# A Hacker-Centric Perspective to Empower Cyber Defense

by

Ericsson Santana Marin

A Dissertation Presented in Partial Fulfillment
of the Requirements for the Degree
Doctor of Philosophy

Approved April 2020 by the
Graduate Supervisory Committee:

Paulo Shakarian, Chair
Adam Doupé
Huan Liu
Emilio Ferrara

ARIZONA STATE UNIVERSITY

May 2020

## ABSTRACT

Malicious hackers utilize the World Wide Web to share knowledge. Previous work has demonstrated that information mined from online hacking communities can be used as precursors to cyber-attacks. In a threatening scenario, where security alert systems are facing high false positive rates, understanding the people behind cyber incidents can help reduce the risk of attacks. However, the rapidly evolving nature of those communities leads to limitations still largely unexplored, such as: who are the skilled and influential individuals forming those groups, how they self-organize along the lines of technical expertise, how ideas propagate within them, and which internal patterns can signal imminent cyber offensives?

In this dissertation, I have studied four key parts of this complex problem set. Initially, I leverage content, social network, and seniority analysis to mine key-hackers on darkweb forums, identifying skilled and influential individuals who are likely to succeed in their cybercriminal goals. Next, as hackers often use Web platforms to advertise and recruit collaborators, I analyze how social influence contributes to user engagement online. On social media, two time constraints are proposed to extend standard influence measures, which increases their correlation with adoption probability and consequently improves hashtag adoption prediction. On darkweb forums, the prediction of where and when hackers will post a message in the near future is accomplished by analyzing their recurrent interactions with other hackers. After that, I demonstrate how vendors of malware and malicious exploits organically form hidden organizations on darkweb marketplaces, obtaining significant consistency across the vendors' communities extracted using the similarity of their products in different networks. Finally, I predict imminent cyber-attacks correlating malicious hacking activity on darkweb forums with real-world cyber incidents, evidencing how social indicators are crucial for the performance of the proposed model. This research is a hybrid of social network analysis (SNA), machine learning (ML), evolutionary computation (EC), and temporal logic (TL), presenting expressive contributions to empower cyber defense.

*To my beloved and inspiring family.*

ACKNOWLEDGMENTS

I would like to thank my Ph.D. advisor, Dr. Paulo Shakarian, for his supervision throughout the dissertation. I am grateful for his methodical advice during the development of my research. I will never forget our weekly meetings, and how day after day, his suggestions significantly contributed to my success as a doctoral researcher. Besides, I would like to thank my defense committee members Dr. Adam Doupé, Dr. Huan Liu, and Dr. Emilio Ferrara, who carefully invested their attention and time to review my work.

I have enjoyed the company of my friends and collaborators from CySIS lab, a team that I am proud to have been part of it: Ahmad Diab, Ashkan Aleali, Dr. Elham Shaabani, Dr. Eric Nunes, Jana Shakarian, Dr. Hamidreza Alvari (Dr. Ghazaleh Beigi), John Robertson, Dr. Mohammed Almukaynizi, Ruocheng Guo, Dr. Soumajyoti Sarkar, and Vivin Paliath.

I also want to thank Professor Farideh Navabi and Dr. Hessam Sarjoughian for the TA assistantships and moments of learning that will help me during my journey as a professor.

I could not forget to thank Dr. Cedric L. de Carvalho (my master's advisor at UFG - Brazil), who encouraged me to continue my research journey through the Ph.D., and also Dr. Thierson C. Rosa and Dr. Telma Soares who helped me to reach ASU.

Finally, I especially thank my beloved family. My beautiful wife Lilian Frota and cute stepdaughter Chloe. My parents Edson Marin and Cássia M. M. S. Marin. My brother, sister, in-laws, nephews, and nieces, Dr. Evelyn C. Marin, Everton Marin, Amanda Zardini, Humberto Barbieri, Enzo M. Barbieri, Lisa M. Barbieri, and Melina Z. Marin. In simple words, I would not have even started this work without their support and encouragement. I know that I always have them to count on, and that is why I love them more than anything.

This dissertation would not have been possible without the funding from the National Council for Scientific and Technological Development (CNPq-Brazil), through the "Science without Borders" program, the Office of Naval Research, the ASU Global Security Initiative (GSI), the Intelligence Advanced Research Projects Activity (IARPA), and CYR3CON, Inc.

TABLE OF CONTENTS

LIST OF TABLES

Table Page

LIST OF FIGURES

Figure Page

Figure Page

# Chapter 1

# INTRODUCTION

With the widespread of cyber-attack incidents, such as those recently experimented by Facebook, Instagram, Dow Jones, AMC Networks, T-Mobile, Disney+, Adobe, Choice Hotels, State Farm, and U.S. Customs and Border Protection [60], cybersecurity has become a serious concern for organizations. A security bulletin published by Kaspersky Lab [66] informed that about 2,672,579 cyber-attacks were repelled daily by the company in 2019 (30 per second), reflecting the average activity of criminals involved in the creation and distribution of cyber threats. No major operating system, application or even hardware seem to be immune to cyber offensive operations [93]. Worldwide, cyber-attacks cost organizations an estimate U$600 billion in 2017 [68] (0.8% of global income) and U$5.2 trillion in additional costs and lost revenue are expected until 2024 [3]. Those attacks have potential to cause serious damage for the target organizations, strengthening the security specialists' claim towards prevention compared to remediation [37].

Information regarding the preparation of cyber-attacks has been increasingly shared by malicious hackers on online communities [104]. In those environments, cybercriminals discuss how to: 1) identify vulnerabilities, 2) create or purchase exploits, 3) choose a target and recruit collaborators, 4) obtain access to the infrastructure needed, and 5) plan and execute the attack [113], making what was once a hard-to-penetrate market becomes accessible to a much wider population. Many works detail how hackers rely on online communities to accomplish their goals [92, 104, 93]. Although this behavior helps to produce a huge amount of malware, it also provides intelligence for defenders, as the information shared online can be leveraged as precursors to various types of cyber-attacks (see examples of attack prediction by using Twitter [109, 35, 63] or darkweb data [7, 9, 8]).

In this context, an intimate understanding of the adversaries present in online hacking communities will greatly aid proactive cybersecurity, allowing security teams to reduce the risk of attacks. However, the rapidly evolving nature of those communities leads to important limitations still largely unexplored, such as: who are the skilled and influential individuals forming those groups, how they self-organize along the lines of technical expertise, how ideas propagate within those communities, and which internal patterns can signal imminent cyber offensives? In this dissertation, I have studied four key parts of this complex problem set: (1.) identification of skilled and influential hackers, (2.) analysis of user/hacker engagement driven by social influence, (3.) disclosure of the community structure of highly specialized technical experts, and (4.) prediction of cyber-attacks by mining malicious hacking activity. The proposed research is a hybrid of social network analysis (SNA), machine learning (ML), evolutionary computation (EC), and temporal logic (TL), being conducted using data from social platforms specialized in malicious hacking on the darkweb and social media.

## 1.1 Motivation

Recent approaches derived from proactive cyber threat intelligence are still facing high false positive rates when predicting cyber-attacks [17, 6, 8], keeping organizations exposed while they counter irrelevant cyber threats. These methods suffer from not knowing which vulnerabilities might be of interest to malicious hackers, as they often concentrate only on the technical aspects involved [93]. However, the correlation between high user engagement on online hacking communities and vulnerability exploitation [5, 7] provides us an important insight: understanding the people behind cyber incidents can help reduce the risk of attacks. Thus, we focus on scrutinizing the actors creating, manipulating, and distributing malicious code online, as well as the groups they form, as an alternative technique to help security teams anticipate the actions of their adversaries. By considering our proposed models, organizations' assets likely to be targeted can be protected before the attackers operate.

## 1.2 Contributions

Figure 1.1 illustrates the four research studies conducted in this dissertation, each with their respective contribution to empower cyber defense.

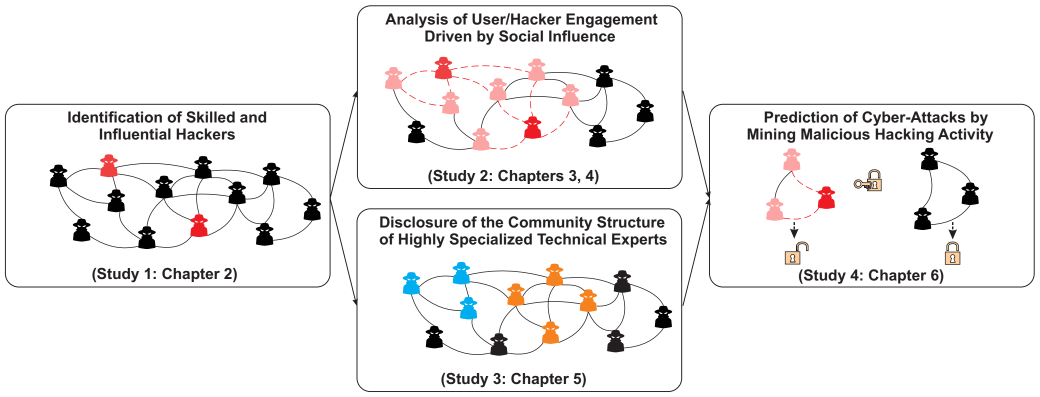
Identification of Skilled and Influential Hackers
(Study 1: Chapter 2)
Analysis of User/Hacker Engagement Driven by Social Influence
(Study 2: Chapters 3, 4)
Disclosure of the Community Structure of Highly Specialized Technical Experts
(Study 3: Chapter 5)
Prediction of Cyber-Attacks by Mining Malicious Hacking Activity
(Study 4: Chapter 6)

Fig. 1.1: Research Studies Carried Out in this Dissertation.

In our first study, we identify skilled and influential users on popular darkweb [1] hacking forums: the so-called "key-hackers". As these individuals are likely to succeed in their cybercriminal goals [89], they foment a promising vulnerability exploitation threat market from where defenders can locate emerging cyber threats. However, as most users on those forums seem to be unskilled or have fleeting interests [13], the identification of key-hackers becomes a complex problem. Moreover, as ground truth data is rare for this task, there is a lack of a method to validate the results. To counter those problems, we develop a profile for each forum member using features derived from content, social network, and seniority analysis, aiming to differentiate standard from key cyber-actors. Then, after defining a metric for collecting ground truth data (key-hackers are formed by the top 10% of users according to their reputation), we train our model on a given forum using optimization (EC) and (ML) algorithms fed with those features to later test its performance on a different

[1]Collection of websites that exist on encrypted networks of the World Wide Web. It is a region intentionally hidden from users, search engines, and regular browsers, being one of the most widespread environment for the investigation of malicious hacking [80, 92, 104, 113].

forum. Our results for ranking consistency show that we are able to identify up to 52% of the existing key-hackers, demonstrating how our model generalizes relatively well.

Additionally, as key-hackers use online platforms to advertise wares, vulnerabilities, and for recruitment [119], we investigate in our second study how social influence contributes to online user engagement. Particularly, we develop two lines of research for analyzing user adoption behavior, one for social media microblogs and the other for darkweb forums.

On social media microblogs, we investigate whether users will adopt a given hashtag considering the influence exerted by their active neighbors. We introduce two time constraints to extend standard (SNA) measures used to quantify social influence, examining their correlation with adoption probability as well as their ability to predict adoption in a (ML) classification task. We observe adoption probability improves for all influence measures analyzed up to 488.24%, while we obtain up to 13.69% improvement in F1 score when comparing to recent machine learning techniques that aim to predict adoption [145].

On darkweb forums, we investigate where and when hackers will post a message in the near future by analyzing their recurrent interactions with other hackers. As lower-skilled individuals are usually influenced to adopt the malicious actions of key-hackers [92], we want to predict in which topic hackers will be influenced to post a message. We formulate this problem as a (ML) sequential rule mining task, whose goal is to discover user posting rules through sequences of user posts and finally use these rules for making predictions over time. We run our experiments using multiple posting time granularities and time-windows for obtaining the rules, observing precision results of up to 0.78 and precision gains up of to 837% when compared to the prior probabilities of hackers' posts. The analysis of user adoption behavior in both research works can be used by security specialists to reveal the potential expansion degree of the key-hackers' networks, providing means for defenders to anticipate who will join a particular malicious hacking activity (e.g., a hacktivist campaign [25] or the acquisition of a hacking product/service online [65]).

Moving to our third study, we analyze whether vendors of malware and malicious exploit organically form hidden organizations on darkweb hacking marketplaces. We search for communities of individuals with similar expertise in specific subfields of hacking, a feature typically owned by key-hackers that can be used for surveillance purposes [94]. For instance, vendors linked to emerging cyber threats can be automatically identified if at least one of the community members is confirmed as offering a similar exploit online, allowing defenders to predict their subsequent product offerings. As there is no direct communication between vendors on those markets, detecting their communities becomes challenging, especially with the absence of ground truth data. Thus, we develop a method based on (SNA) techniques that identifies implicit communities of hacking-related vendors using the similarity of their products. We validate our method cross-checking the community assignments of these individuals on two mutually exclusive sets of marketplaces, achieving 0.445 of consistency between more than 30 communities of vendors revealed in each subset of markets.

Finally, we design an AI tool that uses a (TL) framework to accomplish two tasks: 1) induct rules that correlate malicious hacking activity with real-world cyber incidents in order to predict future cyber-attacks; 2) leverage a deductive approach that combines attack predictions for more accurate security warnings. The framework considers technical and socio-personal indicators of attacks, deriving the latter from the social models proposed in our previous studies. Results demonstrate considerable prediction gains in F1 score (up to 150.24%) compared to the baseline when the pre-conditions of the rules include those socio-personal indicators of attacks, highlighting their relevance for the identification of imminent threats. Besides, we also observe a higher performance of our framework when the predictions made for a given day are combined using deduction, obtaining gains in F1 score of up to 182.38%. Those achievements evidence how the interdisciplinary work conducted in this dissertation allows security specialists to mine the interest of credible malicious hackers, given defenders a better chance in the security battle against attackers.

## 1.3 Applications and Impact

Deeply understand online hacker communities can be the key for designing better attack prediction systems. From the defenders perspective, the hackers' digital traces existing in those environments yield valuable insights into evolving cyber-threats and can signal a pending offensive operation well before malicious activity is detected on a target system. For instance, mining who are the high skilled and influential hackers, as well as their closest disciples, to later observe which are the software vulnerabilities they are interested in, can help security alert systems identify credible threats. We believe this capability affords a reduction on the set of possible targets (organizations/platforms/products) that are at real risk, enhancing the performance of those alert systems while predicting cyber-attacks.

## 1.4 Literature Overview

There are important works that addressed the identification of skilled and influential individuals on hacking forums in the last years [2, 148, 38, 112]. Some of them used content analysis to classify hackers in groups, either by matching lexicon to extract expertise [2], by analyzing post orientations regarding knowledge transfer [148], or by identifying the most active users in each hacking domain [38]. Overall, they found that: 1) the majority of hackers are only average users, not actively engaging on the communities; 2) key-hackers increasingly act as knowledge providers. Differently, Samtani and Chen [112] used (SNA) techniques to calculate the centrality measures of hackers, identifying those who should be the most important users in the networks. In all these works, the authors did not combine the advantages of different approaches to find key-hackers. We also observe an absence of a method to validate the key-hackers identified, which basically makes their results not comparable. In this dissertation, we fill these two gaps by using a hybrid model to identify key-hackers, including a systematic method based on user reputation to validate the results.

We also report three relevant works that analyzed user susceptibility to influence on social media, as they can be used to map the expanding networks of hackers [145, 51, 40]. The first one considered two functions based on pair-wise influence and structural diversity to predict adoptions [145]. The second and third works used joint probabilities to calculate the total influence that active neighbors exert on users to make them adopt a particular behavior [51, 40]. All these works found a positive correlation between the number of active neighbors and probability of influence, specially for hashtags that carry social risks. However, we note those authors have not fully explored the dynamics of social influence, building their models upon static relationships and invariable social stimulus. In our proposed work, we address these issues by dynamically building our social networks to more accurately measure social influence, showing significant improvements for adoption prediction.

To the best of our knowledge, we propose the first applied study where hacker engagement on darkweb forums is investigated through adoption prediction. Even so, we present here some works carried out on the surfaceweb [2] that can be used to predict opinions, activities, and link formation. For instance, the framework proposed in [101] inferred users' stance according to their arguments, interactions, and attributes, but it was unable to estimate where and when a user would engage. The same issue is observed in the model proposed in [49], where the authors tracked online activity of users to predict their future interactions. Although the model estimated browse-content, browse-comments, upvote, downvote, or do-nothing behavior for each post visualized, the technique was not able to anticipate a new message. Also, the authors in [110] developed a time-series methodology for predicting link formation in discussion forums, which was unable to forecast when specific interactions between users would occur. Note how the prediction of hackers' posts, considering patterns of interactions driven mainly by social influence, is an important contribution of our work.

[2] Section of the Web accessed from any browser and regularly indexed by search engines.

Another contribution of this dissertation is an applied study where social network information of malware and exploit vendors is derived from malicious hacking marketplaces on the darkweb, since previous studies only examined characteristics of hacking and non-hacking darkweb forums for this task. For instance, two topic-based social networks were created in [69], one from the topic creator perspective and the other from the repliers perspective. There are also works where the authors tried to form clusters of users based on their messages' timestamps [142] or based on the similarities of the posts' meta-information (author, timestamp, thread, etc.) [10]. It is widely known that social relationships of forum users can be directly inferred from their posts/replies, while on marketplaces there is no explicit communications among vendors, highlighting the novel aspect of our research.

Finally, only few research works focus on predicting cyber-attacks against specific corporations by analyzing online hacking discussions. Most works that proactively investigated cybersecurity either searched for cyber-threats to mitigate risks [103, 7, 93, 113, 5] or predicted the exploitation of software vulnerabilities [109, 9, 17, 132]. However, similar to our goal, Khandpur et al. [63] proposed an unsupervised approach to detect ongoing cyber-attacks discussed on Twitter, by using a limited set of seed event triggers and a query expansion strategy based on convolutional kernels and dependency parses. Goyal et al. [52] described deep neural networks and autoregressive time series models that leveraged signals from security blogs and vulnerability databases to predict attacks. Deb et al. [30] applied sentiment analysis to darkweb forum posts to correlate sentiment trends over time with potential attacks. Almukaynizi et al. [8] proposed a logical framework to predict the magnitude of attacks by analyzing vulnerability mention on the darkweb. Although those approaches contributed with proactive cyber threat intelligence, they neglected the individuals behind the threats. Besides the technical information involved, we also rely on social-personal indicators of attacks in this dissertation. Then, we are able to differentiate the hackers in terms of capability, significantly increasing the accuracy of our attack predictions.

## 1.5 Organization

The remaining of this dissertation is organized as follows:

**Chapter 2: Mining Key-Hackers on Darkweb Forums**. In this Chapter, we describe the proposed model used to identify the existing key-hackers on darkweb forums [83].

**Chapter 3: Temporal Analysis of Influence to Predict User Adoption on Social Media**. In this Chapter, we detail the two proposed time constraints to extend standard (SNA) influence measures while predicting hashtag adoption on social media [81, 82].

**Chapter 4: Predicting Hacker Adoption on Darkweb Forums**. In this Chapter, we describe the proposed model to predict hacker engagement on darkweb forums, anticipating in which topic hackers will be influenced to post a message in the near future [76].

**Chapter 5: Detecting Communities of Malware and Exploit Vendors on Darkweb Marketplaces**. In this Chapter, we describe the proposed model to reveal hidden communities of hacking-related vendors on darkweb marketplaces [77, 80].

**Chapter 6: Reasoning About Future Cyber-Attacks Through Socio-Technical Hacking Information**. In this Chapter, we describe the proposed framework to predict future cyber offensives, considering technical and socio-personal indicators of attacks [78, 79].

**Chapter 7: Final Considerations**. In this chapter, we recapitulate the main ideas and results presented in the dissertation, also considering some directions for future work.

Table 1.1 summarize the contributions presented in each chapter of this dissertation.

Table 1.1: Contributions of this Dissertation.

| Chapters | Contribution |
|---|---|
| 02 | Identification of key-hackers on darkweb forums. |
| 03, 04 | Analysis of user/hacker engagement on social media and darkweb forums. |
| 05 | Disclosure of hidden hacker communities existing on darkweb marketplaces. |
| 06 | Prediction of imminent cyber-attacks using socio-technical hacking information. |

# Chapter 2

# MINING KEY-HACKERS ON DARKWEB FORUMS

## 2.1 Introduction

Malicious hacker communities have participants with different levels of knowledge, and those who want to identify emerging cyber threats need to scrutinize these individuals to find key cybercriminals [148]. We denote those malicious cyber-actors as key-hackers, since they have higher hacking skills and influence when compared to the great majority of users present in online hacking communities. As this select group of hackers foment a promising vulnerability exploitation threat market [5], it forms "natural lens" through which security alert systems can look at while predicting cyber-attacks.

To support our assumption, consider when beginners or standard-level hackers are planning to launch an attack. As those actors are utility-maximizing, they opt for rewarding vulnerabilities for which there exist threats with proved attack and concealment capabilities to increase their chance of success [5]. Overall, the skills to implement and spread those threats belong to key-hackers [7], as they are able to craft advanced hacking tools [1] , find zero-days vulnerabilities [2] , recruit and orchestrate teams in attack campaigns [3] , and maintain low profiles of activity [126, 97]. As key-hackers often succeed in their cybercrimes [89], they provide profitable resources that are more appealing for the others [73].

[1]Ex. of advanced hacking tools crafted by key-hackers: $Retefe$ and $TrickbotGo$ banking Trojans, $Nitol$ and $DoublePulsar$ backdoors, $Gh0st$ RAT, $EternalRocks$ and $MicroBotMassiveNet$ computer worms and $WannaCry$ and $NotPetya$ ransomwares.

[2]Ex. of zero-day exploits crafted by key-hackers: $Stuxnet$ computer worm, 666 RAT, $Tobfy$ ransomware, and $LadyBoyle$ action script.

[3]Ex. of APT watering hole attack campaigns conducted by key-hackers: Web2Crew, Taidoor, th3bug, and Operation Ephemeral Hydra.

The challenge here is that key-hackers form only a small percentage of the community members, making their identification a complex problem. In the literature, two approaches have been empirically considered for this task: content analysis [2, 148, 38] and social network analysis [147, 112]. In both approaches, the idea is to generate features and rank the community users based on their feature values, being the top ranked users considered as key-hackers [2]. However, there is a serious complication for this identification task: the lack of ground truth (the key-hackers of the communities) to validate the results. As it is difficult to obtain this information, previous works neglected this validation task or have it done manually - e.g., by leveraging security consulting companies [91]. Finally, it is unclear if these methods can generalize, as training and testing are done using the same forum data.

In this Chapter, we address the key-hacker identification problem including a systematic method to validate the results. Particularly, we study how content, social network, and also seniority analysis perform individually and combined in this task. We conduct our experiments using informative features extracted from three highly ranked darkweb hacker forums. Information related to activity, expertise, knowledge transfer behavior, structural position, influence, and coverage are mined to develop a profile for each community member, aiming to understand which features characterize key cybercriminals. To train and test our model, we use an optimization metaheuristic and compare its performance with machine learning algorithms. We leverage the users' reputation provided by the forums analyzed to cross-validate the results among those sites - models trained in one forum are generalized to make predictions on different ones. Our work is novel since it offers researchers a strategy to find key-hackers in forums with no users' reputation or with a deficient user reputation system. We observe this is the case of the vast majority of hacking forums, representing over 80% of the 36 scraped for this study. We summarize the main contributions of this work as:

1. We show that a hybridization of features derived from content, social network, and seniority analysis is able to identify key-hackers up to 17% more precisely than those

derived from any of these strategies by itself;

2. We explain and evidence why reputable hackers form a strong indicator of key-cybercriminals;
3. We demonstrate how a model learned in a given forum to identify its key-hackers can be generalized to a different forum which was not used to train the model, obtaining up to 52% of ranking consistency;
4. We compare the performance of different models when trying to identify key-hackers, showing how an optimization metaheuristic obtains up to 35% of predictive improvement over machine learning algorithms.

The remainder of this Chapter is organized as follows. Section 2.2 details darkweb forums and our dataset. Next, we show in Section 2.3 how we leverage users' reputation to obtain ground truth data. Section 2.4 defines our problem. Section 2.5 describes the features we derive to profile hackers. Section 2.6 presents our experiments and corresponding results. Section 2.7 shows some related work. Finally, Section 2.8 summarizes the Chapter.

## 2.2 Darkweb Hacking Forums

Many people involved in malicious cyber activity rely on trustful online communities, among which, forums are one of the most prevalent [2]. For example, the recent "WannaCry" ransomware attack directed against hospitals in the UK and numerous other worldwide targets was discussed several weeks prior on a darkweb forum [127]. Hackers likely involved in this attack discussed the number of unpatched machines, the exploit to be used, the industry verticals, and the method of attack (ransomware). These hacking forums provide user-oriented platforms that enable communication regardless geophysical location, facilitating the emergence of hackers' communities.

The World Wide Web (Web) is a vast network of linked hypertext files where forums are accessed via the Internet. The Web can be maily classified into 3 regions: surfaceweb, deepweb, and darkweb [92]. The Surfaceweb is the open portion of the Internet, where webpages are publicly accessible and indexed by search engines. On the other hand, the deepweb refers to the websites hosted on the surfaceweb but not indexed by search engines, usually because they require authentication. Finally, the darkweb refers to a collection of websites that exist on encrypted networks of the deepweb. It is a region intentionally and securely hidden from users and standard search engines and browsers. This is the reason why darkweb forums constitute one of the most widespread hacking environment, being commonly used for research studies investigating key cybercriminals [2].

### *2.2.1 Dataset*

We collect data from a commercial version of the system proposed in [92]. This system currently provided by CYR3CON [28] is responsible for gathering cyber threat intelligence from various social platforms of the World Wide Web, especially the ones existing on deepnet and darkweb websites. For this particular work, we select three popular English hacking forums on the darkweb. We anonymize these forums representing them as *Forum 1*, *Forum 2*, and *Forum 3*, showing their statistics in Table 2.1. All these forums comprise hacking-related discussions organized in a thread format, where a user initiates a topic that is followed by many users' replies.

Table 2.1: Statistics of the Three Analyzed Darkweb Hacker Forums.

| | *Forum 1* | *Forum 2* | *Forum 3* |
|---|---|---|---|
| Time Period | 2013-12-24 : 2016-03-16 | 2013-12-24 : 2016-08-16 | 2002-09-14 : 2016-03-15 |
| Number of Users | 4,380 | 2,495 | 2,802 |
| Number of Topics | 5,571 | 1,077 | 5,805 |
| Number of Posts | 36,453 | 25,115 | 49,078 |
| Distinct Values of Users' Reputation | 134 | 102 | 37 |

In order to prepare the data for feature extraction, we retrieve the users' interactions over time to generate a network of hackers. We denote a set of users $V$ and connections $E$ as the nodes and edges in a directed graph $G = (V, E)$, while $\Theta$, $\mathcal{M}$, and $T$ correspond to a set of topics, messages, and discrete time points. The symbols $v, \theta, m, t$ will represent a specific node, topic, message, and time point. We denote an activity log $\mathcal{A}$ containing all posts (topics and replies) as a set of tuples of the form $\langle v, \theta, m, t \rangle$, where $v \in V$, $\theta \in \Theta$, $m \in \mathcal{M}$, and $t \in T$. It describes that "$v$ posted in topic $\theta$ a message $m$ at time $t$". A directed edge $(v, v')$ is created when users $v$ and $v'$ post together in a given topic, so that the posting time of $v$ is greater than of $v'$. We formalize the set of direct edges $E$ in equation 2.1:

$$E = \{(v, v') \mid \exists \langle v, \theta, m, t \rangle \in \mathcal{A}, \exists \langle v', \theta, m', t' \rangle \in \mathcal{A},\ s.t.\ v \neq v', t > t'\} \tag{2.1}$$

The intuition with this set of direct edges is to make visible to users that are posting in $\theta$ at time $t$ all other users that have already posted in $\theta$ prior to $t$, but not vice-versa. We believe this strategy can better reproduce the interaction process on online forums (compared to the general strategy of creating a complete undirected graph including all users that post together in a topic [112]), since users will only know about previous posts. Figure 2.1 illustrates this process by showing the original users' posts in panel (a) and the corresponding generated social network in panel (b).

| Topic A | | Topic B | |
|---|---|---|---|
| User | Post Time | User | Post Time |
| 1 | 01-01-2015 10:23:15 | 2 | 01-02-2015 15:20:10 |
| 2 | 01-01-2015 10:25:10 | 1 | 01-02-2015 16:10:05 |
| 3 | 01-01-2015 10:30:20 | 3 | 01-02-2015 16:18:47 |
| 2 | 01-01-2015 10:31:46 | 2 | 01-02-2015 17:04:46 |
| 5 | 01-01-2015 10:40:14 | 4 | 01-02-2015 20:49:14 |

(a)

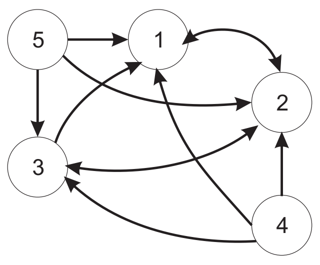

(b)

Fig. 2.1: Directed Graph Generated Using the Users' Posts.

After generating the social networks, we remove all users who do not belong to the giant component of their corresponding forum, since they can produce misleading centrality values. The issue happens because some centralities are computed and normalized for each component, which tends to produce high values for users in small parts of the networks. Because of their few connections, these individuals would hardly be considered as key-hackers. Table 2.2 shows the size of all components of each forum, detailing that 67 users from *Forum 1*, 78 users from *Forum 2*, and 65 users from *Forum 3* were removed.

Table 2.2: Network Component Analysis.

| | *Forum 1* | *Forum 2* | *Forum 3* |
|---|---|---|---|
| Giant Component Size | 4,313 | 2,417 | 2,737 |
| Component Size = 11 | 0 | 1 | 0 |
| Component Size = 3 | 1 | 0 | 0 |
| Component Size = 2 | 19 | 6 | 7 |
| Component Size = 1 | 26 | 55 | 51 |

## 2.3 Leveraging Users' Reputation to Obtain Ground Truth Data

As hacker communities form meritocracies [104, 118], members own different levels of capability, expertise, and influence (to mention a few human factors). According to [31], those factors are organically consolidated in the user reputation score, which is a metric that codifies users' standing, driving engagement by measuring participation, activity, content quality, content rating, etc. Zhang et al. [148] showed that reputable hackers are usually linked to emerging cyber threats, making them a strong indicator of key cybercriminals.

A case study in our data corroborates with the Zhang's assumption. In 2016, Anna Senpai had a high reputation when he released the Mirai Botnet source code on a popular hacker forum [128]. His posts generated a high number of responses, though none more than the post containing the code. Since user reputation is peer-assigned, the reputation score is mirroring how other forum members evaluate the usefulness of the users' contributions. When we analyze the posting patterns of high and low reputable hackers of *Forum 1* presented in Figure 2.2(a), we observe that 36 out of the 44 hackers with the highest reputation ($Top_{1\%}$ of all users) are posting on the 28 spikes of activity (minimal of $4 \times \sigma$ above average), while only 8 of them are not engaged in these conversations.

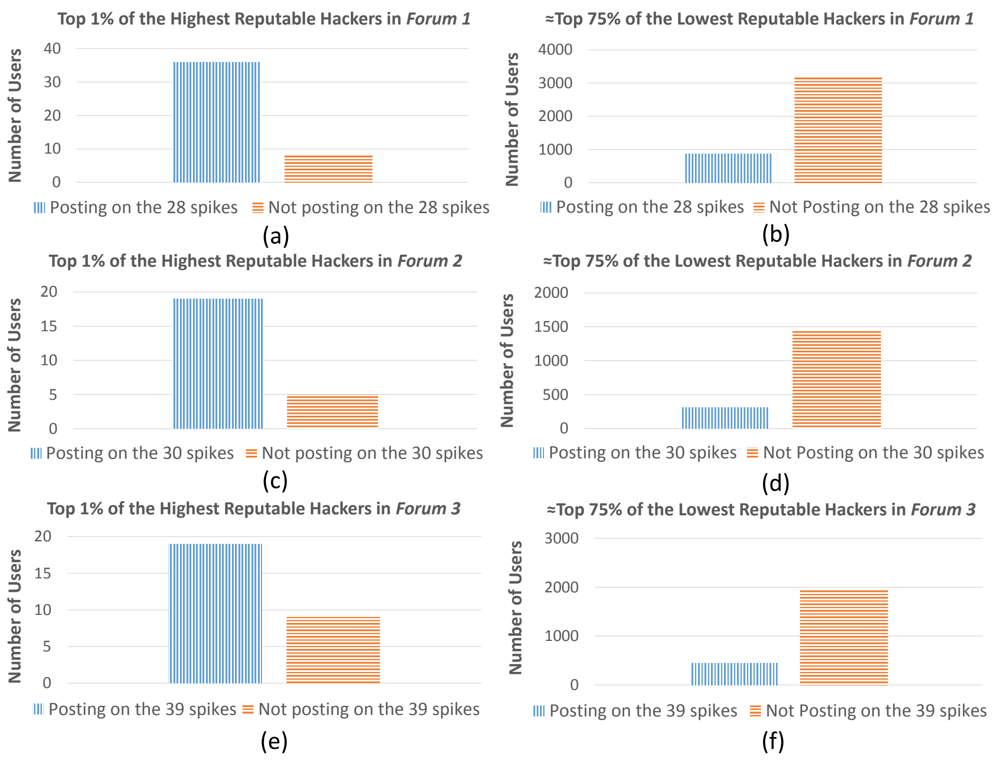

Fig. 2.2: Posting Pattern of the Highest and the Lowest Reputable Hackers on the Three Darkweb Forums Analyzed.

On the other hand, Figure 2.2(b) shows that 870 out of the 4.039 hackers with the lowest reputation ($\approx Top_{75\%}$ of all users) are posting on those spikes, while 3.169 are not engaged in these conversations. A similar pattern is observed for the other two forums analyzed. We investigate those spikes as they offer some intuition about possible interesting topics promoted by skilled and influential hackers on the forums, confirming the user reputation score as a strong indicator for key-hacker identification.

In this study, we also rely on the assumption that users with high reputation form our set of key-hackers, using this metric as our ground truth. Thus, we deliberately select forums that explicitly provide this information, so that the corresponding key-hackers can be identified. Figure 2.3 shows the distribution of the reputation score in (a) *Forum 1*, (b) *Forum 2*, and (c) *Forum 3*, pointing out the existence of a hacking meritocracy (these curves fit power-laws with $p_k \approx k^{-0.92}$, $p_k \approx k^{-0.86}$ and $p_k \approx k^{-0.78}$ respectively, where $k$ is the number of users). As it is observed, only a few number of users (key-hackers) own high reputation in all the forums, although their corresponding scores vary in magnitude. In addition, although Table 2.1 shows that *Forum 1* and *Forum 2* are closer in terms of reputation distinctness (their scores are formed by 134 and 102 different values respectively while *Forum 3* owns only 37), the similar distribution pattern of all those three forums informs that characteristics of the highest reputable hackers should be somehow shared by them.

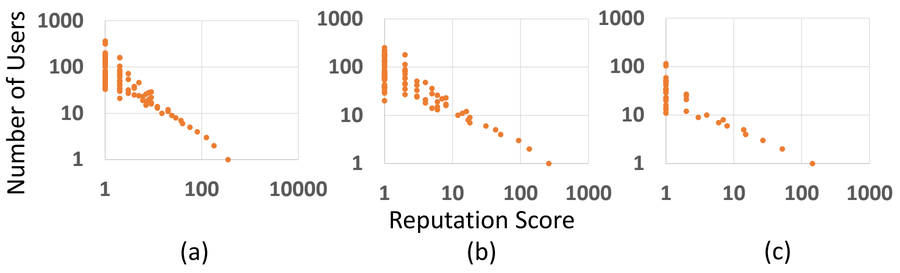

Fig. 2.3: Distribution of Reputation Score in (a) *Forum 1*, (b) *Forum 2*, and (c) *Forum 3* (log-log scale).

## 2.4 Problem Statement

Based on the finding that the highest reputable hackers form our set of key-hackers, we want to estimate the user reputation score in order to find key-hackers in forums that do not provide this score or that have a deficient user reputation system.

## 2.5 Feature Engineering

To estimate users' reputation, we design the 25 features detailed in Table 2.3 to mine relevant characteristics and behaviors of key-hackers.

Table 2.3: Feature Engineering.

| | | | |
|---|---|---|---|
| Content Analysis | Activity | | 01. Topics Created<br>02. Replies Created<br>03. Replies by Month |
| | Expertise | Involvement Quality | 04. Length of Topics<br>05. Length of Replies<br>06. Topics Density<br>07. Replies with Knowledge Provision<br>08. Replies with Knowledge Acquisition<br>09. Topics with Knowledge Provision<br>10. Topics with Knowledge Acquisition |
| | | Cybercriminal Assets | 11. Attachments |
| | | Specialty Lexicons | 12. Technical Jargon<br>13. Darkweb Jargon |
| | Knowledge Transfer Behavior | | 14. Velocity of Knowledge Provision Pattern in Topics<br>15. Velocity of Knowledge Acquisition Pattern in Topics<br>16. Velocity of Knowledge Provision Pattern in Replies<br>17. Velocity of Knowledge Acquisition Pattern in Replies |
| Social Network Analysis | Structural Position | | 18. Degree Centrality<br>19. Betweenness Centrality<br>20. Closeness Centrality |
| | Influence | | 21. Eigenvector Centrality<br>22. Page Rank |
| Seniority Analysis | Coverage | | 23. Interval btw User's & Forum's First Posts<br>24. Distinct Days of Posts<br>25. Interval btw User's & Forum's Last Posts |

From these features, 17 are extracted using *Content Analysis*, subdivided in *Activity* (3), *Expertise* (10), and *Knowledge Transfer Behavior* (4). We subdivide the 10 features related to *Expertise* in *Involvement Quality* (7), *Cybercriminal Assets* (1), and *Specialty Lexicons* (2). In addition, 5 features are extracted using *Social Network Analysis*, subdivided in *Structural*

*Position* (3) and *Influence* (2). Finally, 3 features are extracted using what we denominate *Seniority Analysis*, being all of them related to *Coverage*. We analyze users' seniority since it generates indicators of consistent forum involvement over time, checking how much the users continuously contribute to the hacker environments [55, 89, 102]. We believe this set of features comprises a variety of information that could differentiate key-hackers from the beginners or standard-level hackers, contributing to a better estimation of the users' reputation. All features have their values normalized to avoid problems with different scales [131]. We detail the features below.

### *2.5.1 Activity*

The set of features within this category belongs to the content analysis approach and aims to identify how active the hackers are. It includes the three following features:

**Topics Created (TOC)**. This feature counts how many topics (headers) are initiated by hackers. According to previous works [147], key-hackers usually create relatively few topics but with high relevance to the community. We formalize this feature as:

$$TOC_{(v)} = \sum_{\theta} g(\langle v, \theta, m, t \rangle) \tag{2.2}$$

where $g(\langle v, \theta, m, t \rangle)$ is defined as:

$$g(\langle v, \theta, m, t \rangle) = \begin{cases} 1, \ if \ \langle v, \theta, m, t \rangle \in \mathcal{A} \land \nexists \langle v', \theta, m', t' \rangle \in \mathcal{A}, \ \textit{s.t.} \ t' < t \\ 0, \ otherwise \end{cases} \tag{2.3}$$

**Replies Created (REC)**. This feature counts the amount of times users answer the topics. According to previous works [147, 38, 148, 2], key-hackers usually create a huge quantity of quality replies, offering relevant help to the lower skilled community members. We formalize this feature as:

$$REC_{(v)} = \sum_{\theta} \sum_{m} \sum_{t} |\langle v, \theta, m, t \rangle| - TOC_{(v)}, \text{ s.t. } \langle v, \theta, m, t \rangle \in \mathcal{A} \tag{2.4}$$

**Replies by Month (REM)**. This feature averages the replies created by the hackers monthly, aiming to estimate how often hackers produce answers. Previous works, such as [2], claim that key-hackers usually have a minimum frequency of answers over time, in order to keep the status acquired. We formalize this feature as:

$$REM_{(v)} = \frac{REC_{(v)}}{|MA_{(v)}|} \tag{2.5}$$

where $MA_{(v)}$ is the set of distinct months in which $v$ created at least one topic answer.

### 2.5.2 Expertise

This category of features belongs to the content analysis approach and aims to quantify the users' skills regarding malicious hacking. It includes the ten following features:

**Length of Topics (LET)**. This feature averages the number of words used by hackers to create a topic. Previous works, such as [2], state that key-hackers tend to not create extensive topics since this is a characteristic of low-skilled hackers. We formalize this feature as:

$$LET_{(v)} = \frac{\sum_{\theta} h(\langle v, \theta, m, t \rangle)}{TOC_{(v)}} \tag{2.6}$$

with $h(\langle v, \theta, m, t \rangle)$ being defined as:

$$h(\langle v, \theta, m, t \rangle) = \begin{cases} Length(m), \ if \ \langle v, \theta, m, t \rangle \in \mathcal{A} \ \land \ \nexists \langle v', \theta, m', t' \rangle \in \mathcal{A}, \\ \hfill \text{s.t. } t' < t \\ 0, \ otherwise \end{cases} \tag{2.7}$$

**Length of Replies (LER)**. This feature averages the number of words used by hackers to create a reply. According to previous works [147, 2], key-hackers usually produced detailed answers, as they have interest and knowledge to instruct the other community members. We formalize this feature as:

$$LER_{(v)} = \frac{\sum_{\theta} \sum_{m} \sum_{t} i(\langle v, \theta, m, t \rangle)}{REC_{(v)}} \tag{2.8}$$

with $i(\langle v, \theta, m, t \rangle)$ being defined as:

$$i(\langle v, \theta, m, t \rangle) = \begin{cases} Length(m), \; if \; \langle v, \theta, m, t \rangle \in \mathcal{A} \; \wedge \; \exists \langle v', \theta, m', t' \rangle \in \mathcal{A}, \\ \hfill \textit{s.t. } t' < t \\ 0, \; otherwise \end{cases} \tag{2.9}$$

**Topics Density (TOD)**. This feature averages the number of users posting in a given topic. As discussions started by key-hackers are more relevant to the community, they often promote a higher user engagement [148]. We formalize this feature as:

$$TOD_{(v)} = \frac{\sum_{\theta} j(\langle v, \theta, m, t \rangle)}{TOC_{(v)}} \tag{2.10}$$

with $j(\langle v, \theta, m, t \rangle)$ being defined as:

$$j(\langle v, \theta, m, t \rangle) = \begin{cases} \sum_{v'} \sum_{m'} \sum_{t'} |\langle v', \theta, m', t' \rangle|, \; if \; \langle v, \theta, m, t \rangle \in \mathcal{A} \; \wedge \\ \hfill \nexists \langle v', \theta, m', t' \rangle \in \mathcal{A}, \; \textit{s.t. } t' < t \\ 0, \; otherwise \end{cases} \tag{2.11}$$

**Replies with Knowledge Provision (RKP)**. This feature counts the number of replies containing knowledge provision. Zhang et. al. [148] observed a trend for key-hackers to produce more replies providing than requesting information. To identify knowledge provision, we apply string-match to a predefined set of keywords. Table 2.4 shows a sample of the keywords that match knowledge provision.

Table 2.4: Sample of Keywords Used for String-Match.

| Knowledge Provision | Knowledge Acquisition | Technical Jargon | Darkweb Jargon |
|---|---|---|---|
| advice | request | back door | tor |
| suggest | ask | cookie | blockchain |
| guide | doubt | crack | dispute |
| tutorial | whyd́ | dos | bitcoin |
| recommend | how to | dump | escrow |
| follow | need | zero day | honeypot |
| check | want | xss | i2p |
| yourself | troublesom | spyware | freenet |
| easy-to-follow | fail | shell | onion |
| demonstrate | struggling | phishing | pgp |

We formalize this feature as:

$$RKP_{(v)} = \sum_{\theta}\sum_{m}\sum_{t} k(\langle v, \theta, m, t\rangle) \tag{2.12}$$

with $k(\langle v, \theta, m, t\rangle)$ being defined as:

$$k(\langle v,\theta,m,t\rangle) = \begin{cases} 1, if\ \exists w \in m \wedge w \in Key_{\{kp\}} \wedge \langle v,\theta,m,t\rangle \in \mathcal{A} \wedge \\ \qquad \exists\langle v',\theta,m',t'\rangle \in \mathcal{A},\ s.t.\ t' < t \\ 0,\ otherwise \end{cases} \tag{2.13}$$

where $Key_{\{kp\}}$ is the predefined set of knowledge provision keywords.

**Replies with Knowledge Acquisition (RKA)**. This feature counts the number of replies containing knowledge acquisition. As the opposite of the previous feature, Zhang et. al. [148] observed a tendency for key-hackers to produce fewer replies acquiring than providing information. To identify a knowledge acquisition, we also apply string-match to a predefined set of keywords illustrated in Table 2.4. We formalize this feature as:

$$RKA_{(v)} = \sum_{\theta} \sum_{m} \sum_{t} l(\langle v, \theta, m, t \rangle) \tag{2.14}$$

with $l(\langle v, \theta, m, t \rangle)$ being defined as:

$$l(\langle v, \theta, m, t \rangle) = \begin{cases} 1, if \ \exists w \in m \land w \in Key_{\{ka\}} \land \langle v, \theta, m, t \rangle \in \mathcal{A} \land \\ \hfill \exists \langle v', \theta, m', t' \rangle \in \mathcal{A}, \ \textit{s.t.} \ t' < t \\ 0, \ otherwise \end{cases} \tag{2.15}$$

where $Key_{\{ka\}}$ is the predefined set of knowledge acquisition keywords.

**Topics with Knowledge Provision (TKP)**. This feature counts the number of topics containing knowledge provision. It has the same pattern observed for the feature *RKP*, but with a different magnitude. We formalize this feature as:

$$TKP_{(v)} = \sum_{\theta} n(\langle v, \theta, m, t \rangle) \tag{2.16}$$

with $n(\langle v, \theta, m, t \rangle)$ being defined as:

$$n(\langle v, \theta, m, t \rangle) = \begin{cases} 1, if \ \exists w \in m \land w \in Key_{\{kp\}} \land \langle v, \theta, m, t \rangle \in \mathcal{A} \land \\ \hfill \nexists \langle v', \theta, m', t' \rangle \in \mathcal{A}, \ \textit{s.t.} \ t' < t \\ 0, \ otherwise \end{cases} \tag{2.17}$$

**Topics with Knowledge Acquisition (TKA)**. This feature counts the number of topics containing knowledge acquisition. It has the same pattern observed for the feature *RKA*, but with a different magnitude. We formalize this feature as:

$$TKA_{(v)} = \sum_{\theta} o(\langle v, \theta, m, t \rangle) \tag{2.18}$$

with $o(\langle v, \theta, m, t \rangle)$ being defined as:

$$o(\langle v, \theta, m, t \rangle) = \begin{cases} 1, if \ \exists w \in m \wedge w \in Key_{\{ka\}} \wedge \langle v, \theta, m, t \rangle \in \mathcal{A} \wedge \\ \qquad \nexists \langle v', \theta, m', t' \rangle \in \mathcal{A}, \ s.t. \ t' < t \\ 0, \ otherwise \end{cases} \tag{2.19}$$

**Attachments (ATH)**. This feature checks for attachments in the posts (topics and replies). According to [2], key-hackers usually provide relevant cybercriminal assets in form of attachments. We apply string-match to a predefined set of keywords such as “href” or “http”, formalizing this feature as:

$$ATH_{(v)} = \sum_{\theta} \sum_{m} \sum_{t} p(\langle v, \theta, m, t \rangle) \tag{2.20}$$

with $p(\langle v, \theta, m, t \rangle)$ being defined as:

$$p(\langle v, \theta, m, t \rangle) = \begin{cases} 1, if \ \exists w \in m \wedge w \in Key_{\{at\}} \wedge \ \langle v, \theta, m, t \rangle \in \mathcal{A} \\ 0, \ otherwise \end{cases} \tag{2.21}$$

where $Key_{\{at\}}$ is the predefined set of keywords related to attachments.

**Technical Jargon (TEJ)**. This feature checks for technical jargon in the posts. According to [2], key-hackers often use technical jargon to reference some specific hacking technique or tool. To identify technical jargon, we apply string-match to a set of keywords extracted from a predefined dictionary. Table 2.4 shows a sample of the keywords that match technical jargon. We formalize this feature as:

$$TEJ_{(v)} = \sum_{\theta} \sum_{m} \sum_{t} q(\langle v, \theta, m, t \rangle) \tag{2.22}$$

with $q(\langle v, \theta, m, t \rangle)$ being defined as:

$$q(\langle v, \theta, m, t \rangle) = \begin{cases} 1, if \ \exists w \in m \wedge w \in Key_{\{ja\}} \wedge \ \langle v, \theta, m, t \rangle \in \mathcal{A} \\ 0, \ otherwise \end{cases} \tag{2.23}$$

where $Key_{\{ja\}}$ is the predefined set of keywords related to technical jargon.

**Darkweb Jargon (DWJ)**. This feature checks for darkweb jargon in the posts. According to [2], key-hackers often use darkweb jargon to reference some specific hacker environment, technique or tool. To identify darkweb jargon, we apply string-match to a set of keywords extracted from a predefined dictionary. Table 2.4 shows a sample of the keywords that match darkweb jargon. We formalize this feature as:

$$DWJ_{(v)} = \sum_{\theta} \sum_{m} \sum_{t} r(\langle v, \theta, m, t \rangle) \tag{2.24}$$

with $r(\langle v, \theta, m, t \rangle)$ being defined as:

$$r(\langle v, \theta, m, t \rangle) = \begin{cases} 1, if \ \exists w \in m \wedge w \in Key_{\{dw\}} \wedge \ \langle v, \theta, m, t \rangle \in \mathcal{A} \\ 0, \ otherwise \end{cases} \tag{2.25}$$

where $Key_{\{dw\}}$ is the predefined set of keywords related to the darkweb.

### *2.5.3 Knowledge Transfer Behavior*

The set of features within this category belongs to the content analysis approach and aims to identify the behavioral trend of hackers related to knowledge provision and knowledge acquisition over time. It includes the four following features:

**Velocity of Knowledge Provision Pattern in Topics (VPT)**. This feature checks how fast the knowledge provision pattern increases or decreases in the topics created by hackers. The idea is inspired in [148], who examined how this pattern changes by analyzing sequential posts. According to [148], key-hackers usually present increasing knowledge provision over time, and this feature measures the velocity of this behavior in the topics. Specifically, for every sequential 10 topics $i$ where user $v$ engaged, we create a data point $x_i(v)$ and assign the number of topics created by $v$ containing knowledge provision to $y_i(v)$. Then, we analyze all points created using linear regression, checking the slope $a$ of the line generated ($y = ax$). We formalize this feature as:

$$VPT_{(v)} = \frac{y_2(v) - y_1(v)}{x_2(v) - x_1(v)} = \frac{y_2(v) - y_1(v)}{2 - 1} = y_2(v) - y_1(v) = a \tag{2.26}$$

with $y_i(v)$ being defined as:

$$y_i(v) = \sum_{\theta \in TOP_{(v)},\, \theta = [(i-1)*10]+1}^{[(i-1)*10]+10} n(\langle v, \theta, m, t \rangle) \tag{2.27}$$

where $TOP_{(v)}$ is the set of sorted topics created by $v$ and $n$ is defined in equation 2.17.

**Velocity of Knowledge Acquisition in the Topics (VAT)**. This feature checks how fast the knowledge acquisition pattern increases or decreases in the topics created by hackers. We use the same strategy mentioned for the previous feature, but considering knowledge acquisition now. According to [148], key-hackers usually present decreasing knowledge acquisition over time, and this feature measures the velocity of this behavior in the topics. We formalize this feature as:

$$VAT_{(v)} = \frac{y_2(v) - y_1(v)}{x_2(v) - x_1(v)} = \frac{y_2(v) - y_1(v)}{2 - 1} = y_2(v) - y_1(v) = a \tag{2.28}$$

with $y_i(v)$ being defined as:

$$y_i(v) = \sum_{\theta \in TOP_{(v)}, \theta = [(i-1)*10]+1}^{[(i-1)*10]+10} o(\langle v, \theta, m, t \rangle) \tag{2.29}$$

where $TOP_{(v)}$ is the set of sorted topics created by $v$ and $o$ is defined in equation 2.19.

**Velocity of Knowledge Provision in the Replies (VPR)**. This feature checks how fast the knowledge provision pattern increases or decreases in the replies created by hackers. The pattern here should follow the pattern identified by the feature *VPT*, but with different magnitude. We formalize this feature as:

$$VPR_{(v)} = \frac{y_2(v) - y_1(v)}{x_2(v) - x_1(v)} = \frac{y_2(v) - y_1(v)}{2 - 1} = y_2(v) - y_1(v) = a \tag{2.30}$$

with $y_i(v)$ being defined as:

$$y_i(v) = \sum_{\theta \in REP_{(v)}, \theta = [(i-1)*10]+1}^{[(i-1)*10]+10} k(\langle v, \theta, m, t \rangle) \tag{2.31}$$

where $REP_{(v)}$ is the set of sorted replies created by $v$ and $k$ is defined in equation 2.13.

**Velocity of Knowledge Acquisition in the Replies (VAR)**. This feature checks how fast the knowledge acquisition pattern increases or decreases in the replies created by hackers. The pattern here should follow the pattern identified by the feature *VAT*, but with different magnitude. We formalize this feature as:

$$VAR_{(v)} = \frac{y_2(v) - y_1(v)}{x_2(v) - x_1(v)} = \frac{y_2(v) - y_1(v)}{2 - 1} = y_2(v) - y_1(v) = a \tag{2.32}$$

with $y_i(v)$ being defined as:

$$y_i(v) = \sum_{\theta \in REP_{(v)}, \theta = [(i-1)*10]+1}^{[(i-1)*10]+10} l(\langle v, \theta, m, t \rangle) \tag{2.33}$$

where $REP_{(v)}$ is the set of sorted replies created by $v$ and $l$ is defined in equation 2.15.

### *2.5.4 Structural Position*

The set of features within this category belongs to the social network analysis approach and aims to define the hackers' relevance based on their structural position in the networks. This category includes the three following features:

**Degree Centrality (DEC)**. This feature measures the number of direct neighbors connected to a node [143]. As we deal with directed networks, we defined this measure as the number of outgoing edges [143]. According to [112], key-hackers usually present high degree centralities, since each of their many replies produces an outgoing edge. We formalize this feature as:

$$DEC_{(v_i)} = d_i^{out} \tag{2.34}$$

where $d_i^{out}$ is the out-degree of $v_i$.

**Betweenness Centrality (BEC)**. This feature measures the number of shortest paths that pass through a node [143], indicating its importance for the information flow. According to [147], key-hackers usually present high betweenness centralities, since they are very well connected users who often appear in those shortest paths. We formalize this feature as:

$$BEC_{(v_i)} = \sum_{s \neq t \neq v_i} \frac{\sigma_{st}(v_i)}{\sigma_{st}} \tag{2.35}$$

where $\sigma_{st}$ is the number of shortest paths from node $s$ to $t$ and $\sigma_{st}(v_i)$ is the number of shortest paths from node $s$ to $t$ that pass through $v_i$.

**Closeness Centrality (CLC)**. This feature measures how close an individual is to everyone else [143]. As key-hackers have a central position in the networks that shrinks distances to the others, they usually present high closeness centralities. We formalize this feature as:

$$CLC_{(v_i)} = \frac{1}{\bar{l}_{v_i}} \tag{2.36}$$

where $\bar{l}_{v_i} = \frac{1}{n-1} \sum_{v_j \neq v_i} l_{i,j}$ is node $v_i$'s average shortest path length to other nodes and $n$ is the number of nodes.

### *2.5.5 Influence*

The set of features within in this category belongs to the social network analysis approach and aims to identify the level of prestige of hackers. It includes the two following features:

**Eigenvector Centrality (EIC)**. This feature assigns importance to a node if other important nodes are linked to it [143]. According to [91], key-hackers usually present high eigenvector centralities, since they form connections among themselves. We formalize this feature as:

$$EIC_{(v_i)} = \frac{1}{\lambda} \sum_{j=1}^{n} A_{j,i} EIC(v_j) \tag{2.37}$$

where $\lambda$ is a fixed constant, $A_{j,i}$ is the adjacent matrix of the directed graph $G = (V, E)$ and $n$ is the number of nodes.

**Page Rank (PAR)**. As a variant of *EIC*, this feature also checks the quality of the links pointing to a hacker [143]. According to [91], key-hackers often present high page rank, since they are likely to receive more links from other key-hackers. We formalize this feature as:

$$PAR_{(v_i)} = \alpha \sum_{j=1}^{n} A_{j,i} \frac{PAR(v_j)}{d_j^{out}} + \beta \tag{2.38}$$

where $\lambda$, $\alpha$, and $\beta$ are fixed constants, $A_{j,i}$ is the adjacent matrix of the directed graph $G = (V, E)$ and $n$ is the number of nodes.

### *2.5.6 Coverage*

This category of features belongs to the seniority analysis approach and aims to identify the active long-term hackers in the forums. It includes the three following features:

**Interval between User's and Forum's First Posts (IFP)**. This feature checks the time interval between the first post in the forum and the first post of a specific hacker. Previous works [13, 2] argue that founding members are usually key-hackers, being actively involved in the discussions since the beginning. We formalize this feature as:

$$IFP(v) = \sum_{\theta}\sum_{m}\sum_{t} s(\langle v,\theta,m,t\rangle) - \sum_{v'}\sum_{\theta'}\sum_{m'}\sum_{t'} u(\langle v',\theta',m',t'\rangle) \tag{2.39}$$

where $s(\langle v,\theta,m,t\rangle)$ and $u(\langle v',\theta',m',t'\rangle)$ are defined as:

$$s(\langle v,\theta,m,t\rangle) = \begin{cases} t,\ if\ \langle v,\theta,m,t\rangle \in \mathcal{A} \wedge \nexists \langle v,\theta'',m'',t''\rangle \in \mathcal{A},\ s.t.\ t'' < t \\ 0,\ otherwise \end{cases} \tag{2.40}$$

$$u(\langle v',\theta',m',t'\rangle) = \begin{cases} t,\ if\ \langle v',\theta',m',t'\rangle \in \mathcal{A} \wedge \nexists \langle v'',\theta'',m'',t''\rangle \in \mathcal{A}\ ,\ s.t.\ t'' < t' \\ 0,\ otherwise \end{cases} \tag{2.41}$$

**Distinct Days of Postings (DDP)**. This feature checks the hackers' posting frequency. Previous works [13, 148] argue that continuous participants are more likely to be key-hackers, since they are often contributing to the communities. We formalize this feature as:

$$DDP_{(v)} = |Days_{(v)}| \tag{2.42}$$

where $Days_{(v)}$ returns the set of distinct days in which $v$ posted.

**Interval between User's and Forum's Last Posts (ILP)**. This feature checks the time interval between the last post in the forum and the last post of a specific hacker. Previous works [13, 2] argue that key-hackers are usually active in the communities with no fleeting interests. We formalize this feature as:

$$ILP(v) = \sum_{\theta}\sum_{m}\sum_{t} x(\langle v,\theta,m,t\rangle) - \sum_{v'}\sum_{\theta'}\sum_{m'}\sum_{t'} y(\langle v',\theta',m',t'\rangle) \tag{2.43}$$

where $x(\langle v,\theta,m,t\rangle)$ and $y(\langle v',\theta',m',t'\rangle)$ are defined as:

$$x(\langle v,\theta,m,t\rangle) = \begin{cases} t,\ if\ \langle v,\theta,m,t\rangle \in \mathcal{A} \wedge \nexists \langle v,\theta',m',t'\rangle \in \mathcal{A},\ s.t.\ t' > t \\ 0,\ otherwise \end{cases} \tag{2.44}$$

$$y(\langle v',\theta',m',t'\rangle) = \begin{cases} t,\ if\ \langle v',\theta',m',t'\rangle \in \mathcal{A} \wedge \nexists \langle v'',\theta'',m'',t''\rangle \in \mathcal{A}\ ,\ s.t.\ t'' > t' \\ 0,\ otherwise \end{cases} \tag{2.45}$$

## 2.6 Supervised Learning Experiments

This section presents our supervised learning experiments to mine key-hackers. We first introduce how we perform training and testing using four different algorithms, including an optimization metaheuristic and three machine learning methods. Our intention is to verify which algorithms generalize better when estimating user reputation, using the hackers' characteristics learned in one forum to test on another one. Then, we compare the performance of our model under two conditions: 1) when it is trained/tested using the features related to each approach individually and combined; 2) when it is trained/tested using different ranges for the definition of key-hackers.

We use the 25 features engineered as input to the supervised learning algorithms. We compare the algorithms' performance when they use features of content, social network, and seniority analysis individually and combined. To perform that, we leverage the user reputation score to maximize the overlap of two distinct sets of hackers: the $Top_{10\%}$ found with their *Estimated Reputation Score (ERS)* and the $Top_{10\%}$ found with their *Actual Reputation Score (ARS)*. The *ARS* represents the user's reputation informed by the forums, and we want to use this information as our ground truth. This way, we sort the users according to their reputation in descending order, and the $Top_{10\%}$ will represent the key-hackers - for instance, the $Top_{10\%}$ of *Forum 1* are the 431 hackers with the highest *ARS*. The *ERS* is the reputation to be estimated by our algorithms based on the features extracted, and we also want to use the $Top_{10\%}$ to infer who should be the key-hackers. With these both metrics in hands, our goal is to maximize the value of $Overlap_{10\%}$ presented in equation 2.46, which is a metric that provides a measure for user ranking consistency [16].

$$Overlap_{10\%} = \frac{|ERS_{10\%} \cap ARS_{10\%}|}{|ERS_{10\%} \cup ARS_{10\%}|} \tag{2.46}$$

### 2.6.1 Genetic Algorithms

We train and test four different supervised learning algorithms. The first one comprises an optimization metaheuristic inspired by the natural selection process: Genetic Algorithms (GA) [87]. In the training phase, we use this algorithm to perform a linear combination of our 25 features, calibrating the *ERS*'s feature weights in equation 2.47 so that $Overlap_{10\%}$ is maximized. As this approach relies on genetic operators such as *selection*, *crossover*, and *mutation* to produce high-quality solutions to optimization problems [87] (we apply the elitist, two-points, and order-changing methods respectively), we expect it searches through a huge combination of feature weights to find the ones generating the highest value for $Overlap_{10\%}$. Then, we use the calibrated linear system trained in a particular forum to test its performance on a different one, also using the $Overlap_{10\%}$.

$$ERS(v) = \sum_{i=1}^{n} w_i * v_{x_i} \tag{2.47}$$

where $w_i$ is the weight of feature $i$, $v_{x_i}$ is the value of the feature $i$ for user $v$, and $n$ is the set of considered features.

### 2.6.2 Multiple Linear Regression

The second algorithm is a Multiple Linear Regression (MLR) [131]. In the training phase, we want to model the relationship between our dependent variable (reputation) and our 25 independent variables (features). This relationship is modeled using linear predictor functions, whose parameters are estimated from the data to fit a curve that produces the highest value for $Overlap_{10\%}$. Then, we want to use this curve fitted to a particular forum to test its performance on a different one, also using the $Overlap_{10\%}$. Note that the correct order of hackers based on reputation is not required, only the presence of the correct individuals in the $Top_{10\%}$.

### 2.6.3 Random Forests and Support Vector Machines

The next two algorithms comprise classifiers: Random Forests (RF) and Support Vector Machines (SVM) [131]. Here, we define a binary classification problem to identify the individuals belonging to the positive class (key-hackers). Random Forests are an ensemble method that use multiple decision trees for training, outputting the class that is the mode of the classes. Support Vector Machines (SVM) are a discriminative classifier formally defined by a separating hyperplane that gives the largest minimum distance to the training examples. For both classifiers in the training phase, we want to learn the feature values of the $Top_{10\%}$ reputable hackers of a given forum, in order to apply this knowledge to another forum (testing phase) maximizing the value of $Overlap_{10\%}$.

### *2.6.4 Results*

Figure 2.4 presents the performance of the algorithms when they are trained using *Forum 1* and tested using *Forum 2* and *Forum 3*. We detail the performances when the algorithms learn only the features of individual approaches, and when they learn all the features combined (hybrid approach).

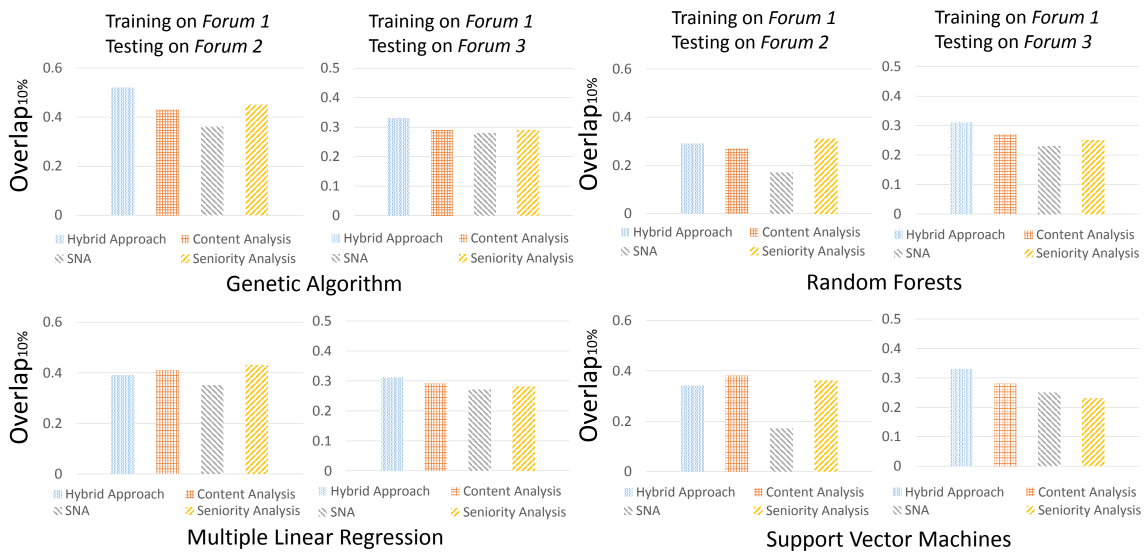

Fig. 2.4: $Overlap_{10\%}$ Performance when Algorithms are Trained on *Forum 1* and Tested on *Forum 2*/*Forum 3*.

We observe 5 cases when the hybrid approach obtains the best performance, while 1 and 2 cases are verified for content and seniority analysis respectively. The highest value for

$Overlap_{10\%}$ when testing on *Forum 2* (0.52) is achieved by Genetic Algorithms using the hybrid approach. This result implies that more than half of the $Top_{10\%}$ reputable hackers were identified, which for this forum represents around 121 users. Also, the highest value for $Overlap_{10\%}$ when testing on *Forum 3* (0.33) is achieved by using Genetic Algorithms and SVM using the hybrid approach. This result implies that more than one third of the $Top_{10\%}$ reputable hackers were identified, which for this forum represents around 92 users. Note these performances correspond to find only 10% of the hackers (those with the highest reputation), which represents a strict filter of users.

Figure 2.5 presents the performance of the algorithms when they are trained using *Forum 2* and tested using *Forum 1* and *Forum 3*. We observe 5 cases when the hybrid approach obtains the best performance, while 1 case is verified for each of the other approaches. The highest value for $Overlap_{10\%}$ when testing on *Forum 1* (0.43) is achieved by Genetic Algorithms using the hybrid approach. This result implies that almost half of the $Top_{10\%}$ reputable hackers were identified, which for this forum represents around 186 users.

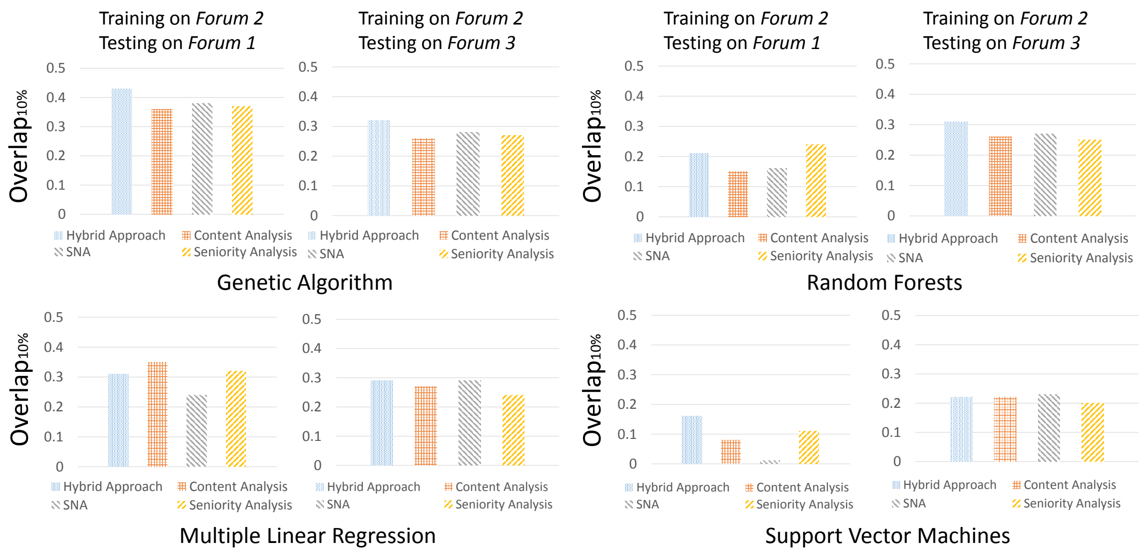

Fig. 2.5: $Overlap_{10\%}$ Performance when Algorithms are Trained on *Forum 2* and Tested on *Forum 1*/*Forum 3*.

In addition, the highest value for $Overlap_{10\%}$ when testing on *Forum 3* (0.32) is achieved by Genetic Algorithms and Random Forests using the hybrid approach. This result implies that almost one third of the $Top_{10\%}$ reputable hackers were identified, which for this forum represents around 88 users.

Figure 2.6 shows the algorithms' performance when they are trained using *Forum 3* and tested using *Forum 1* and *Forum 2*. We note 5 cases when the hybrid approach has the best performance, while 1 and 2 cases are verified for content/seniority and social network analysis respectively. The highest value for $Overlap_{10\%}$ when testing on *Forum 1* (0.45) is achieved by Genetic Algorithms using the hybrid approach. This result implies that almost half of the $Top_{10\%}$ reputable hackers were identified, which for this forum represents around 194 users. Also, the highest value for $Overlap_{10\%}$ when testing on *Forum 2* (0.5) is achieved by Genetic Algorithms using the hybrid approach. This result implies that half of the $Top_{10\%}$ reputable hackers were identified, which for this forum represents around 121 users.

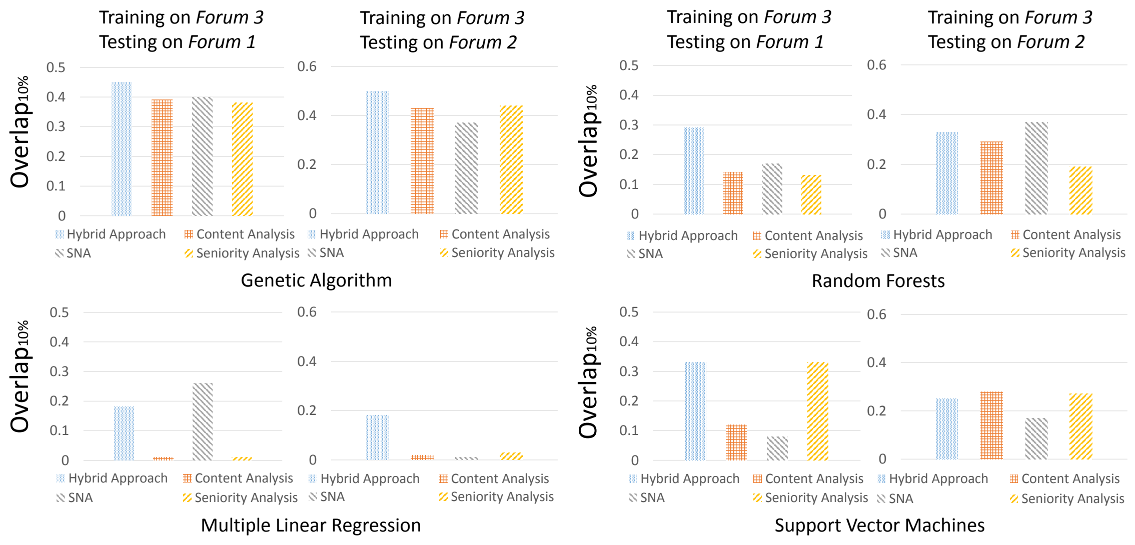

Fig. 2.6: $Overlap_{10\%}$ Performance when Algorithms are Trained on *Forum 3* and Tested on *Forum 1*/*Forum 2*.

These results show that the hybrid approach is preferable comparing to the individual ones, specially if used by Genetic Algorithms. Overall, the generalization of the model is satisfying, since we are able to retrieve a considerable part of the existing key-hackers in all situations analyzed.

**Varying the Overlap**. In order to observe how the results change according to the fraction of users that represent the key-hackers, we test different values for $Overlap_{X\%}$. The idea is to cover different zones for the identification of key-hackers, including $Overlap_{1\%}$, $Overlap_{5\%}$, $Overlap_{10\%}$, and also what we denominate $Overlap_{10}$, which means only the top 10 reputable hackers in the forums. Figure 2.7 presents the performance of the four algorithms with the exact same previous setting, except that we only consider the hybrid approach. We include a random key-hacker identification approach for comparison purposes.

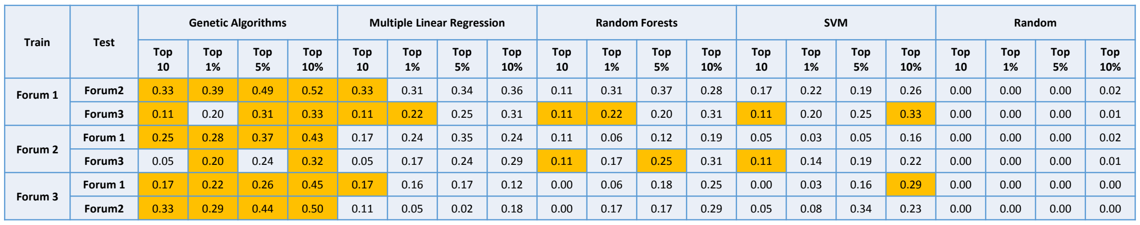

| Train | Test | Genetic Algorithms | | | | Multiple Linear Regression | | | | Random Forests | | | | SVM | | | | Random | | | |
|---|---|---|---|---|---|---|---|---|---|---|---|---|---|---|---|---|---|---|---|---|---|
| | | Top 10 | Top 1% | Top 5% | Top 10% | Top 10 | Top 1% | Top 5% | Top 10% | Top 10 | Top 1% | Top 5% | Top 10% | Top 10 | Top 1% | Top 5% | Top 10% | Top 10 | Top 1% | Top 5% | Top 10% |
| Forum 1 | Forum2 | 0.33 | 0.39 | 0.49 | 0.52 | 0.33 | 0.31 | 0.34 | 0.36 | 0.11 | 0.31 | 0.37 | 0.28 | 0.17 | 0.22 | 0.19 | 0.26 | 0.00 | 0.00 | 0.00 | 0.02 |
| | Forum3 | 0.11 | 0.20 | 0.31 | 0.33 | 0.11 | 0.22 | 0.25 | 0.31 | 0.11 | 0.22 | 0.20 | 0.31 | 0.11 | 0.20 | 0.25 | 0.33 | 0.00 | 0.00 | 0.00 | 0.01 |
| Forum 2 | Forum 1 | 0.25 | 0.28 | 0.37 | 0.43 | 0.17 | 0.24 | 0.35 | 0.24 | 0.11 | 0.06 | 0.12 | 0.19 | 0.05 | 0.03 | 0.05 | 0.16 | 0.00 | 0.00 | 0.00 | 0.02 |
| | Forum3 | 0.05 | 0.20 | 0.24 | 0.32 | 0.05 | 0.17 | 0.24 | 0.29 | 0.11 | 0.17 | 0.25 | 0.31 | 0.11 | 0.14 | 0.19 | 0.22 | 0.00 | 0.00 | 0.00 | 0.01 |
| Forum 3 | Forum 1 | 0.17 | 0.22 | 0.26 | 0.45 | 0.17 | 0.16 | 0.17 | 0.12 | 0.00 | 0.06 | 0.18 | 0.25 | 0.00 | 0.03 | 0.16 | 0.29 | 0.00 | 0.00 | 0.00 | 0.00 |
| | Forum2 | 0.33 | 0.29 | 0.44 | 0.50 | 0.11 | 0.05 | 0.02 | 0.18 | 0.00 | 0.17 | 0.17 | 0.29 | 0.05 | 0.08 | 0.34 | 0.23 | 0.00 | 0.00 | 0.00 | 0.00 |

Fig. 2.7: Analysis of Algorithms' Performance Using Different Values for $Overlap_{X\%}$.

The highlighted cells of Figure 2.7 correspond to the highest values of $Overlap_{X\%}$ computed among all the algorithms analyzed. We observe that Genetic Algorithms have the best performances in 87.5% of the cases, since they are able to work under very strict search conditions: the number of individuals to be filtered is considerably low and the search space is very large. Finally, we show in Figure 2.8 the curves of $Overlap_{X\%}$ for all implemented algorithms, comparing the performances according to the forums used for training and test. As verified, Genetic Algorithms produce a superior fit. We believe the characteristic of this strategy - population of candidates searching in multiple directions simultaneously - produces more adapted solutions, avoiding local optima and overfitting. This condition makes this optimization metaheuristic suitable to the key-hacker identification problem, leading opportunities for evolutionary algorithms to be considered in cybersecurity research.

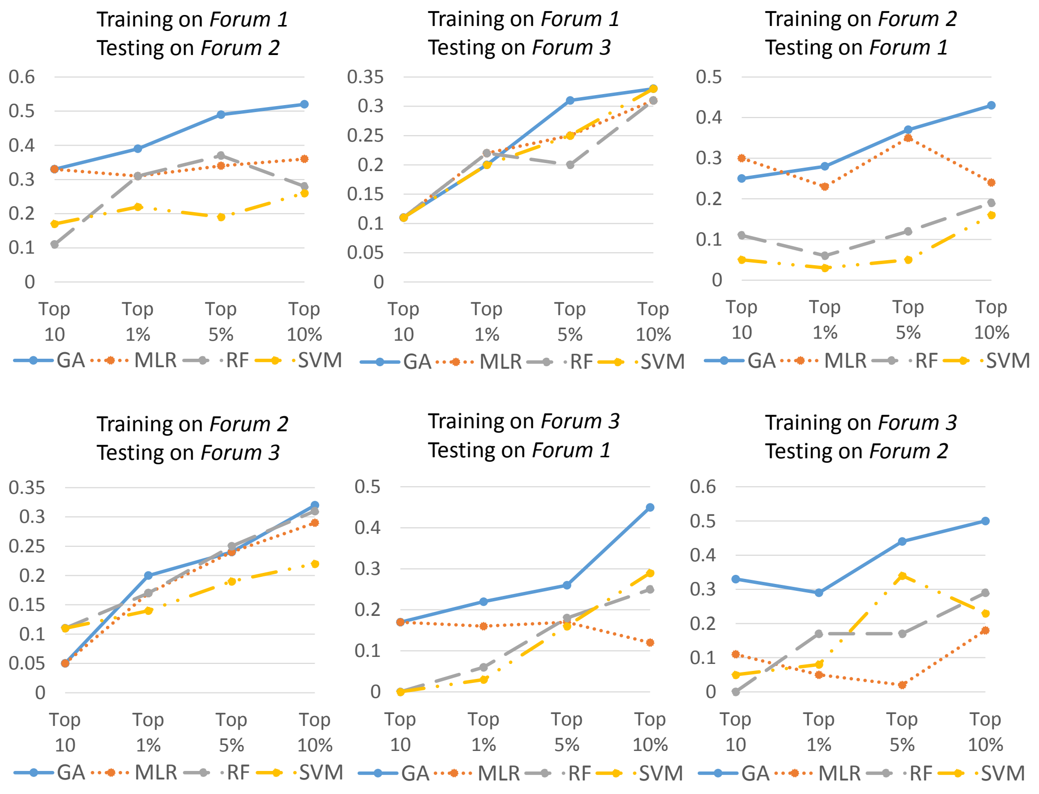

Fig. 2.8: Comparison Between the $Overlap_{X\%}$ Curves.

## 2.7 Related Work

Different works have addressed the key-hacker identification problem in the last years. Abbasi et al. [2] proposed a framework to identify expert hackers in web forums based on content-mining. First, the authors represented each user with three categories of features: cybercriminal assets, specialty lexicons, and forum involvement. Then, they profiled the users into four groups based on their specialties: black market activists, founding members, technical enthusiasts, and average users. Analyzing the hackers' interactions, they noted the average users (86% of the total) were participants that did not actively engage in the community, being the other groups constituted by key-hackers. Later, Zhang et al. [148] also used a content-mining approach on a hacking forum to analyze post orientations regarding knowledge transfer. Knowledge acquisition and knowledge provision were noted as the patterns to construct user profiles, classified by the authors into four ordinal types: guru, casual, learning, and novice hackers. They found that guru hackers act as key knowledgeable and respectable members in the communities, increasingly acting as knowledge providers. In a sequence, Fang et al. [38] developed a framework with a set of topic models for extracting popular topics, tracking topic evolution, and identifying key-hackers with their specialties. Using Latent Dirichlet Allocation (LDA), Dynamic Topic Model (DTM), and Author Topic Model (ATM), they identified five major popular topics, trends related to new communication channels, and key-hackers in each expertize area.

Using a different approach, Seebruck proposed a weighted arc circumplex model to capture hacker motivations [115]. The author created a hacker typology based on 5 motivations: recreation, prestige, revenge, profit, and ideology, and also based on 8 levels of expertise: novices, crowdsourcers, punks, hacktivists, insiders, criminals, coders, and cyber warriors. Then, the model should determine (as no experiments were performed) the likelihood of an organization being targeted by a certain type of hacker. Samtani and Chen [112] performed social network analysis to identify key-hackers on hacking forums. They analyzed users' interactions by leveraging metrics such as network diameter and average path length, and found the importance of users to their communities using centrality measures. Also, Zhang and Li performed survival analysis using Cox proportional hazard regression model to examine what generates a high reputable hacker on online forums [147]. They found that users should reply detailed posts and broaden their interests in multiple topics.

In all these works, we noted the authors did not fully explore a hybrid model to find key-hackers online, considering the advantages of different approaches. In addition, there is still a lack of a validation method, which makes the results of these previous works not comparable. Here, we take the next steps to fill these two gaps, proposing a hybrid model to identify key-hackers on darkweb forums and a systematic method to validate the results.

## 2.8 Summary

In this Chapter, we address the key-hacker identification problem on darkweb forums using a hybrid approach that combines content, social network, and seniority analysis. We start by showing how different algorithms (specially the Genetic Algorithms) perform better when all the 25 engineered features are used together, highlighting that a hybridization of approaches improve the results. Then, we demonstrate that our model is able to generalize, learning features in one particular forum that can be applied to another one. This generalization is evaluated by leveraging the user reputation score to systematically cross-validate the key-hackers identified, providing a strategy to find these users in environments that do not offer a reputation system or offer a deficient one. Although improvements are necessary in this area, we explore in this work some ideas to pavement the road - including a comparison between genetic and machine learning algorithms when they use our predictive model to identify the high skilled and influential users on malicious hacker forums: the key-hackers. These insights offer security researchers an alternative strategy for predicting cyber-attacks: find the key-hackers first, and consequently, their emerging cyber threats.

Chapter 3

# TEMPORAL ANALYSIS OF INFLUENCE TO PREDICT USER ADOPTION ON SOCIAL MEDIA

## 3.1 Introduction

Hacker communities are continually evolving. Due to the social influence effects, values are transmitted from one person to another (see examples in economy [74], psychology [4], sociology [18, 26], business [33], public health [22], politics [20]), and this behavior is also observed among malicious hackers [42, 124, 100, 88]. Holding acknowledged reputation, key-hackers generally use online platforms to advertize exploits, vulnerabilities, techniques, code samples, targets, and also to recruit individuals for malicious campaigns [55, 12], attracting lower-level individuals who aim to quickly improve their skills. Those influential activities not only expand the key-hackers' networks, bringing like-minded collaborators and learners, but also help them to increase their revenue. Therefore, cybersecurity can benefit with the study of user adoption behavior online, using it as crowdsourced sensor to gain insight about future users' activities that may lead to cyber-attacks. Consider for instance, the prediction of hacktivist campaigns on social media, where notorious hacking collectives such as Anonymous and LizardSquad often recruit individuals for attacks [25, 104]. This task would be feasible if we could anticipate the users joining the campaign, leveraging for that the influence produced by key-hackers who mainly form those malicious groups.

In this Chapter, we use this insight to investigate whether microblog users will adopt a new behavior given the influential activities produced by their peers, a technique that might reveal the potential expansion degree of the key-hackers' networks. We introduce two simple time constraints to improve standard influence measures and consequently adoption prediction performance: *Susceptible Span* and *Forgettable Span*. *Susceptible Span* ($\tau_{sus}$) refers to the interval when people are able to receive social signals from their neighbors, "blinding" these individuals to actions coming from connections that are not interesting anymore. *Forgettable Span* ($\tau_{fos}$) refers to the interval when people are able to remember the actions performed by their neighbors, making these actions be eventually forgotten due to a natural human brain limitation. Intuitively, the proposed time constraints specify dynamic graphs from where influence can be estimated more correctly. Figure 3.1 illustrates this process for a given behavior (e.g. the adoption of a malicious exploit advertized by a group of hackers online).

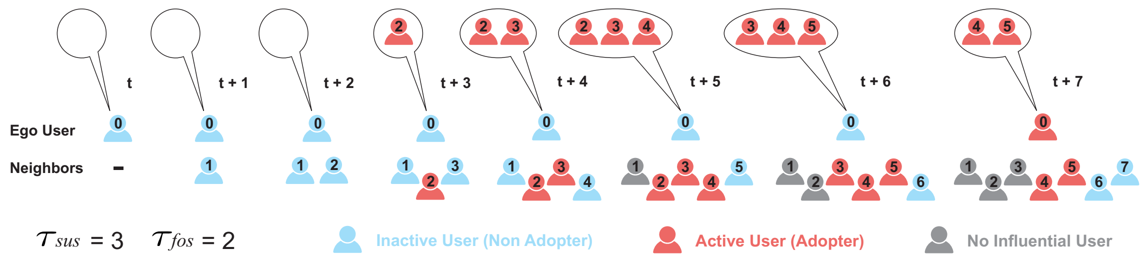

Fig. 3.1: Effects of *Susceptible Span* and *Forgettable Span* for Estimating Social Influence.

At time $t$, node 0 has no neighbors. At $t + 1$, node 0 has one neighbor (node 1, shown beneath node 0). From this moment, node 0 will be aware of (visualize) node 1's future adoptions. At $t + 2$, node 0 has two neighbors, nodes 1, 2, extending its awareness to the adoptions of both users. This cumulative process continues until $t + 4$, since $\tau_{sus}$ was defined as 3. After this time, node 1 is a node 0's neighbor who has its new adoptions no more visualized by node 0, which makes node 0 not be influenced by them. A similar process happens with another node 0's neighbor (node 2) from $t + 6$. The illustration also shows the node 0's memory inside the balloons. As we made $\tau_{fos}$ = 2, node 2's adoption at $t + 3$ fades away from node 0's memory after $t + 5$, when node 0 is no longer influenced by it. The same process happens with node 3's adoption after $t + 6$. Therefore, at $t + 7$, node 0 is activated only because of the influence of nodes 4 and 5, since: 1) these 2 neighbors had their adoptions visualized by node 0 in the past; 2) their adoptions are still in node 0's memory at t+7.

By conducting an engineering study that investigates retweet networks from Twitter and Sina Weibo datasets, we tune those two parameters while we examine the correlation between standard measures of social influence and the probability of adoption as well as the ability to predict adoption, estimating the real susceptibility and influence that microblog users are dynamically subjected to. Although there are limitations about using retweets to analyze influence phenomenon, we observe a better ability to measure influence and predict adoption when the time constraints are applied. For example, for a simple count of the "active" neighbors, we obtain up to a 518.75% improvement in correlation with the probability of adoption, observing comparable results for the other measures analyzed. Further, when comparing to recent machine learning techniques that aim to predict adoption, F1 score improves up to 18.89%. Here, we summarize the main contributions of this work:

- We introduce a framework to analyze the effects of $\tau_{sus}$ and $\tau_{fos}$ while we measure social influence, considering multiple network arrangements produced by different thresholds of user activity;
- We investigate the correlation of 10 standard influence measures with probability of adoption analyzing 144 combinations of $\tau_{sus}$ and $\tau_{fos}$, showing improvements of up to 518.75%;
- We examine the performance of contemporary methods [147, 40, 51] for adoption prediction, demonstrating how our model outperforms them in up to 18.89% and how they can have their own performance improved up to 10.57% when integrating $\tau_{sus}$ and $\tau_{fos}$ into their models.

The remaining of this Chapter is structured as follows. Section 3.2 shows the formalization of our framework for considering the proposed time constraints when measuring social influence. In Section 3.3, we formalize the adoption prediction problem. Section 3.4 presents the experimental setup to create samples. Section 3.5 introduces the influence measures and their correlation with adoption probability. Section 3.6 details the classification experiments and results. Section 3.7 presents the related work. Finally, section 3.8 summarizes the Chapter.

## 3.2 Framework for Consideration of Time Constraints

In this section, we describe the notations of this work and how we produce our dynamic social networks. We denote a set of users $V$ and a set of connections $E$ as the nodes and edges in a directed social graph $G = (V, E)$. In addition, we define a set of topics (hashtags) $\Theta$ and a set of discrete time points $T$. We will use the symbols $v, \theta, t$ to represent a specific node, topic, and time point. To define the active nodes (adopters) w.r.t $\theta$, we use a similar adoption concept of [147, 144, 149, 141, 146]. According to these works, an adopter of $\theta$ is as a user who retweeted a tweet with $\theta$, and users can only adopt a topic by retweeting it from previously active neighbors. Note that this adoption concept might produce some late user activations, which happen when users tweet a hashtag before retweeting the same hashtag from someone else. However, we show in our experiments how social influence is still captured in its great magnitude, probably because of the ephemeral aspect of the hashtags [106, 71, 57]. This ephemerality minimizes the time interval between a possible real activation (tweet) and the late activation (retweet), reducing the loss of our predictive model.

This way, we denote an activity log $\mathcal{A}$ - containing all retweets performed by users - as a set of tuples of the form $\langle v_1, v_2, \theta, t\rangle$, where $v_1, v_2 \in V$. It describes that "$v_1$ adopted $\theta$ retweeting $v_2$ at time $t$", creating a directed edge $(v_1, v_2) \in E$ which makes $v_2$ a neighbor of

$v_1$ but not vice-versa. The intuition behind this edge is that $v_1$, for a limited time, will be aware of (visualize) future actions of $v_2$, and then can be influenced by $v_2$ with respect to a new $\theta$' that eventually $v_2$ adopts after $t$. Based on this definition, we formalize the set of neighbors of a node $v$ at time $t$ as:

$$\mathcal{H}_{v,t} \quad = \{v' | \quad \exists \langle v, v', \theta, t' \rangle \in \mathcal{A},\ s.t.\ t' \leq t\} \tag{3.1}$$

Figure 3.2 illustrates this neighborhood creation process. In panel (a), user 0 retweeted user 1 for the first time, at $t$. In panel (b), user 0 retweeted user 2 for the first time, at $t + 1$. Finally, in panel (c), user 0 retweeted user 3 for the first time, at $t + 2$. The topic of those retweets is indifferent for this analysis. At time $t + 2$, user 0 has 3 neighbors, or three outgoing neighbors specifically: user 1, user 2, and user 3. Although the edges are created from user 0 to user 1, user 2, and user 3, the possible influence of future actions (social signals) flows from these three users to user 0, but not vice-versa.

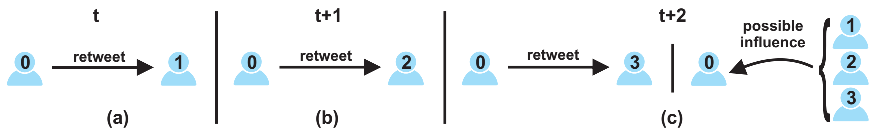

Fig. 3.2: Neighborhood Creation Process.

After defining the users' neighborhood, we integrate into our model the two proposed time constraints: *Susceptible Span* ($\tau_{sus}$) and *Forgettable Span* ($\tau_{fos}$). Due to their different effects, the social signals coming from the neighborhood of a user change over time, affecting the influence measures that result in this user's decision to adopt a particular topic. With this insight, we formalize the set of neighbors of $v$ that can have their actions visualized by $v$ at time $t$ as:

$$\eta_{v,t} \quad = \{v' | \quad \exists \langle v, v', \theta, t' \rangle \in \mathcal{A},\ s.t.\ t' \leq t\ and\ \ t - t' \leq \tau_{sus}\} \tag{3.2}$$

$\eta_{v,t}$ is a subset of $\mathcal{H}_{v,t}$ that contains the neighbors of $v$ whose adoptions since $t - \tau_{sus}$ until $t$ will be presented to $v$. After $t' + \tau_{sus}$, the adoptions of $v'$ will not be visualized by $v$ and therefore will not influence it. Figure 3.3 illustrates this process, considering the retweets shown in Figure 3.2.

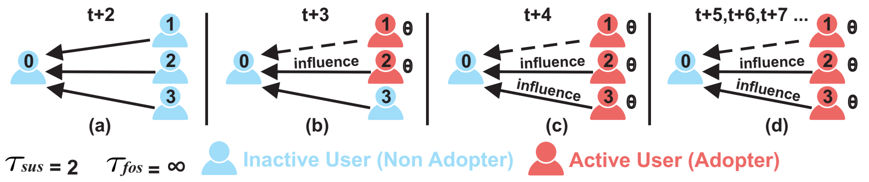

Fig. 3.3: Effect of Susceptible Span.

As we made in this illustration $\tau_{sus} = 2$, user 0 will be aware of (visualize) user 1, user 2, and user 3 activations from $t$ until $t + 2$, from $t + 1$ until $t + 3$, and from $t + 2$ until $t + 4$, respectively. In panel (a), at $t + 2$, none of the user 0's neighbors activates. In panel (b), at $t + 3$, two of them activate w.r.t $\theta$, user 1 and user 2. However, user 0 cannot visualize the actions of user 1 from this time, since $\tau_{sus}$ avoids that. In panel (c), at $t + 4$, one more of the user 0's neighbors activates w.r.t $\theta$ (user 3). This way, only the adoptions of users 2 and 3 are visualized by user 0, becoming a possible source of influence w.r.t $\theta$ with no time limit, since $\tau_{fos}$ was defined in this example as $\infty$. The idea behind this constraint is to "blind" people from actions coming from out-of-date connections.

In Twitter for instance, after a user $v$ starts following a user $u$, all activity of $u$ is automatically presented to $v$. However, we believe this static relationship does not explain users' retweeting behavior as expected. After a period without interacting with $u$, $v$ can lose interest in the relationship, no longer checking updates from $u$ (as also suggested by [21, 141]). We want to approximate this behavior in our model using $\tau_{sus}$. In addition, as influential actions do not last forever [145, 144], we formalize the active neighbors of $v$ that can influence it to adopt $\theta$ at time $t$ as:

$$\eta^{\theta}_{v,t} = \{v' | \quad \exists\langle v, v', \theta', t'\rangle \in \mathcal{A} \textit{ and } \exists\langle v', v'', \theta, t''\rangle \in \mathcal{A}, \textit{ s.t. } t'' - t' \leq \tau_{sus} \quad \textit{and}$$
$$t - t'' \leq \tau_{fos} \textit{ and } t' \leq t'' \leq t\} \qquad (3.3)$$

$\eta^{\theta}_{v,t}$ is a subset of $\mathcal{H}_{v,t}$ that contains the relevant users to be found in this work: the ***influential active neighbors*** of users. As verified in the equation, $v'$ comprehend the neighbors of $v$ who had their adoptions at $t''$ w.r.t $\theta$ visualized by $v$ (considering here $\tau_{sus}$). Therefore, the adoptions of $v'$ are influencing $v$ to adopt $\theta$ at or after $t''$. Nevertheless, $\tau_{fos}$ guarantees that after $t'' + \tau_{fos}$, the fact that $v'$ adopted $\theta$ is forgotten by $v$, with $v'$ no more influencing $v$ in terms of $\theta$. Figure 3.4 illustrates this process considering the retweets of Figure 3.2.

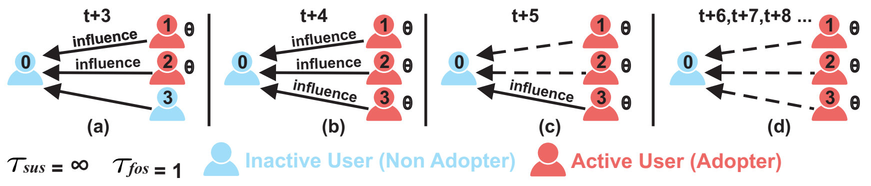

Fig. 3.4: Effect of Forgettable Span.

As we made in this illustration $\tau_{fos} = 1$, user 0 will be influenced by the visualized activations of its neighbors for only 1 time unit. In panel (a), at $t + 3$, two of the user 0's neighbors activate, user 1 and user 2. User 0 is able to visualize both activations (as we defined in this example $\tau_{sus}$ as $\infty$), being influenced by them from $t + 3$ on. However, the influence of those activations disappears after $t + 4$, due to the effects of $\tau_{fos}$. In panel (b), at $t + 4$, one more of the user 0's neighbors activates, user 3. The same influence process happens for this activation, but now from $t + 4$ until $t + 5$. This way, from $t + 6$ on, none of the activations of users 1, 2 and 3 are still influencing user 0 to adopts $\theta$.

In Twitter, once a user adopts a hashtag, all its followers can find it in their timelines. However, as pointed by [40], the hashtag fades away after some time, making it more difficult to be remembered in the future. We want to approximate this behavior in our model using $\tau_{fos}$. Our intention with both time constraints is to mimic the dynamics of online social networks, aiming to better measure the social influence produced by the set of influential active neighbors of users.

**Conditions for Social Influence**. Multiple works argue that there exist three main conditions that prompt users to perform an action - such as a repost - in online social networks [51, 141]:

- Condition 1: users can be influenced by their friends and family members;
- Condition 2: users can be affected by some external event(s), out of their immediate neighborhood (1 degree of separation);
- Condition 3: users can be very active, doing things without influence. These users are often considered in the literature as innovators [138, 39].

In this work, we focus on modeling and learning the influence observed just in condition 1. Given only social network data, influence in condition 2 is hard to be measured, and user actions conducted because of condition 3 are basically unpredictable.

In the social sciences, there is a standing debate over the primacy of *peer influence* or *homophily* in shaping human behavior [143, 120]. Peer influence is the process in which one influences the other's decision, making the influenced node similar to the influential one. Homophily is realized when similar individuals become friends due to their high similarity. We believe that homophily is more related to conditions 2 and 3, while peer influence is more related to condition 1. This assumption makes retweets a natural indicator to accomplish our goal since they overall bound the neighborhood of users, limiting the choices and opportunities available in the networks.

## 3.3 Problem Formalization

Given the set of activities (retweets) of a user $v$ that belong to $\mathcal{A}$, and also the set of activities of its neighbors that belong to $\mathcal{A}$ w.r.t $\theta$, the social influence measurements $x^{\theta}_{v,t}$ can be calculated based on its corresponding set $\eta^{\theta}_{v,t}$. The adoption prediction problem is defined as: given the features $x^{\theta}_{v,t}$, the goal is to predict the class label $y^{\theta}_{v,t}$. This class label states if $v$ will adopt or not the hashtag $\theta$ until time $t$.

## 3.4 Experimental Setup

This section details our datasets, how we collect samples using different values for the time constraints, which types of filters of users' activity are applied, and how we measure the correlation of our features with the probability of adoption. The features included in the samples will be introduced in the next section.

### *3.4.1 Microblogs Dataset*

Table 3.1 presents the statistics of the two datasets used in this work. The first one provided by [140] contains a sample of retweets made on Twitter from March 24 to April 25, 2012, offering us the following information regarding each retweet: 1) the pair of users, 2) hashtag(s), and 3) timestamp. In this dataset, there might be multiple sources (tweets) including the analyzed hashtag considered for adoption, and all of these innovators can be retweeted by other users.

The second dataset provided by [145] contains a sample of retweets made on Sina Weibo from October 10 to November 11, 2012, offering the following information to each retweet: 1) the pair of users and 2) timestamp. Although this dataset does not provide the hashtag information, it does provide a unique identification number for all posted messages,

Table 3.1: Statistics of the Datasets.

| Twitter | | Sina Weibo | |
|---|---|---|---|
| Retweets | 1,687,700 | Retweets | 2,553,588 |
| Number of users retweeting | 314,756 | Number of users retweeting | 601,769 |
| Number of users retweeted | 251,342 | Number of users retweeted | 10,539 |
| Number of distinct users | 366,291 | Number of distinct users | 605,622 |
| Number of distinct hashtags | 226,490 | Number of distinct hashtags | 28,645 |

including tweets and retweets. Then, we use this number to simulate a hashtag, adding it to the original message (tweet) and all its corresponding retweets. In this scenario, there is only one source (tweet) including the analyzed hashtag considered for adoption, and therefore, there is only one innovator.

Figure 3.5 shows the histogram of the number of retweets over users in both datasets. The first distribution (a) fits a power-law with $p_k \approx k^{-1.8}$ while the second distribution (b) fits a power-law with $p_k \approx k^{-1.7}$, where $k$ represents the number of retweets.

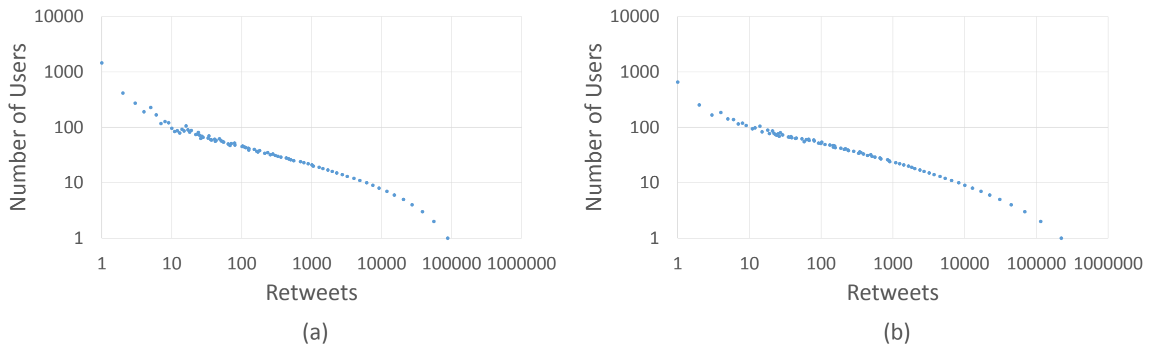

Fig. 3.5: Histogram of the Number of Retweets Over Users in Log-Log Scale for (a) Twitter, (b) Sina Weibo.

### *3.4.2 Sampling*

Following previous works that avoided the problem of imbalanced datasets [145], we create balanced sets of samples for our experiments. We use a 1:1 ratio strategy to avoid bias in the samples created. According to this strategy, for a given activity $\langle v, v_2, \theta, t\rangle$ which will generate a positive sample using $v$, we create a negative sample uniformly getting a user $v'$ from the set:

$$\left\{v' | v_1 \in \eta^{\theta}_{v,t} \wedge v_1 \in \eta^{\theta}_{v',t} \wedge \langle v', v_3, \theta, t'\rangle \notin \mathcal{A}, \forall v_3 \in \eta^{\theta}_{v',t}, \forall t' \leq t\right\} \tag{3.4}$$

where $v_1$ is the influential active neighbor of $v$ who first adopted $\theta$.

This set includes all users under influence of $v_1$ w.r.t $\theta$ at $t$ (considering the time constraints) who did not adopt $\theta$ before or at time $t$. Thus, we create $\langle v', v_1, \theta, t\rangle$ as the negative sample for $\langle v, v_2, \theta, t\rangle$ (our positive sample). We choose $v_1$ so that more information can be collected during the interval between its activation and $t$ (the time when $v$ activates). Also, we keep the same timestamp $t$ for the positive sample $v$ and its negative counterpart $v'$, allowing them to have approximately the same amount of time to accumulate social influence. Note that positive and negative samples should have at least one active neighbor $(v_1)$ to be considered in the sampling process.

Figure 3.6 illustrates this process. Although both time constraints are applied during sampling, we eliminate them here only to facilitate comprehension. User $v$ is a positive sample, since it activates w.r.t $\theta$ at $t$, influenced by 4 of its 6 neighbors. As our model needs a corresponding negative sample, we first look for another user who did not adopt $\theta$ until $t$. However, this user should be, before $t$, also under the influence of the user $v$'s neighbor who first adopted $\theta$, in this case, user $v_1$. This illustration shows that user $v'$ satisfies all these requirements, since it did not adopt $\theta$ until $t$, and it was under the influence of user $v_1$

before this time (at total, user $v'$ was being influenced by 2 of its 6 neighbors w.r.t $\theta$ at $t$). Thus, user $v'$ can be chosen as a negative sample of user $v$. We believe this 1:1 ratio strategy reduces the likelihood of producing bias in the sampling process, providing a reasonable method to sample users for our model.

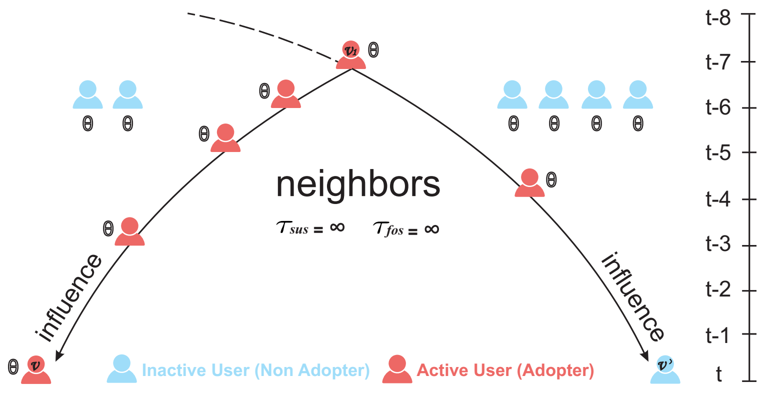

Fig. 3.6: Sampling Process.

### *3.4.3 Filters of User Activity*

We apply the three filters of user's activity presented in Table 3.2 to exclude users with less activity than a certain threshold, as their behaviors are hardly explainable by social influence measures [40, 21] [1] . We follow the researchers' settings done in [141], who defined that microblogs users present a minimum activity if they tweet 10-200 per week. Thus, considering that our both datasets comprise 30 days, we make our users retweet on average at least 15 times per week, or roughly 60 times per month (filter $R60$). We also use the lower bound value of user activity suggested by [141] (40 tweets per month) to create our second filter of distinct hashtags ($H40$). Finally, we use a value of 0.5 for the influenciability score proposed by Goyal et al. at [51]. This score is calculated dividing the number of reposts for which there is evidence a user $v$ was influenced, by the total number

[1]Without those filters, most of the predictions would be "no adoption", since a great part of users do not interact with others.

of reposts performed by $v$. We use a threshold of one active neighbor to claim for evidence of influence. According to Goyal, users with a high influenciability score may exhibit a high likelihood of being influenced by their neighbors, and we want to capture this behavior filtering out individuals who half of the time are influenced by someone. In summary, we want to demonstrate how the proposed framework is robust to various types of bias in data, analyzing dynamic social graphs created using three filters of user activity. Note how after applying the filters, we still have more than 1,000 users for each network to be considered in our model.

Table 3.2: Filters of Users' Activity.

| Description | Threshold | Label | Remaining users retweeting | |
|---|---|---|---|---|
| | | | Twitter | Sina Weibo |
| Minimum Number of Retweets | 60 | $R60$ | 1,246 | 1,218 |
| Minimum Number of Hashtags | 40 | $H40$ | 1,128 | 2,462 |
| Minimum Influenciability Score | 0.50 | $I50$ | 1,094 | 2,004 |

### 3.4.4 Correlation Between Influence Measures and Adoption Probability

To analyze the quality of our social influence measures computed with and without the time constraints, we study how they correlate with the probability of adoption. For this task, we use the Pearson correlation coefficient ($r$) [34], which indicates the degree of linear dependence between two variables: ($x$ and $y$). This metric $r_{xy} = 1$ is obtained when $y_i = ax_i + b$ for all ($x_i$,$y_i$), where $a > 0$, while $r_{xy} = -1$ is obtained when $y_i = ax_i + b$ for all ($x_i$,$y_i$), where $a < 0$. When $r_{xy} \in (-1, 1)$, it indicates the degree of linear dependence between the variables, with values close to zero showing lower correlation. We want to understand how the correlation coefficient varies when we make $\tau_{sus}, \tau_{fos} \in$

$\{8, 16, 24, 48, 72, 96, 120, 144, 168, 336, 504, 720\}(hours)$, so that we can identify the time constraints trade-off which produces high-quality social influence measurements (high positive correlation with probability of adoption). For $n$ samples, the Pearson's correlation coefficient is calculated as [105]:

$$r_{xy} = \frac{n \sum x_i y_i - \sum x_i \sum y_i}{\sqrt{n \sum {x_i}^2 - (\sum x_i)^2} \sqrt{n \sum {y_i}^2 - (\sum y_i)^2}} \tag{3.5}$$

## 3.5 Influence Measures

In this section, we describe the 10 measures we use to estimate the influence in the active neighborhood of users in our both datasets. We leverage those measures to recognize the different structural arrangements in this zone that can affect a user's decision to adopt or not a certain topic. For each measure, we first give a formal definition based on the activity $a = \langle v, v', \theta, t \rangle$ by which we create the sample. Then, we compare the Pearson correlation coefficient of all possible 144 combinations of $\tau_{sus}$ and $\tau_{fos}$ analyzed with the situation when the time constraints are not applied, plotting the result values using heat maps. The cell in the right lower corner is always with value zero, as the pair $(\tau_{sus}, \tau_{fos}) = (720, 720)$ is equivalent to applying no time constraints (both datasets duration comprehends 1 month or 720 hours). The other cells show the gain (in red color) or loss (in blue color) of correlation coefficient according to:

$$r_{xy}(gain\_loss) = \frac{r_{xy} - r'_{xy}}{|r'_{xy}|} \times 100\% \tag{3.6}$$

where $r_{xy}$ is computed with $(\tau_{sus}, \tau_{fos}) \neq (720, 720)$, while $r'_{xy}$ is computed with $(\tau_{sus}, \tau_{fos}) = (720, 720)$.

We opt to do the correlation gain analysis to show the significance of applying the time constraints. Thus, readers can easily observe which combinations of $\tau_{sus}$ and $\tau_{fos}$ improve the probability of influence for each measure analyzed, something that would be much harder to be visualized if we had shown only the individual correlation values, for instance.

Table 3.3 presents how we group the 10 social influence measures into 7 distinct categories created according to their particular characteristics. We discuss each category and influence measure in the following.

Table 3.3: Social Influence Measures.

| Category | Description | Code |
|---|---|---|
| 01 - Connectivity | 01 - Number of Influential Active Neighbors | NAN |
| | 02 - Personal Network Exposure | PNE |
| 02 - Temporal | 03 - Continuous Decay of Influence | CDI |
| 03 - Recurrence | 04 - Previous Reposts | PRR |
| 04 - Transitivity | 05 - Closed Triads | CLT |
| | 06 - Clustering Coefficient | CLC |
| 05 - Centrality | 07 - Hubs | HUB |
| 06 - Reciprocity | 08 - Mutual Reposts | MUR |
| 07 - Structural Diversity | 09 - Active Strongly Connected Components Count | ACC |
| | 10 - Active Strongly Connected Components Ratio | ACR |

### *3.5.1 Connectivity*

This group of measures is computed using the influential active neighborhood of users. Specifically, we study two measures in this category:

**Number of Influential Active Neighbors (NAN)**. Given an activity $a = \langle v, v', \theta, t \rangle$, this measure verifies how many neighbors can influence a user $v$, w.r.t. $\theta$, at time $t$, under ($\tau_{sus}$ and $\tau_{fos}$). Most works that analyzed influence considered a plain form of this measure as a baseline [40], claiming that the likelihood of adoption increases with the number of active neighbors. Because of the time constraints, we adapt here the number of active neighbors to the number of influential active neighbors, formally representing this measure as:

$$NAN_{v,t}^{\theta} = |\eta_{v,t}^{\theta}| \tag{3.7}$$

Figure 3.7 shows the heat maps (one for each filter) of gain (or loss) of correlation coefficients between $NAN$ and probability of adoption for our both datasets (panel (a) for Twitter and panel (b) for Sina Weibo).

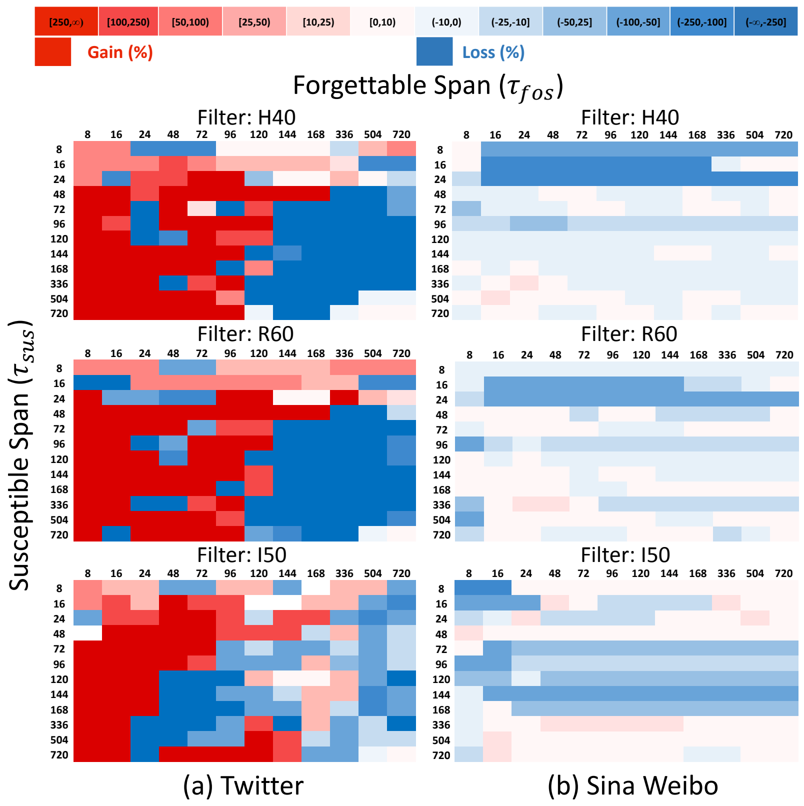

Fig. 3.7: Gain (or Loss) of the Correlation Coefficient Between $NAN$ and Probability of Adoption When the Time Constraints are Applied.

Previous works [51, 40] that have not included the time constraints argue that a positive correlation is expected here. Even so, in Figure 3.7, many cells in all heat maps show correlation gains, which can be understood as combinations of $\tau_{sus}$ and $\tau_{fos}$ strengthening the ability of $NAN$ to explain users' behaviors under social influence. Nevertheless, other combinations of the time constraints actually hurt the performance, and they will probably have a lower chance of being chosen by our model when predicting user adoption. Another observed trend for $NAN$ is that hot red cells dominate the left lower region of the heat maps where $\tau_{sus}$ is relatively high and $\tau_{fos}$ is relatively low. For the Twitter dataset, we observe this pattern especially when $72 \leq \tau_{sus} \leq 720$ and $8 \leq \tau_{fos} \leq 24$, with correlation coefficient gains varying from 6.25$\%$ to 518.75$\%$. For the Sina Weibo dataset, although with a lower magnitude, we still observe the same pattern especially when $336 \leq \tau_{sus} \leq 720$ and $8 \leq \tau_{fos} \leq 48$, with correlation coefficient gains varying from 1.16$\%$ to 23.46$\%$. Note how this phenomenon repeats for all three filters of user activity in both datasets.

**Personal Network Exposure (PNE)**. This value is defined as the division between the number of active neighbors to the total number of neighbors. According to [135], this is a relevant measure to compute the level of user's exposure. Considering the time constraints, we formally represent this measure by:

$$PNE^{\theta}_{v,t} = \frac{|\eta^{\theta}_{v,t}|}{|\eta_{v,t}|} \tag{3.8}$$

Figure 3.8 presents the heat maps for $PNE$, with filters $R60$ and $H40$ presenting comparable results in Twitter. For these filters, red cells with correlation gains are mainly distributed in the area where $\tau_{sus}$ is relatively high and $\tau_{fos}$ is relatively low (especially when $168 \leq \tau_{sus} \leq 504$ and $8 \leq \tau_{fos} \leq 16$). Although filter $I50$ presents the highest correlation gains in the same zone of the others, it also tends to keep these gains when $\tau_{fos}$ is higher. In general, the gains observed for $PNE$ are between 2.44$\%$ and 192.31$\%$. When analyzing Sina Weibo, filters $R60$ and $I50$ present comparable results, with correlation gains mainly distributed in the area where $120 \leq \tau_{sus} \leq 504$ and $8 \leq \tau_{fos} \leq 24$. In addition, for filter $H40$, the gains are roughly spread where the values of $\tau_{sus}$ and $\tau_{fos}$ are intermediate. We observe correlation gains between $1.39\%$ and $414.29\%$.

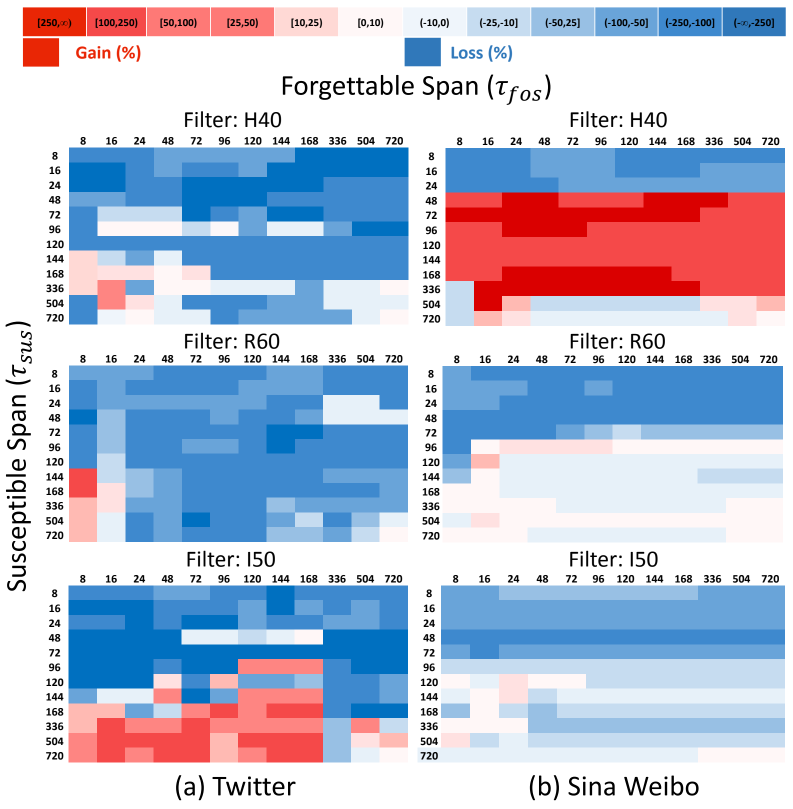

Fig. 3.8: Gain (or Loss) of the Correlation Between $PNE$ and Probability of Adoption When the Time Constraints are Applied.

## 3.5.2 Temporal

Temporal measures are used to detect how social influence changes over time. We study the following temporal measure in this work:

**Continuous Decay of Influence (CDI)**. We propose this measure in order to quantify the continuous decay of influence, since it is known that the neighbors' influence over users decays exponentially over time [51]. We formalize this metric as:

$$CDI_{v,t}^{\theta} = \sum_{u \in \eta_{v,t}^{\theta}} \mathrm{e}^{\frac{-(t_{u(max)} - t_u)}{\sigma}} \tag{3.9}$$

where $t_{u(max)}$ is the time when the latest neighbor in $\eta_{v,t}^{\theta}$ adopted $\theta$ and $\sigma$ is the globally longest identified time-delay for adoption.

Figure 3.9 presents the heat maps for *CDI*. In Twitter, all filters present a similar patter (although filter $I50$ has lower correlation gains). We observe gains between 15.79% and 252.63% for this measure, with the highest ones found where $120 \le \tau_{sus} \le 336$ and $8 \le \tau_{fos} \le 24$. In Sina Weibo, we observe gains between 2.44% and 129.27% for this measure, with the highest ones found in the intermediate zone of the heat maps.

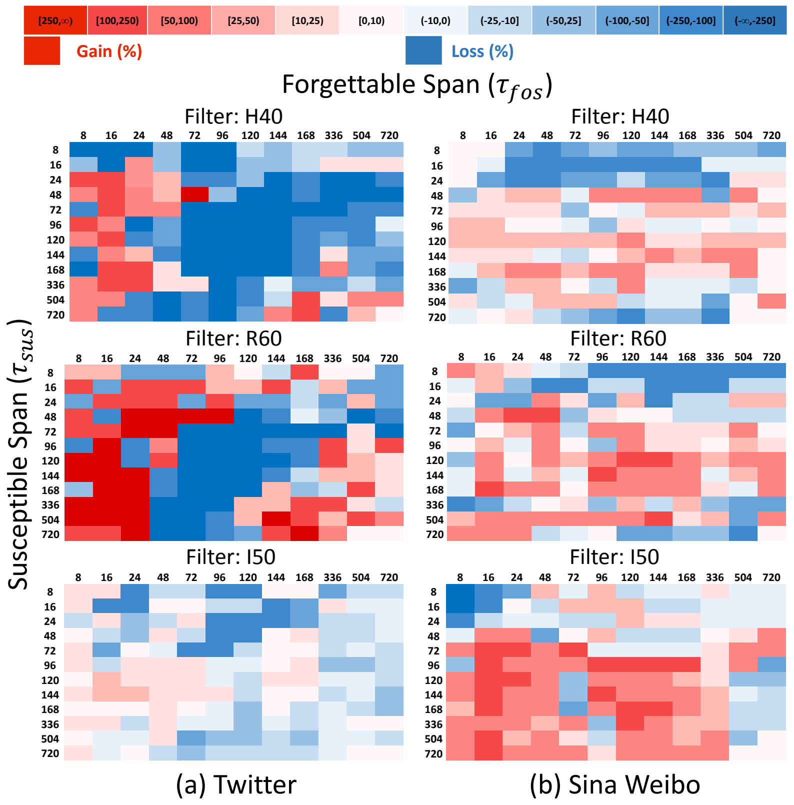

Fig. 3.9: Gain (or Loss) of the Correlation Between *CDI* and Probability of Adoption When the Time Constraints are Applied.

### *3.5.3 Recurrence*

These measures are designed to capture patterns of interaction between users [86]. In this work, we study one measure regarding recurrence:

**Previous Reposts (PRR)**. This measure verifies how many times an influential active neighbor in $\eta^{\theta}_{v,t}$ was previously retweeted by $v$, as a way to detect how strong is the corresponding relationship. We formalize this measure as:

$$PRR^{\theta}_{v,t} = \sum_{\theta'} \sum_{u \in \eta^{\theta}_{v,t}} \sum_{t' \leq t} |\langle v, u, \theta', t' \rangle| \tag{3.10}$$

Figure 3.10 presents the heat maps for *PRR*, with filters $H40$ and $R60$ presenting similar results in the Twitter dataset. Because of the cumulative nature of this measure, there is a slight tendency that high values to $\tau_{sus}$ and intermediate values to $\tau_{fos}$ results in higher correlation coefficient gains for these 2 filters, especially where $336 \leq \tau_{sus} \leq 720$ and $96 \leq \tau_{fos} \leq 144$. We observe here gains between $9.52\%$ and $328.57\%$.

For filter $I50$, gains are found when the values for $\tau_{fos}$ are slightly lower. When analyzing the Sina Weibo dataset, we observe the highest gains (between $1.2\%$ and $85.37\%$) for filters $R60$ and $I50$, where $336 \leq \tau_{sus} \leq 720$ and $8 \leq \tau_{fos} \leq 16$. For filter $H40$, low gains are basically spread throughout the majority of cells.

### *3.5.4 Transitivity*

Transitivity measures check how influential active neighbors are connected to each other. Higher values imply a more cohesive neighborhood, which produces more influence for their followers [108]. Two measures are studied here:

**Closed Triads (CLT)**. This measure enumerates how many triangles are formed by $v$ and its influential active neighbors in the entire dataset [143]. As our social graphs are directed,

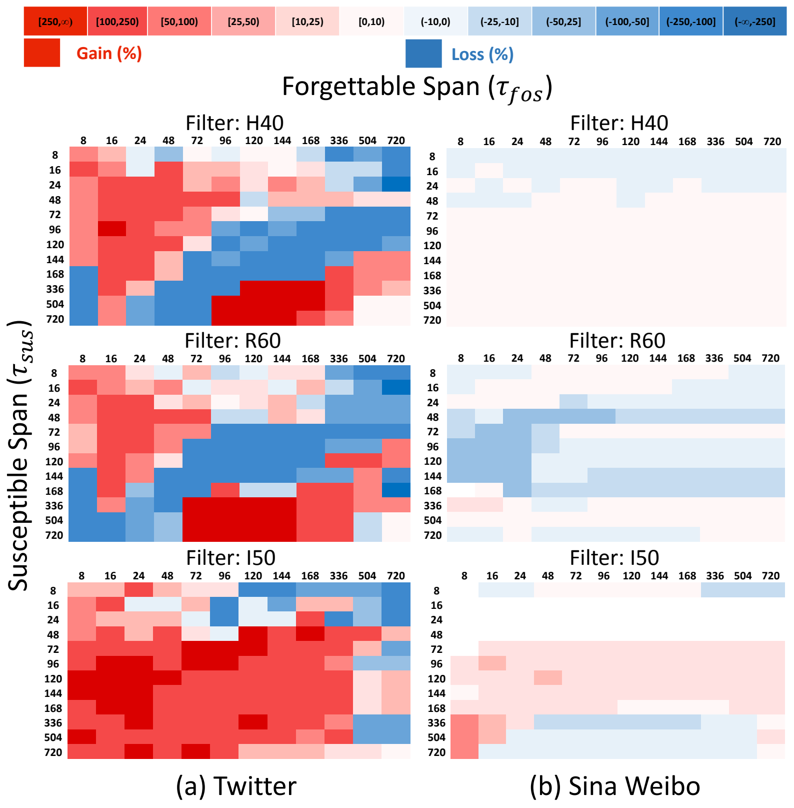

Fig. 3.10: Gain (or Loss) of the Correlation Between *PRR* and Probability of Adoption When the Time Constraints are Applied.

both directions of potential edges are checked in this analysis. We formally define this measure as:

$$CLT^{\theta}_{v,t} = \sum_{\{u,z\} \in \eta^{\theta}_{v,t}, u \neq z} f((u,z)_t) \tag{3.11}$$

where $f((u,z)_t)$ is defined as:

$$f((u,z)_t) = \begin{cases} 1, \ if \ \langle u, z, \theta', t' \rangle \in \mathcal{A} \wedge t' \leq t \\ 0, \ otherwise \end{cases} \tag{3.12}$$

Figure 3.11 presents the heat maps for *CLT*. In Twitter, this measure obtains correlation gains between 10% and 800% through all heat maps in a great part of the cells, especially over the area where both $\tau_{sus}$ and $\tau_{fos}$ have intermediate values. In Sina Weibo, we observe a similar pattern, although this measure obtains lower gains between 2.08% and 56.36%.

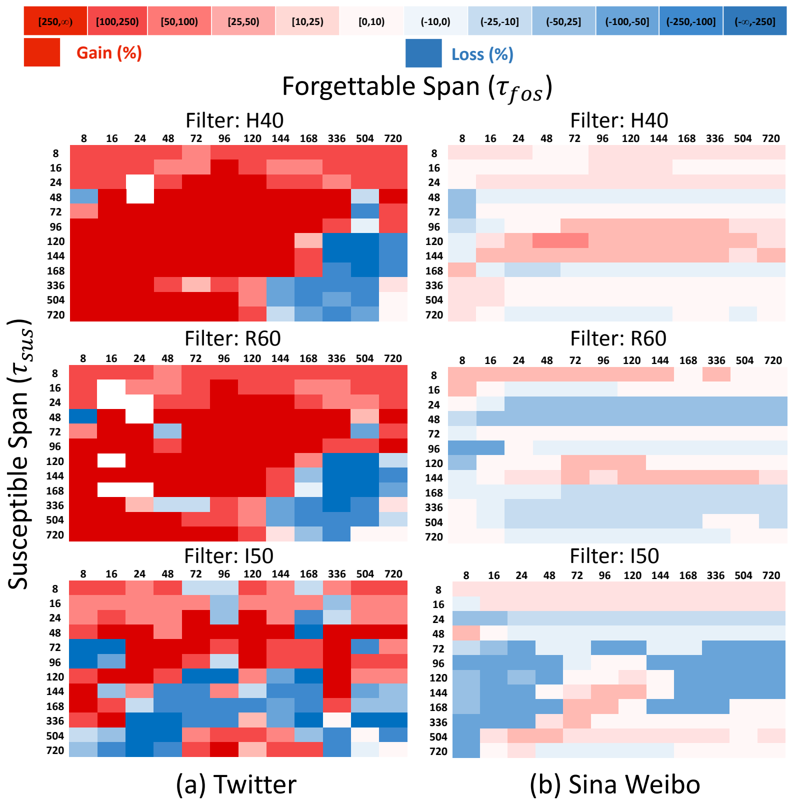

Fig. 3.11: Gain (or Loss) of the Correlation Between *CLT* and Probability of Adoption When the Time Constraints are Applied.

**Clustering Coefficient (CLC).** The Clustering coefficient is calculated using the number of closed triads divided by the possible number of triads [143]. It is a normalized value for transitivity that can be formalized as:

$$CLC_{v,t}^{\theta} = \frac{CLT_{v,t}^{\theta}}{|\eta_{v,t}^{\theta}| * (|\eta_{v,t}^{\theta}| - 1)} \tag{3.13}$$

Figure 3.12 presents the heat maps for *CLC*. For filters $H40$ and $R60$ in the Twitter dataset, relatively high values for $\tau_{sus}$ and low values for $\tau_{fos}$ produce higher correlation gains that vary between 6.67% and 313.33% (pattern observed where $48 \leq \tau_{sus} \leq 504$ and $16 \leq \tau_{fos} \leq 48$). The highest gains for filter $I50$ are lower and found in intermediate zones of both time constraints. In Sina Weibo, high values for $\tau_{sus}$ and low values for $\tau_{fos}$ produce higher correlation gains that vary between 2.78% and 466.67% (pattern observed where $336 \leq \tau_{sus} \leq 504$ and $8 \leq \tau_{fos} \leq 16$ for all filters of user activity).

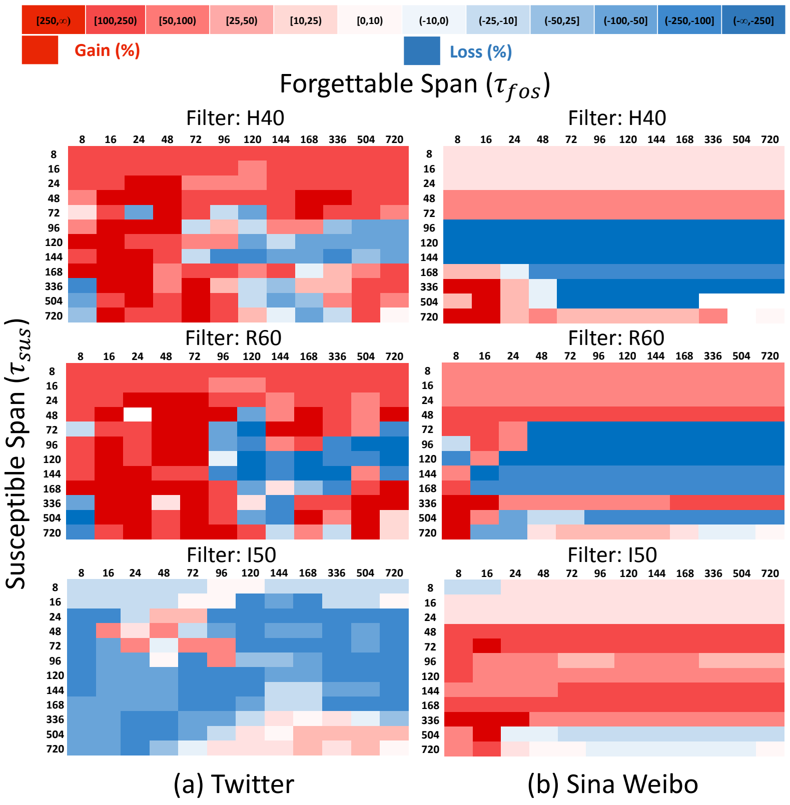

Fig. 3.12: Gain (or Loss) of the Correlation Between *CLC* and Probability of Adoption When the Time Constraints are Applied.

### 3.5.5 Centrality

Measures related to centrality try to identify the most important nodes within a graph. We use the following measure for this category:

**Hubs (HUB)**. This measure enumerates how many hubs are present in the influential active neighborhood of users. As hubs are highly connected individuals with a number of links that greatly exceeds the average, they are considered influential [11]. We define this measure as:

$$HUB_{v,t}^{\theta} = \sum_{u \in \eta_{v,t}^{\theta}} g(u,t) \tag{3.14}$$

where $g(u,t)$ is defined as:

$$g(u,t) = \begin{cases} 1, \ if \ \sum_{\theta'} \sum_{x \in V} \sum_{t' \leq t} |\langle x, u, \theta', t' \rangle| >= \gamma \\ \\ 0, \ otherwise \end{cases} \tag{3.15}$$

with $\gamma$ being the minimum number of messages reposted by a user to be considered a hub in our work.

Upon data analysis, we made $\gamma = 104$ and $\gamma = 991$ for the Twitter and Sina Weibo datasets respectively, which corresponds to 0.5% of the users (the best-connected) in Twitter and 5% of the users in Sina Weibo. To reach this value, users should be retweeted daily on average 3.5 times in Twitter or 33 times in Sina Weibo during the month analyzed in this work. Figure 3.13 presents the heat maps for *HUB*. In Twitter, we can again observe the existence of hot red cells in zones where $\tau_{sus}$ is relatively high and $\tau_{fos}$ is relatively low, especially where $72 \leq \tau_{sus} \leq 336$ and $8 \leq \tau_{fos} \leq 24$ for all filters. We found correlation gains here between 141.67% and 691.67%. In Sina Weibo, the highest gains (up to 20.78%) are also present in zones where $\tau_{sus}$ is relatively high and $\tau_{fos}$ is relatively low, especially where $168 \leq \tau_{sus} \leq 504$ and $8 \leq \tau_{fos} \leq 72$ for all filters of user activity.

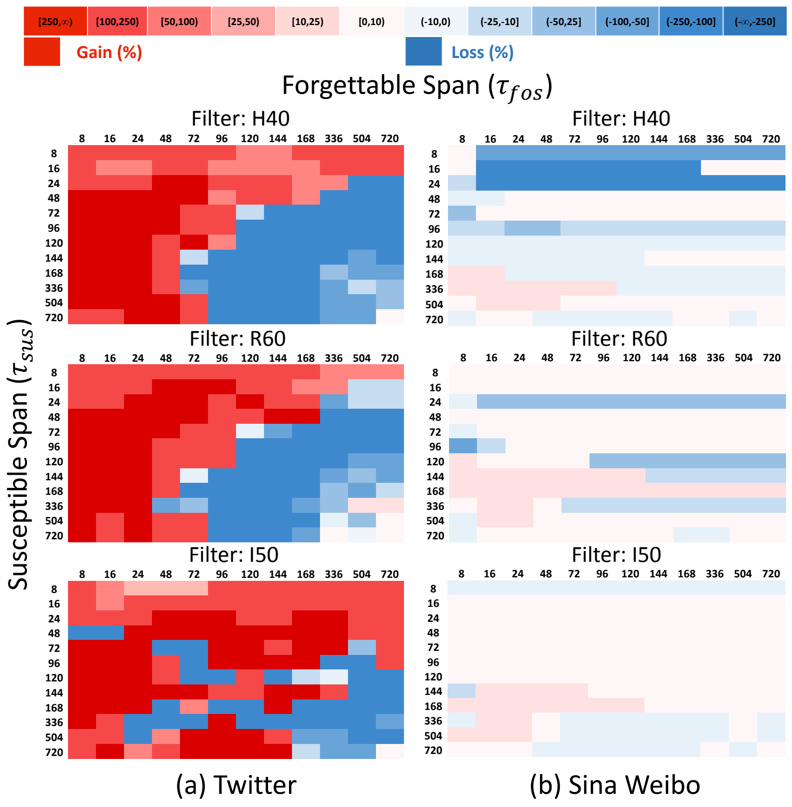

Fig. 3.13: Gain (or Loss) of the Correlation Between *HUB* and Probability of Adoption When the Time Constraints are Applied.

### *3.5.6 Reciprocity*

We compute a category of measures to capture reciprocal behaviors between users, since this information is relevant for measuring influence [143]. There are many studies analyzing the importance of reciprocity in interpersonal relationships, and how a lack of this behavior produces a negative effect [19, 59]. We use the following metric for this measure:

**Mutual Reposts (MUR)**. Mutual reposts represent one of the main forms of reciprocity existing in Twitter and Sina Weibo. We formalized this metric as:

$$MUR^{\theta}_{v,t} = \sum_{u \in \eta^{\theta}_{v,t}} h(u,t) \tag{3.16}$$

where $h(u,t)$ is defined as:

$$h(u,t) = \begin{cases} 1, \ if \ \langle u, v, \theta', t' \rangle \in \mathcal{A} \wedge t' \leq t \\ 0, \ otherwise \end{cases} \tag{3.17}$$

Figure 3.14 presents the heat maps for *MUR*. In Twitter, we observe the highest correlation gains (up to 343.90%) in the area above the diagonal that links the lower-left corner and the upper-right corner of the heat maps, especially where $96 \leq \tau_{sus} \leq 336$ and $8 \leq \tau_{fos} \leq 24$ for all filters. In Sina Weibo, we observe the highest correlation gains (up to 38.03%) in the area where $\tau_{sus}$ has intermediate values and $\tau_{fos}$ has relatively low values, especially where $48 \leq \tau_{sus} \leq 144$ and $8 \leq \tau_{fos} \leq 16$ for all filters of user activity.

### 3.5.7 Structural Diversity

This group of measures takes into consideration the diversity of communities in the influential active neighborhood of users. Uganda et al. studied this measure in [134], highlighting its importance for influence analysis. Two metrics are studied in this category: **Active Strong Connected Components Count (ACC)**. This measure is defined as the number of adjacent strongly connected components that include $v$ and at least one of its influential active neighbors. The function $P(V') : V' \rightarrow C$ maps the set of nodes $V'$ to the set of strongly connected components $C$. Then we formalize this metric as:

$$ACC^{\theta}_{v,t} = |P(\eta^{\theta}_{v,t})| \tag{3.18}$$

Figure 3.15 presents the heat maps for *ACC*. In Twitter, the highest correlation gains are distributed where $\tau_{sus}$ is intermediate and $\tau_{fos}$ is relatively low for all filters (although

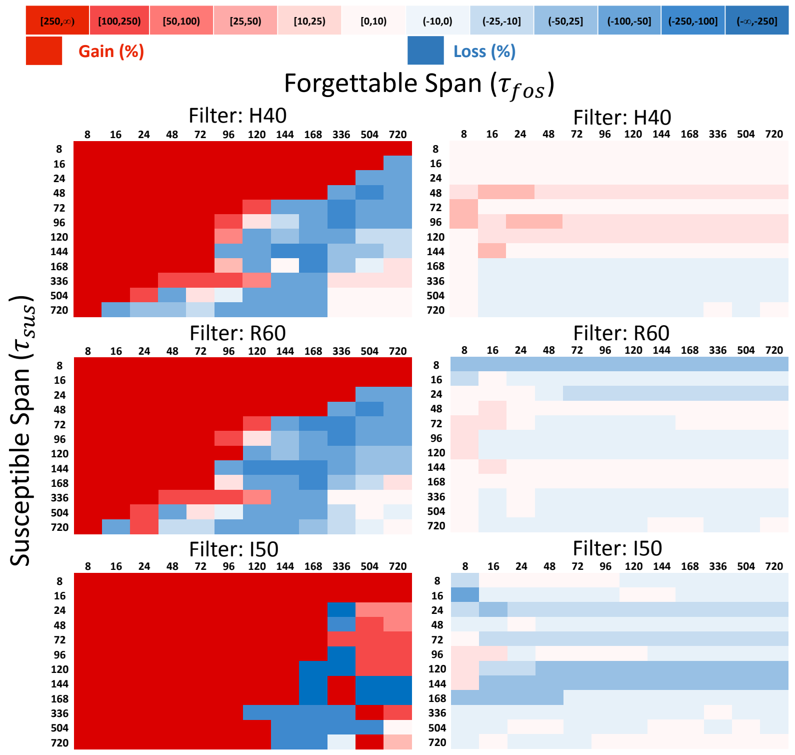

Fig. 3.14: Gain (or Loss) of the Correlation Between *MUR* and Probability of Adoption When the Time Constraints are Applied.

filter $I50$ keeps the gains when $\tau_{fos}$ becomes intermediate). The gains vary between 6.67% and 66.67% where $72 \leq \tau_{sus} \leq 168$ and $8 \leq \tau_{fos} \leq 16$. In Sina Weibo, the highest correlation gains (up to 74.51%) are distributed where $\tau_{sus}$ is relatively high and $\tau_{fos}$ is intermediate for all filters, although filter $H40$ keeps the gains when $\tau_{sus}$ becomes intermediate.

**Active Strongly Connected Components Ratio (ACR).** Since we have defined *ACC*, we can normalize this value by the total number of adjacent strongly connected components. Thus, we define *ACR* as:

$$ACR^{\theta}_{v,t} = \frac{|P(\eta^{\theta}_{v,t})|}{|P(\eta_{v,t})|} \tag{3.19}$$

Figure 3.16 presents the heat maps for *ACR*. The highest correlation gains in the Twitter dataset are spread through the area where $\tau_{sus}$ is relatively high and $\tau_{fos}$ is relatively low,

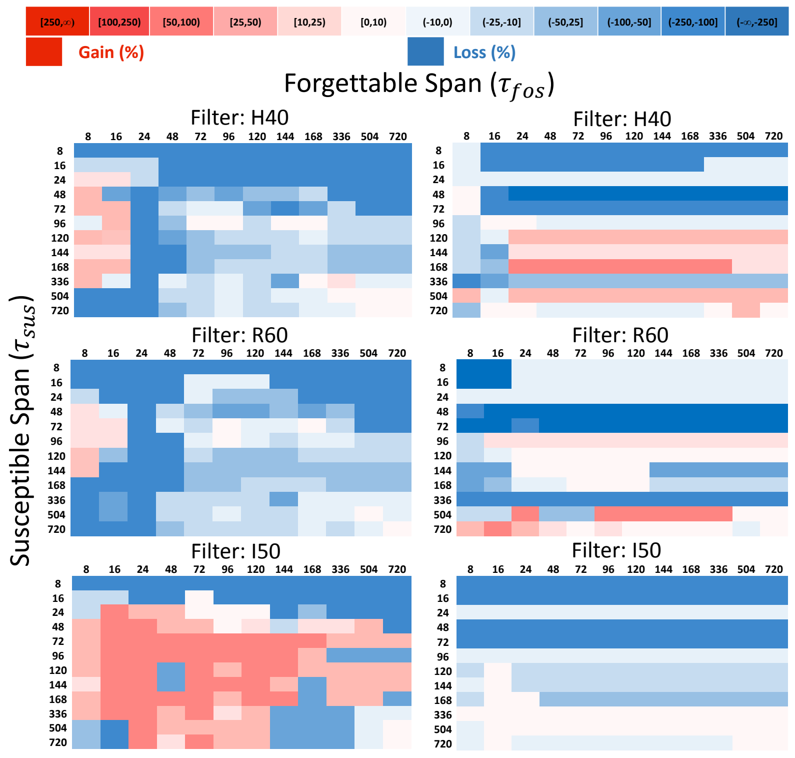

Fig. 3.15: Gain (or Loss) of the Correlation Between *ACC* and Probability of Adoption When the Time Constraints are Applied.

especially where $72 \leq \tau_{sus} \leq 720$ and $8 \leq \tau_{fos} \leq 16$ for all filters. The gains computed for this measure are between 20.00% and 860.00%. In Sina Weibo, the highest correlation gains are spread where $\tau_{sus}$ and $\tau_{fos}$ have intermediate values. The gains computed for this measure are between 1.75% and 203.85%.

## 3.6 Classification Experiments

This section presents our classification experiments and results for the adoption prediction task. We first introduce how we do training and testing and the baselines for comparison. Then, we show the performance of our model when it is trained and tested with the features individually and combined, analyzing the results when we apply and do not apply the time constraints. Finally, we demonstrate how our model overcomes the baseline methods and how those baselines can have their own performance boosted, if the time constraints are

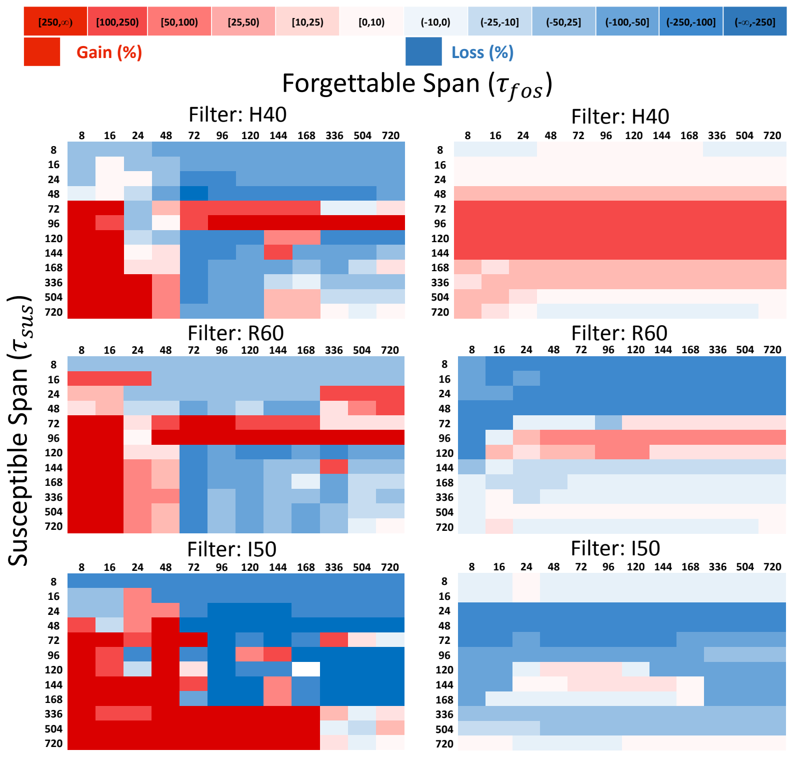

Fig. 3.16: Gain (or Loss) of the Correlation Between *ACR* and Probability of Adoption When the Time Constraints are Applied.

integrated into their models.

### 3.6.1 Training and Testing

Our 10 influence measures are treated here as features for classifiers in a machine learning approach, where we measure their performance for adoption prediction. We design experiments to study features individually and combined. We sort our samples chronologically and use the first 90% for training and the rest for testing, obeying causality which is sometimes neglected by works that attempt to predict adoption. We train and test two classifiers: Logistic Regression and Random Forest, but only report the corresponding F1 score (harmonic mean of precision and recall) for Random Forest, since Logistic Regression produces comparable results.

### 3.6.2 Individual Feature Analysis

Table 3.4 presents the individual classification performance of our 10 features for both datasets, illustrating the F1 score of the positive class.

Table 3.4: Individual Feature Performances.

| Twitter | | | | | | Sina Weibo | | | | | |
|---|---|---|---|---|---|---|---|---|---|---|---|
| Measure w/ time constraints | | | | Measure w/o time constraints | | Measure w/ time constraints | | | | Measure w/o time constraints | |
| Filter | $\tau_{sus}$ | $\tau_{fos}$ | F1 score | Filter | F1 score | Filter | $\tau_{sus}$ | $\tau_{fos}$ | F1 score | Filter | F1 score |
| NAN | | | | NAN | | NAN | | | | NAN | |
| R60 | 144 | 120 | 0.666 | R60 | 0.605 | R60 | 72 | 48 | 0.766 | I50 | 0.629 |
| H40 | 336 | 120 | 0.664 | H40 | 0.567 | H40 | 96 | 16 | 0.704 | R60 | 0.550 |
| I50 | 504 | 504 | 0.541 | I50 | 0.502 | I50 | 168 | 168 | 0.678 | H40 | 0.492 |
| PNE | | | | PNE | | PNE | | | | PNE | |
| I50 | 336 | 96 | 0.671 | R60 | 0.600 | R60 | 504 | 168 | 0.738 | H40 | 0.709 |
| H40 | 144 | 120 | 0.669 | I50 | 0.598 | H40 | 720 | 72 | 0.715 | R60 | 0.704 |
| R60 | 72 | 16 | 0.634 | H40 | 0.597 | I50 | 144 | 168 | 0.713 | I50 | 0.637 |
| CDI | | | | CDI | | CDI | | | | CDI | |
| H40 | 336 | 72 | 0.627 | H40 | 0.563 | I50 | 120 | 16 | 0.676 | I50 | 0.550 |
| R60 | 120 | 96 | 0.622 | R60 | 0.560 | H40 | 72 | 48 | 0.644 | H40 | 0.488 |
| I50 | 144 | 96 | 0.596 | I50 | 0.483 | R60 | 72 | 72 | 0.601 | R60 | 0.460 |
| PRR | | | | PRR | | PRR | | | | PRR | |
| H40 | 144 | 24 | 0.657 | I50 | 0.561 | R60 | 336 | 24 | 0.689 | I50 | 0.614 |
| R60 | 96 | 24 | 0.642 | R60 | 0.524 | H40 | 16 | 8 | 0.659 | H40 | 0.557 |
| I50 | 504 | 8 | 0.626 | H40 | 0.485 | I50 | 120 | 8 | 0.629 | R60 | 0.406 |
| CLT | | | | CLT | | CLT | | | | CLT | |
| R60 | 168 | 48 | 0.680 | R60 | 0.606 | R60 | 96 | 24 | 0.735 | I50 | 0.644 |
| H40 | 120 | 16 | 0.671 | H40 | 0.600 | H40 | 96 | 96 | 0.678 | H40 | 0.4 |
| I50 | 144 | 504 | 0.610 | I50 | 0.474 | I50 | 168 | 48 | 0.657 | R60 | 0.339 |
| CLC | | | | CLC | | CLC | | | | CLC | |
| R60 | 96 | 72 | 0.664 | I50 | 0.561 | R60 | 96 | 16 | 0.735 | I50 | 0.629 |
| H40 | 120 | 96 | 0.664 | R60 | 0.533 | H40 | 96 | 16 | 0.680 | R60 | 0.614 |
| I50 | 504 | 504 | 0.538 | H40 | 0.500 | I50 | 168 | 120 | 0.675 | H40 | 0.378 |
| HUB | | | | HUB | | HUB | | | | HUB | |
| H40 | 336 | 48 | 0.683 | H40 | 0.634 | R60 | 72 | 16 | 0.770 | I50 | 0.629 |
| R60 | 336 | 120 | 0.662 | R60 | 0.609 | I50 | 120 | 24 | 0.734 | R60 | 0.561 |
| I50 | 96 | 72 | 0.623 | I50 | 0.472 | H40 | 72 | 24 | 0.693 | H40 | 0.479 |
| MUR | | | | MUR | | MUR | | | | MUR | |
| R60 | 24 | 16 | 0.637 | I50 | 0.574 | I50 | 96 | 8 | 0.384 | I50 | 0.335 |
| H40 | 96 | 24 | 0.628 | H40 | 0.494 | R60 | 16 | 16 | 0.308 | R60 | 0.282 |
| I50 | 72 | 96 | 0.620 | R60 | 0.481 | H40 | 16 | 8 | 0.302 | H40 | 0.275 |
| ACC | | | | ACC | | ACC | | | | ACC | |
| H40 | 96 | 72 | 0.673 | R60 | 0.628 | H40 | 96 | 16 | 0.710 | I50 | 0.655 |
| R60 | 120 | 72 | 0.673 | H40 | 0.615 | R60 | 72 | 48 | 0.704 | H40 | 0.544 |
| I50 | 144 | 336 | 0.662 | I50 | 0.203 | I50 | 168 | 144 | 0.680 | R60 | 0.538 |
| ACR | | | | ACR | | ACR | | | | ACR | |
| R60 | 16 | 24 | 0.661 | I50 | 0.623 | H40 | 144 | 96 | 0.785 | H40 | 0.695 |
| I50 | 336 | 120 | 0.655 | H40 | 0.557 | R60 | 720 | 16 | 0.739 | R60 | 0.649 |
| H40 | 96 | 72 | 0.647 | R60 | 0.526 | I50 | 120 | 24 | 0.663 | I50 | 0.588 |

We present all performances among the 3 filters of user activity, showing the results when they include or not the time constraints. For the great majority of cases (80%), $\tau_{sus}$ present values greater than $\tau_{fos}$, and in more than half of the cases, $\tau_{sus}$ present values much greater than $\tau_{fos}$ so that adoption is more precisely predicted. This pattern repeats what we observe for correlation gain between influence measures and the probability of adoption, pointing a clear requirement of a longer time interval to *Susceptible Span* when compared to *Forgettable Span*. We also confirm this tendency noting that $\tau_{sus}$ has a value greater or equal to 96 (hours) in 78.83% of the cases analyzed, while $\tau_{fos}$ has a value lower or equal to 96 (hours) in 78.66% of these cases.

In the Twitter dataset, the top 5 features which present the highest values for F1 score when considering the time constraints are: 1) *HUB* with 0.683, 2) *CLT* with 0.680, 3) *ACC* with 0.673, 4) *PNE* with 0.671, and 5) *NAN* with 0.666. In the Sina Weibo dataset, the top 5 features with the highest F1 score are: 1) *ACR* with 0.785, 2) *HUB* with 0.770, 3) *NAN* with 0.766, 4) *PNE* with 0.738, and 5) *CLT-CLC* with 0.735. These results demonstrate the relevance of features such as *HUB*, *PNE*, and *NAN* for capturing social influence, since they are all present in the set of features with the highest performances in Twitter and Sina Weibo. Although the adoption predictions here are considerably high for both datasets, we note that our model performs slightly better in Sina Weibo, probably because of the limitation of the Twitter API that produces some indirect links between users retweeting. Another relevant finding we observe with these results refers to the fact that all three filters of user activity analyzed in this work obtain roughly comparable performances in each dataset, although filter $I50$ has lower performances in some cases. This phenomenon demonstrates the robustness of the two time constraints regardless of the method used for filtering users.

To complete this individual feature analysis, we sort the features according to their F1 score gain when compared to applying no time constraints in Table 3.5. For this analysis, we consider only the highest F1 score among the three filters for each feature. Our intention is to check the magnitude with which our features have their prediction performance boosted when they are subject to $\tau_{sus}$ and $\tau_{fos}$. In Twitter, $CLC$ presents the highest performance improvement in F1 score (18.36%), followed by *PRR*, *CLT*, *PNE*, and *CDI*, while *ACR* is the feature with the lowest one. In Sina Weibo, $CDI$ presents the highest performance improvement in F1 score (22.90%), followed by *HUB*, *NAN*, *CLC*, and *MUR*, while *PNE* is the feature with the lowest one. In general, we observe F1 score gains varying between 4.09% and 22.90% for all filters analyzed.

Table 3.5: Individual Feature Performances Considering the Time Constraints.

| Twitter | | | | | | Sina Weibo | | | | | |
|---|---|---|---|---|---|---|---|---|---|---|---|
| Feature | Filter | $\tau_{sus}$ | $\tau_{fos}$ | F1 score | Improvements (%) | Feature | Filter | $\tau_{sus}$ | $\tau_{fos}$ | F1 score | Improvements (%) |
| CLC | R60 | 96 | 72 | 0.664 | 18.36 | CDI | I50 | 120 | 16 | 0.676 | 22.90 |
| PRR | H40 | 144 | 24 | 0.657 | 17.11 | HUB | R60 | 72 | 16 | 0.770 | 22.41 |
| CLT | R60 | 168 | 48 | 0.680 | 12.21 | NAN | R60 | 72 | 48 | 0.766 | 21.78 |
| PNE | I50 | 336 | 96 | 0.671 | 11.83 | CLC | R60 | 96 | 16 | 0.735 | 16.85 |
| CDI | H40 | 336 | 72 | 0.627 | 11.36 | MUR | I50 | 96 | 8 | 0.384 | 14.62 |
| MUR | R60 | 24 | 16 | 0.637 | 10.97 | CLT | R60 | 96 | 24 | 0.735 | 14.13 |
| NAN | R60 | 144 | 120 | 0.666 | 10.08 | ACR | H40 | 96 | 16 | 0.710 | 12.94 |
| HUB | H40 | 336 | 48 | 0.683 | 7.72 | PRR | R60 | 336 | 24 | 0.689 | 12.21 |
| ACC | H40 | 96 | 72 | 0.673 | 7.16 | ACC | H40 | 96 | 16 | 0.710 | 8.39 |
| ACR | I50 | 16 | 24 | 0.661 | 6.09 | PNE | R60 | 504 | 168 | 0.738 | 4.09 |

### 3.6.3 Combined Feature Analysis

Besides evaluating the performance of features individually, we check the performance of our model when the 10 features are applied combined, comparing the results when we apply and when we do not apply the time constraints. We show the corresponding results for both datasets in Table 3.6, sorting them by the F1 score gain. We detect an improvement of 14.88% and 12.82% in Twitter and Sina Weibo datasets respectively, showing how the time constraints also work when we use all features together. In addition, the pattern noticed before for the individual features (adoption is better predicted when $\tau_{sus} \gg \tau_{fos}$) is observed again for the features combined, with the performances achieving significant improvements when $\tau_{sus}$ reaches values between 144 and 504 and when $\tau_{fos}$ reaches values between 16 and 96. Averaging all these top performances, we can interpret our results as: 1) users will stop observing their neighbors roughly after 2 weeks on average, if they do not retweet them anymore; 2) users will no more remember the activations of their neighbors after a period of approximately 1.5 days. Therefore, an accordingly parameter tuning is needed to apply the proposed methods for adoption prediction.

Table 3.6: Performances of All Features Combined.

| Twitter | | | | | | | Sina Weibo | | | | | | |
|---|---|---|---|---|---|---|---|---|---|---|---|---|---|
| All features w/ time constraints | | | | | All features w/o time constraints | | All features w/ time constraints | | | | | All features w/o time constraints | |
| Filter | $\tau_{sus}$ | $\tau_{fos}$ | F1 score | Improv. (%) | Filter | F1 score | Filter | $\tau_{sus}$ | $\tau_{fos}$ | F1 score | Improv. (%) | Filter | F1 score |
| H40 | 504 | 24 | 0.741 | 14.88 | H40 | 0.645 | R60 | 336 | 16 | 0.862 | 12.82 | R60 | 0.764 |
| R60 | 144 | 16 | 0.722 | 13.16 | R60 | 0.638 | H40 | 504 | 48 | 0.849 | 10.11 | H40 | 0.771 |
| I50 | 504 | 16 | 0.713 | 9.35 | I50 | 0.652 | I50 | 168 | 96 | 0.792 | 8.49 | I50 | 0.730 |

### *3.6.4 Performance of Baseline Methods*

We compare our model with 3 baselines for measuring social influence and predicting adoptions. The main idea is to compare the classification results and answer two questions: 1) if our method can outperform all baselines; 2) if the baselines can be improved when the time constraints are applied to their models. We list the 3 baseline methods below:

- **Influence Locality model (LRC-Q).** Provided by [145], it was defined by the combination of peer influence and structural diversity (function $Q$). Peer influence is computed as a linear combination of the geometric mean of random walk probabilities of active neighbors while structural diversity combines the social circles formed by these neighbors.

- **Static Bernoulli (SB).** In the work proposed in [51], the SB model learns the influence probability $P^t_{u,u'}$ for each edge $(u, u')$ at time $t$, predicting the adoption probability of user $v$ at time $t$ given the set of active neighbors $S$ as: $p^v_t(S) = 1 - \prod_{u \in S}(1 - p^t_{u,v})$.

- **Complex Probability Model (CPM).** The authors in [40] translated the General Threshold Model [62] to a probabilistic adoption model where the likelihood of adoption increases with more active neighbors. To approximate threshold-like behavior, they used a logistic sigmoid function to calculate the joint probability of exposures.

Table 3.7 presents the results of those three baselines in our both datasets.

Table 3.7: Baselines comparisons.

| Twitter | | | | | | | Sina Weibo | | | | | | |
|---|---|---|---|---|---|---|---|---|---|---|---|---|---|
| LRC-Q w/ time constraints | | | | | LRC-Q w/o time constraints | | LRC-Q w/ time constraints | | | | | LRC-Q w/o time constraints | |
| Filter | $\tau_{sus}$ | $\tau_{fos}$ | F1 score | Improv. (%) | Filter | F1 score | Filter | $\tau_{sus}$ | $\tau_{fos}$ | F1 score | Improv. (%) | Filter | F1 score |
| R60 | 336 | 16 | 0.659 | 9.46 | R60 | 0.602 | I50 | 168 | 16 | 0.664 | 5.73 | I50 | 0.628 |
| H40 | 48 | 8 | 0.646 | 8.20 | H40 | 0.597 | R60 | 120 | 48 | 0.658 | 5.44 | R60 | 0.624 |
| I50 | 504 | 16 | 0.626 | 3.98 | I50 | 0.602 | H40 | 96 | 48 | 0.639 | 3.56 | H40 | 0.617 |
| SB w/ time constraints | | | | | SB w/o time constraints | | SB w/ time constraints | | | | | SB w/o time constraints | |
| Filter | $\tau_{sus}$ | $\tau_{fos}$ | F1 score | Improv. (%) | Filter | F1 score | Filter | $\tau_{sus}$ | $\tau_{fos}$ | F1 score | Improv. (%) | Filter | F1 score |
| H40 | 168 | 24 | 0.662 | 8.34 | H40 | 0.611 | H40 | 96 | 72 | 0.708 | 9.42 | H40 | 0.647 |
| R60 | 504 | 72 | 0.654 | 7.38 | R60 | 0.609 | R60 | 72 | 24 | 0.693 | 8.79 | R60 | 0.637 |
| I50 | 336 | 16 | 0.628 | 5.36 | I50 | 0.596 | I50 | 336 | 48 | 0.659 | 6.11 | I50 | 0.621 |
| CPM w/ time constraints | | | | | CPM w/o time constraints | | CPM w/ time constraints | | | | | CPM w/o time constraints | |
| Filter | $\tau_{sus}$ | $\tau_{fos}$ | F1 score | Improv. (%) | Filter | F1 score | Filter | $\tau_{sus}$ | $\tau_{fos}$ | F1 score | Improv. (%) | Filter | F1 score |
| R60 | 336 | 96 | 0.669 | 10.57 | R60 | 0.605 | H40 | 96 | 72 | 0.721 | 9.07 | H40 | 0.661 |
| H40 | 336 | 72 | 0.671 | 9.10 | H40 | 0.615 | R60 | 72 | 24 | 0.725 | 8.20 | R60 | 0.670 |
| I50 | 504 | 48 | 0.633 | 8.20 | I50 | 0.585 | I50 | 336 | 8 | 0.686 | 6.19 | I50 | 0.646 |

As verified, our model outperforms the baselines in both situations: when we use an individual feature such as *HUB* and when we use all the features combined. For instance, we observe that by considering all features together, we reach improvements from 7.92% to 12.63% in Twitter, while improvements from 15.45% to 18.89% are computed in Sina Weibo (both compared to *CPM*). Note that similar results hold for all filters of user activity. In addition, we inform in this table how much the time constraints can improve the predictions of the baseline methods. Basically, $\tau_{sus}$ and $\tau_{fos}$ boost all baselines' performances, with gains of 9.46% for *LRC-Q*, 8.34% for *SB*, and 10.57% for *CPM* in Twitter. In Sina Weibo, we have gains of 5.73% for *LRC-Q*, 9.42% for *SB*, and 9.07% for *CPM*. These results highlight the effectiveness of both time constraints for all tested models, recognizing the pattern detected throughout this work: when $\tau_{sus} \gg \tau_{fos}$, social influence is better measured and adoption is more precisely predicted by the baseline models.

## 3.7 Related Work

Many works have been proposed to measure social influence and predict users' adoption. For instance, the seminal work of Kempe et al. [62] describes two popular models for information diffusion that were generalized with the General Threshold Model (GTM). In the GTM, the collective influence produced by the infected neighbors of a person will trigger its infection once its threshold is exceeded. Later, Saito et al. [111] worked with predictions of influence probabilities in complex networks, also considering the GTM's diffusion concept. They formulated the problem of likelihood maximization and applied the EM algorithm to solve it, showing reasonable results with the proposed method. In a sequence, Goyal et al. [51] leveraged a variety of models learned with pairwise influence probability, finding that the probability of adoption increases with the number of previously adopters among friends. State and Adamic [125] also found evidence of Goyal's findings, looking for evidence of social influence on Facebook. They checked when users overlay their profile pictures to support same-sex marriage, discovering that the probability of adoption increases as more neighbors adopt the same behavior.

With an alternative approach, Zhang et al. [145] proposed the *influence locality* model, developing two instantiated functions based on pair-wise influence and structural diversity to predict adoptions. Their analysis reveals that a retweet behavior is positively correlated with the number of friends who have retweeted the same message before, but it is negatively correlated with the number of connected circles (a group of socially interconnected people) formed by these friends. Although the model proposed is quite simple, the authors showed how it performs relatively well. Comparing two different perspectives, Fink et al. [40] proposed probabilistic contagion models for simple and complex contagion phenomena, testing their models on 20 Nigerian events in Twitter. By optimizing the threshold for the complex model and the single adoption probability for the simple model, they showed that for politically-themed hashtags, the complex contagion model produces a superior fit, reinforcing the idea that influence grows with more active neighbors.

In addition, there is a wide range of work focusing on cascades prediction in social networks, whose goal is to detect when information has the potential to go viral through consecutive user adoptions [138]. For instance, Watts and Dodds demonstrated how cascades are driven not by "influentials" but by a critical mass of easily influenced individuals [139]. By introducing and using the concept of structural virality, Goel et al. found that popular events grow through broadcast and also peer-to-peer spreading [50]. Jenders et al. presented probabilistic models for predicting the spread of tweets, considering a combination of structural, content, and sentimental-based features [61]. Weng et al. showed how the popularity of a message on Twitter can be predicted by quantifying its early spreading pattern in terms of community concentration [140]. Selecting important nodes as sensors, Cui et al. analyzed historical data to predict cascades based on the behaviors of these sensors [27]. On a large sample of photo reshare cascades on Facebook, Cheng et al. confirmed that initially, breadth, rather than depth in a cascade is a better indicator of viral messages [23].

In all these works, we note the authors have not fully explored the dynamics of influence, building their models basically upon static relationships and invariable social stimulus. Here, while we also focus on measuring influence to predict adoption, we take the next steps to apply a pair of time constraints to dynamically build our social graphs, presenting evidence that influence and adoptions are better measured and predicted when the two proposed time constraints are considered in both processes.

## 3.8 Summary

In this Chapter, we conduct an engineering study that investigates how a simple pair of time constraints can considerably contribute to measuring influence and predict user adoption in social media, as a way to identify potential future collaborators of the ever-expanding networks of key-hackers. First, we integrate and tune these constraints in a model composed of 10 standard influence measures, all of them capable of quantifying different influential factors in the active neighborhood of users. Then, we formulate a binary classification problem where those influence measures are used as features in a machine learning approach for predicting whether an individual will adopt a new behavior. Through the designed and implemented experiments, we show how the dynamic graphs produced by both time constraints better capture the influence between users over time (especially when the values of $\tau_{sus}$ and $\tau_{fos}$ are relatively high and low respectively), improving the performance of approaches introduced by us and others. We validate our approach under a variety of conditions using a sample of Twitter and Sina Weibo datasets, showing how it outperforms the state of the art methods and enables practical usage of the concepts for adoption prediction.

Chapter 4

# PREDICTING HACKER ADOPTION ON DARKWEB FORUMS

## 4.1 Introduction

Based on the findings presented in Chapter 3 regarding how social influence affects online user behavior, we postulate whether it would be possible to leverage the spread of adoption behavior among hackers to predict their activities on online hacking communities. One direct application of this study would be the prediction of which hackers would buy a specific hacking product/service that has been offered on a darkweb forum [65]. As standard hackers, who are often influenced by reputable ones, rely on darkweb hacking forums to improve their skills and capabilities [83], the anticipation of this interaction could be accomplished. Finally, adoption behavior could also be used for addressing online cascade predictions [53] in those environments, whose primary goal is the detection of an early-stage post with potential to “go viral”, generating multiple subsequent adoptions that strongly signal imminent cyber-attacks [104].

In this Chapter, we study adoption behavior trying to predict in which topic of a darkweb hacking forum users will post in the near future, given the influence of their peers. We formulate our problem as a sequential rule mining task [47], where the goal is to discover user posting rules through sequences of user posts. Then, we use the mined rules to make predictions of users posting in a particular forum topic. In general, sequential rule mining is an important data mining technique that tries to predict event(s) that are likely to follow other events(s) with a given probability, using patterns mined from sequences [46].

Adapting the problem to our context, we make each rule of the form $X \Rightarrow Y$ only contain the users responsible for the posts, being interpreted as “if $X$ (a set of users) engages in a given forum topic, $Y$ (a unique user) is likely to engage in the same topic (or adopt it) with a given confidence afterward, mainly because of the influence of $X$". Additionally, as we demonstrated that influence decreases over time because of effects of time constraints such as *Forgettable Span* [81], we only consider rules occurring within defined time-windows. We also verify how the precision of our model changes according to two posting time granularities (day and hour). Finally, we compare our results with those produced by the prior probabilities of hackers' posts, showing how our predictions and prediction gains are considerably higher. This Chapter makes the following main contributions:

1. We collect more than 330,000 hacker posts of a popular darkweb forum to create a sequential rule mining model capable of predicting future posts of hackers;
2. We consider 2 posting time granularities (day and hour) and 10 different time-windows for each time granularity;
3. During training, we mine more than 362,617 sequential rules with different sizes (number of users);
4. During testing, we obtain prediction precision results of up to 0.78, while a baseline model reaches up to 0.18;
5. We observe the highest precision gain [785%, 837%] for time-windows in [3,5] days, confirming the *Forgettable Span* [81] effects also on hacking forums of the darkweb.

The remaining of this Chapter is structured as follows. Section 4.2 presents our dataset. Section 4.3 formalizes our sequential rule mining task applied to hacker adoption prediction. Section 4.4 presents our experiments and results. Section 4.5 shows some related work. Finally, Section 4.6 summarizes the Chapter.

## 4.2 Darkweb Dataset

In this work, we collect data from a popular hacker forum on the darkweb (anonymized as $ForumX$) provided by CYR3CON [28]. We show information from $ForumX$ in Table 4.1, which includes a wide range of hacking-related messages posted by community members.

Table 4.1: $ForumX$ Information.

| | |
|---|---|
| Time Period | 06/09/2014 : 08/02/2017 |
| Number of Users | 4,112 |
| Number of Topics | 95 |
| Number of Posts | 331,384 |

## 4.3 Sequential Rule Mining Task

Discovering temporal relationships between events stored in large databases is important in many domains (e.g. stock market data, biological data, patient hospital records, and customer data), as it sets a basis for event prediction. Various methods have been proposed for mining these relationships (see a survey in [67]), being sequential rule mining one of the most popular in the data mining field [44]. Basically, this technique discovers rules in a single sequence [32], across sequences [29] or common to multiple sequences [44]. These rules are potentially useful for analyzing data in sequential format, indicating that if some event(s) occur, some other event(s) are likely to occur with a given confidence afterward. Sequential rule mining has been applied in several domains such as stock market analysis [29], where the goal is to predict stock prices going up or down, e-learning [47], where it is used to predict the behavior of learners in educational data, e-commerce [99], aiming to determine the purchase pattern of customers, weather observation [54], where it is used to forecast the weather, and also drought prediction [32], among other applications.

Bringing to our context, we leverage sequential rule mining applied to multiple sequences to study the spread of adoption behavior among malicious hackers. The goal is to predict in which topic of $ForumX$ hackers will post in the near future (topic adoption), given the influence produced by their peers. This way, we make each of the 95 topics of the forum analyzed represents a particular sequence, which starts with the oldest post of the topic and ends with the latest one. In the following, we give a detailed formalization of our problem.

### *4.3.1 Problem Formalization*

We follow the definitions of [47] to specify a sequence database as a set of topics $\Theta = \{\theta_1, \theta_2 ... \theta_k\}$ and a set of users (malicious hackers) $U = \{u_1, u_2, ... u_m\}$ posting in these topics. Each topic $\theta_x$ is an ordered list of usersets (set of users) $\theta_x = U_1, U_2, ... U_n$ such that $U_1, U_2, ... U_n \subseteq U$. Figure 4.1 illustrates a timeline where users are posting on 4 topics.

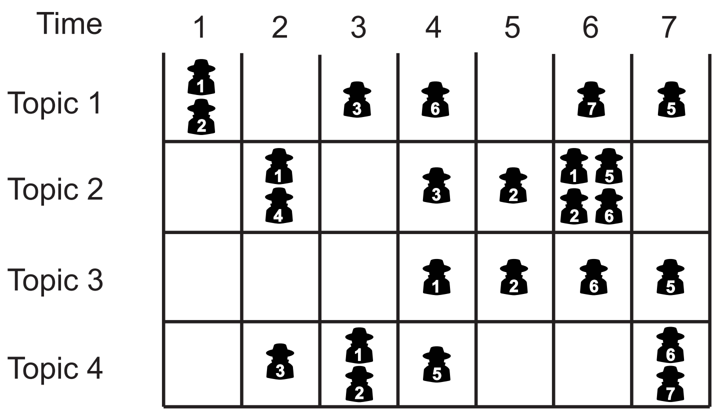

Fig. 4.1: Sample Timeline of Forum Topics.

Table 4.2 depicts a sequence database encoding the data presented in Figure 4.1. For instance, topic $\theta_1$ states that users $u_1$ and $u_2$ posted at the same particular time point $t_i$, being followed successively by: nobody at $t_i + 1$, user $u_3$ at $t_i + 2$, $u_6$ at $t_i + 3$, nobody at $t_i + 4$, $u_7$ at $t_i + 5$, and $u_5$ at $t_i + 6$.

Table 4.2: Modeling a Forum as a Sequence Database.

| Topics | Sequences of Post Users |
|---|---|
| $\theta_1$ | $\{u_1,u_2\},\{\},\{u_3\},\{u_6\},\{\},\{u_7\},\{u_5\}$ |
| $\theta_2$ | $\{u_1,u_4\},\{\},\{u_3\},\{u_2\},\{u_1,u_2,u_5,u_6\}$ |
| $\theta_3$ | $\{u_1\},\{u_2\},\{u_6\},\{u_5\}$ |
| $\theta_4$ | $\{u_3\},\{u_1,u_2\},\{u_5\},\{\},\{\},\{u_6,u_7\}$ |

In our context, a sequential rule $X \Rightarrow Y$ is defined as a relationship between two usersets $X$ (antecedent), $Y$ (consequent) $\subseteq U$ such that $X \cap Y = \emptyset$ and $X, Y \neq \emptyset$. A rule $X \Rightarrow Y$ is said to occur in a topic $\theta_x = U_1, U_2, ...U_n$ if there exists an integer $u$ such that $1 \leq u < n, X \subseteq \cup_{i=1}^{u} U_i$ and $Y \subseteq \cup_{i=u+1}^{n} U_i$. For example, the rule $\{u_1, u_2, u_3\} \Rightarrow \{u_5\}$ occurs in the topics $\theta_1$, $\theta_2$ and $\theta_4$ of Table 4.2.

According to [47], a rule $X \Rightarrow Y$ is said to be of size $v{*}w$ if $|X| = v$ and $|Y| = w$. Thus, the rule $\{u_1, u_5\} \Rightarrow \{u_6\}$ is of size $2{*}1$. We only consider in this work sequential rules containing a single user in the rule consequent ($w = 1$), since we want to predict one hacker at a time for the adoption prediction task. Furthermore, a rule of size $f{*}g$ is larger than another rule of size $h{*}i$ if $f > h$ and $g \geq i$, or if $f \geq h$ and $g > i$ [47].

There are two standard measures that we leverage to evaluate the quality of our rules: the *sequential support*, which is the fraction of topics where all the users of $X$ appear before the user of $Y$ and the *sequential confidence*, which is the number of topics where all the users of $X$ appear before the user of $Y$ divided by the number of topics where all the users of $X$ appear. Therefore, the problem of mining sequential rules consists in finding all rules with support and confidence no less than the user-defined thresholds $minsup$ and $minconf$ respectively. Those rules are interpreted as "if the users of $X$ post in a given topic, the user of $Y$ is likely to post in (or adopt) the same topic with a given confidence afterward, mainly because of the influence of $X$". Note that in addition to predicting the next user to post in the near future ($Y$), the rules also provide information about the reason for that post (influence of $X$), allowing easy interpretation.

There is also one important point about the non-requirement of ordering restriction between users in $X$. Fournier pointed out that mining sequential rules has the following three drawbacks when a strict ordering is applied between items (our users) of the antecedent or consequent of a rule [45]:

1. **Rules may have many variations:** There are different variations of the rule $\{u_1\}, \{u_3\} \Rightarrow \{u_5\}$ as illustrated with the following rules $r_i, r_{i'}, r_{i''}$. However, all these variations describe the same situation: if users $u_1$ and $u_3$ post in a given topic in any order, then user $u_5$ is likely to post in the same topic after them.

$$r_i : \{u_1\}, \{u_3\} \Rightarrow \{u_5\},$$

$$r_{i'} : \{u_3\}, \{u_1\} \Rightarrow \{u_5\},$$

$$r_{i''} : \{u_1, u_3\} \Rightarrow \{u_5\}.$$

2. **Similar rules are rated very differently:** Considering a strict order, the rules $r_i$ and $r_{i'}$ have support/confidence of 0.5/1.0 and 0.25/0.5 respectively, while the rule $r_{i''}$ does not appear in our sample database. This condition produces a wrong impression about the existing sequential relationships. Taken as a whole, the support of the rule $\{u_1, u_3\} \Rightarrow \{u_5\}$ grows to 0.75.

3. **Rules are less likely to be useful:** Rules with a strict order are are less likely to match with a sequence for future adoption predictions. For example, no rule can be retrieved from the sample database to match the sequence $\{u_1\}, \{u_2\}, \{u_3\}$ in this strict order.

Thus, in order to avoid these drawbacks of standard sequential rules, we consider in our model partially-ordered sequential rules [45]. They define a more broad type of sequential rules common to multiple sequences, such that users in the rule antecedent are unordered. However, the requirement of a sequential relationship between the antecedent and consequent of a rule is preserved. According to this partially-ordered definition, the rules $r_i, r_{i'}, r_{i''}$ presented before can be represented by a single rule $\{u_1, u_3\} \Rightarrow \{u_5\}$. We show in Table 4.3 some rules found in our sample database (Table 4.2), considering $minsup = 0.5$ and $minconf = 0.5$.

Table 4.3: Sample of Mined Sequential Rules from Table 4.2.

| ID | Rule | Support | Confidence |
|---|---|---|---|
| $r_1$ | $\{u_1, u_2, u_3\} \Rightarrow \{u_5\}$ | 0.75 | 1.00 |
| $r_2$ | $\{u_1, u_2, u_6\} \Rightarrow \{u_5\}$ | 0.50 | 0.50 |
| $r_3$ | $\{u_1, u_2\} \Rightarrow \{u_5\}$ | 1.00 | 1.00 |
| $r_4$ | $\{u_2, u_3\} \Rightarrow \{u_6\}$ | 0.75 | 1.00 |
| $r_5$ | $\{u_3\} \Rightarrow \{u_2\}$ | 0.50 | 0.66 |
| $r_6$ | $\{u_1\} \Rightarrow \{u_2\}$ | 0.50 | 0.50 |

Finally, we only consider in our model rules occurring within a time-window ($\Delta_t$), which is a constraint used by many applications that wish to discover relevant sequential patterns within a limited time interval [98, 116, 46, 45]. As research has already demonstrated how social influence decreases over time, mainly because of effects of time constraints such as *Forgettable Span* [81], we use time-windows to discard found patterns irrelevant for social influence. They constitute sequential user posts happening within an interval greater than the one specified by the time-window, bringing spurious information to our model that is not related to influence.

This way, we make a time-window as a group of consecutive time points in our sequences of hacker posts. Then, we check how many time-windows can be generated from the beginning of a forum topic to its end, one time point at a time (defined by [46] as a sliding time-window). For example, for $\Delta_t = 3$, there are 5 different time-windows $w_1, w_2, w_3, w_4, w_5$ for the topic $\theta_1$ of Table 4.2 depicted in Figure 4.2.

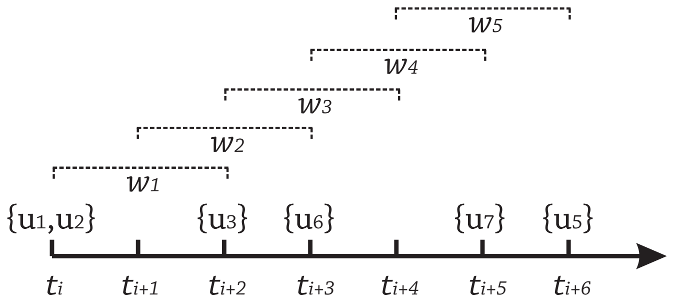

Fig. 4.2: Considered Time-Windows When $\Delta_t = 3$ for Topic $\theta_1$ of Table 4.2.

Formally, we follow the concepts proposed in [47] and define the problem of mining sequential rules with a time-window as being the same as the problem of mining sequential rules, except that a rule $X \Rightarrow Y$ occurs in a topic $\theta_x = U_1, U_2, ...U_n$ if there exist integers $j$, $k$, $m$ such that $1 \leq j \leq k < m \leq n, X \subseteq \cup_{i=j}^{k} U_i$, $Y \subseteq \cup_{i=k+1}^{m} U_i$ and $m{-}j + 1 \leq \Delta_t$, where $\Delta_t$ is defined by the user. We also consider the border cases keeping rules only for $j \leq n - \Delta_t + 1$, so that we always have $\Delta_t$ time points, and not less, to find the consequent of a rule.

We include the time-window constraint to compute the values of the two measures used to evaluate the rules. After defining a time-window ($\Delta_t$), the sequential support becomes the fraction of topics where all the users of $X$ appear before the user of $Y$ within $\Delta_t$, while the sequential confidence becomes the number of topics where all the users of $X$ appear before the user of $Y$ within $\Delta_t$ divided by the number of topics where all the users of $X$ appear within $\Delta_t$. We show in Table 4.4 how the sequential support and confidence of the rules presented in the Table 4.3 changes for $\Delta_t$ in [3,4,5].

Table 4.4: Sequential Rule Measures Considering Different Time-Windows.

| $\Delta_t$ = 3 | | | |
|---|---|---|---|
| ID | Rule | Support | Confidence |
| $r_1$ | $\{u_1, u_2, u_3\} \Rightarrow \{u_5\}$ | 0.25 | 0.33 |
| $r_2$ | $\{u_1, u_2, u_6\} \Rightarrow \{u_5\}$ | 0.00 | 0.00 |
| $r_3$ | $\{u_1, u_2\} \Rightarrow \{u_5\}$ | 0.25 | 0.25 |
| $r_4$ | $\{u_2, u_3\} \Rightarrow \{u_6\}$ | 0.25 | 0.33 |
| $r_5$ | $\{u_3\} \Rightarrow \{u_2\}$ | 0.50 | 0.66 |
| $r_6$ | $\{u_1\} \Rightarrow \{u_2\}$ | 0.25 | 0.25 |
| $\Delta_t$ = 4 | | | |
| ID | Rule | Support | Confidence |
| $r_1$ | $\{u_1, u_2, u_3\} \Rightarrow \{u_5\}$ | 0.25 | 0.33 |
| $r_2$ | $\{u_1, u_2, u_6\} \Rightarrow \{u_5\}$ | 0.25 | 0.33 |
| $r_3$ | $\{u_1, u_2\} \Rightarrow \{u_5\}$ | 0.50 | 0.50 |
| $r_4$ | $\{u_2, u_3\} \Rightarrow \{u_6\}$ | 0.50 | 0.66 |
| $r_5$ | $\{u_3\} \Rightarrow \{u_2\}$ | 0.50 | 0.66 |
| $r_6$ | $\{u_1\} \Rightarrow \{u_2\}$ | 0.50 | 0.50 |
| $\Delta_t$ = 5 | | | |
| ID | Rule | Support | Confidence |
| $r_1$ | $\{u_1, u_2, u_3\} \Rightarrow \{u_5\}$ | 0.50 | 0.66 |
| $r_2$ | $\{u_1, u_2, u_6\} \Rightarrow \{u_5\}$ | 0.25 | 0.25 |
| $r_3$ | $\{u_1, u_2\} \Rightarrow \{u_5\}$ | 0.75 | 0.75 |
| $r_4$ | $\{u_2, u_3\} \Rightarrow \{u_6\}$ | 0.50 | 0.66 |
| $r_5$ | $\{u_3\} \Rightarrow \{u_2\}$ | 0.50 | 0.66 |
| $r_6$ | $\{u_1\} \Rightarrow \{u_2\}$ | 0.50 | 0.50 |

## 4.4 Experimental Setting

In this section, we present our experiments designed to predict hacker adoption of a particular forum topic of the darkweb, mining sequential rules of hacker posts. We detail how we train and test our model under a variety of conditions and also how we compare our results with a standard baseline.

### *4.4.1 Training*

In the training phase, we mine sequential rules from $ForumX$ which contains 95 hacking-related topics. These topics comprise sequences of hacker posts, where each sequence starts with the oldest post of the topic and ends with the latest one. Our goal here is to discover the sequential rules that will be used for hacker adoption prediction. As our dataset has approximately 38 months of sequential data, we use the first 34 months ($\approx$ 90% of the period analyzed) to form our training set, which totals 298,245 posts.

Aiming to remove infrequent rules from our training data, since they have a lower chance of reflecting influence, we define $minsup = 0.1$ after analyzing some other possible values. This support value means that any sequential rule of posts must be present in at least 10 out of 95 topics within the defined time-window. In addition, to increase the correlation between the antecedent and consequent of the rules during training, we define $minconf = 0.8$, also after considering other possible values. This confidence value means that any sequential rule must have its consequent predicted in 80% of the cases within the defined time-window.

We also use two granularities (day and hour) to represent the hacker posting time (granularities commonly used for adoption prediction [81]), aiming to observe whether these granularities affect our prediction results. Table 4.5 illustrates this representation with random sequential data. As verified, when the time granularity is defined as "day", the first three posts are assigned to the same time point "01/01/2017 00:00:00", since the hours, minutes, and seconds of these posts are discarded. Following the same idea, the last two posts are assigned to the same time point "01/02/2017 00:00:00". On the other hand, when the time granularity is defined as "hour", only the first two posts are assigned to the time point "01/01/2017 10:00:00", since the hours are not discarded now. Then, the next post is assigned to the time point "01/01/2017 11:00:00", while the last two posts are assigned to the time point "01/02/2017 13:00:00".

Table 4.5: Representation of Different Posting Time Granularities.

| Time Granularity (day) | | | |
|---|---|---|---|
| Topic | User | Original Post Time | Representation |
| $\theta_5$ | $u_1$ | 01/01/2017 10:20:18 | 01/01/2017 00:00:00 |
| $\theta_5$ | $u_2$ | 01/01/2017 10:25:32 | 01/01/2017 00:00:00 |
| $\theta_5$ | $u_3$ | 01/01/2017 11:10:55 | 01/01/2017 00:00:00 |
| $\theta_5$ | $u_2$ | 01/02/2017 13:25:12 | 01/02/2017 00:00:00 |
| $\theta_5$ | $u_4$ | 01/02/2017 13:32:19 | 01/02/2017 00:00:00 |
| Time Granularity (hour) | | | |
| Topic | User | Original Post Time | Representation |
| $\theta_5$ | $u_1$ | 01/01/2017 10:20:18 | 01/01/2017 10:00:00 |
| $\theta_5$ | $u_2$ | 01/01/2017 10:25:32 | 01/01/2017 10:00:00 |
| $\theta_5$ | $u_3$ | 01/01/2017 11:10:55 | 01/01/2017 11:00:00 |
| $\theta_5$ | $u_2$ | 01/02/2017 13:25:12 | 01/02/2017 13:00:00 |
| $\theta_5$ | $u_4$ | 01/02/2017 13:32:19 | 01/02/2017 13:00:00 |

These two representations produce different sequences of user posts as demonstrated in Figure 4.3, where panel (a) and panel (b) show the sequences created when the time granularity is defined as "day" and "hour" respectively. In panel (a), there are only two time points, with the userset $\{u_1, u_2, u_3\}$ being assigned to the time point "01/01/2017 00:00:00" and the userset $\{u_2, u_4\}$ being assigned to the time point "01/02/2017 00:00:00".

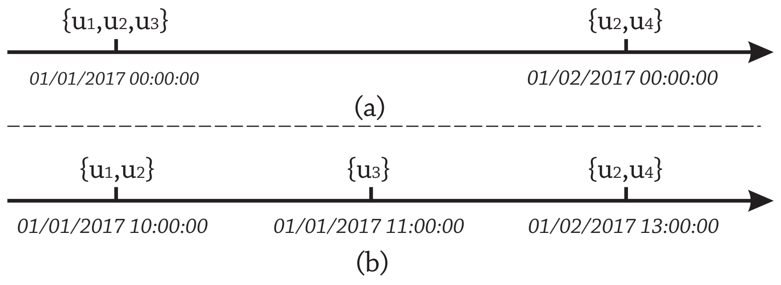

Fig. 4.3: Sequential Representation of Posts Using Different Time Granularities.

However, in panel (b), there are three time points, being the userset $\{u_1, u_2\}$ assigned to the time point "01/01/2017 10:00:00", the userset $\{u_3\}$ assigned to the time point "01/01/2017 11:00:00", and the userset $\{u_2, u_4\}$ assigned to the time point "01/02/2017

13:00:00”. Note how panel (b) contains the sequential rules $\{u_1\} \Rightarrow \{u_3\}$ and $\{u_2\} \Rightarrow \{u_3\}$, while panel (a) does not, which makes the user $u_3$ predictable only for panel (b). Setting the time granularity as “hour” generates more sequences, and we want to investigate if this implies a higher performance of our model.

In addition, we analyze 10 increasing time-window values for each time granularity, being $\Delta_t \in (2, 3, 4, 5, 6, 7, 8, 15, 22, 31)$ (sequence $d$) when considering “days” and $\Delta_t \in (48, 72, 96, 120, 144, 168, 192, 360, 528, 744)$ (sequence $h$) when considering “hours”. We want to vary $\Delta_t$ while generating rules during training in order to check which configuration leads to a better prediction accuracy during testing. Although we change the time-windows magnitude for the corresponding indices of sequences $d$ and $h$, we maintain the same time interval for all of them (e.g., 2 days = 48 hours, 3 days = 72 hours, 4 days = 96 hours, ... 31 days = 744 hours). Our intention is to have a fair comparison between both time granularities when predicting hacker adoption.

**TRuleGrowth algorithm**. To proceed with the generation of rules, we implement an extension of the TRuleGrowth algorithm [47, 46]. This algorithm was originally proposed to discover all partially-ordered sequential rules common to several sequences that have a support and confidence respectively higher than $minsup$ and $minconf$. It accepts a sliding-window constraint to find rules occurring within a maximum amount of time and the specification of the maximum number of items that can appear in the antecedent and consequent of a rule. Thus, TRuleGrowth was a natural choice to produce our training data. It allows us to specify all required constraints to our problem, also providing us an optimized performance when compared with other algorithms that address the same sequential rule mining task, such as CMDeo or CMRules [44].

We show in Figure 4.4 the number of rules generated by TRuleGrowth, considering the 10 defined values of $\Delta_t$ for each time granularity and the values assigned for $minsup$, $mincon$. The number of rules grows as we increase the value of $\Delta_t$, since there is more time to find all users that belong to a specific rule, respecting the sequential constraint among the antecedent and consequent. Also, there is a considerable difference in the number of generated rules when "hour" is set as the time granularity. Remember we are dealing with partially-ordered sequential rules that comprise a set of users in the antecedent, which makes TRuleGrowth eliminate antecedent variations of the same rule consequent. For instance, if the algorithm stores the rule $\{u_1, u_2, u_3\} \Rightarrow \{u_4\}$ it eliminates the rules as $\{u_2, u_1, u_3\} \Rightarrow \{u_4\}$ or $\{u_3, u_1, u_2\} \Rightarrow \{u_4\}$. However, TRuleGrowth stores all consequent variations of the same rule antecedent, since this condition implies in multiple hacker adoptions derived from the influence of the same individuals. For instance, both rules $\{u_1, u_3\} \Rightarrow \{u_5\}$ and $\{u_1, u_3\} \Rightarrow \{u_6\}$ are stored by the algorithm.

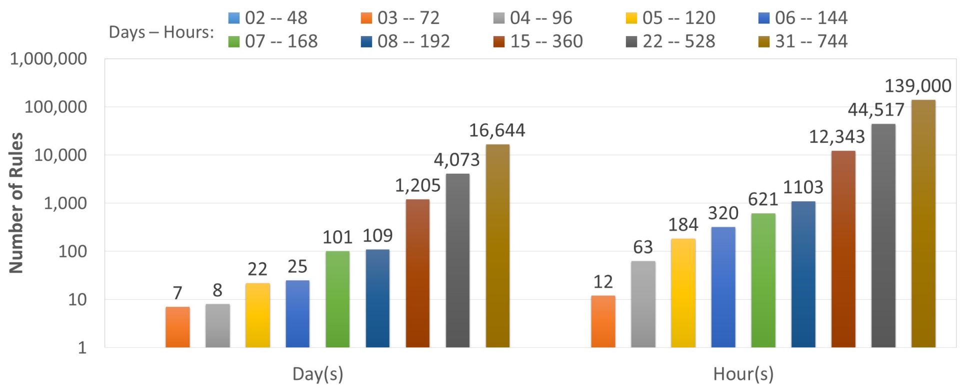

Fig. 4.4: Number of Rules Generated for 10 Values of $\Delta_t$ Considering Each Time Granularity (y-axis is in log-scale to better visualization).

As verified, no rule is generated when $\Delta_t$ = 2 and $\Delta_t$ = 48 for granularities "day" and "hour" respectively. This condition informs that there is no sequence of hackers posts among 2 consecutive days (the consequent is observed one day after the observation of the antecedent) or 48 consecutive hours in our forum data for this particular set up, pointing out that a longer time interval is required for social influence to effectively take place. Actually, many research works claim that social influence gets stronger as the number of "active neighbors" of a given user increases as time goes by (until reaches some kind of limit), since this user becomes more influenced by all these individuals together [81, 51, 40, 147].

We count in Table 4.6 the number of distinct users in the antecedent $a_{\Delta_t}$ and in the consequent $c_{\Delta_t}$ of the generated rules for each time granularity and time-window ($\Delta_t$). Note how the former is greater than the corresponding number of rules for some cases, which means that rules with different antecedent sizes (more people influencing together) are generated. The latter indicates that different consequents (influenced individuals) can be predicted by the rules.

Table 4.6: Number of Distinct Users in the Generated Rules.

| Rule Antecedent. Time Granularity (days). | | | | |
|---|---|---|---|---|
| $a_2$ = 0 | $a_3$ = 7 | $a_4$ = 8 | $a_5$ = 29 | $a_6$ = 32 |
| $a_7$ = 68 | $a_8$ = 72 | $a_{15}$ = 187 | $a_{22}$ = 227 | $a_{31}$ = 266 |
| Rule Antecedent. Time Granularity (hours). | | | | |
| $a_{48}$ = 0 | $a_{72}$ = 18 | $a_{96}$ = 52 | $a_{120}$ = 91 | $a_{144}$ = 121 |
| $a_{168}$ = 147 | $a_{192}$ = 177 | $a_{360}$ = 250 | $a_{528}$ = 283 | $a_{744}$ = 312 |
| Rule Consequent. Time Granularity (days). | | | | |
| $c_2$ = 0 | $c_3$ = 2 | $c_4$ = 3 | $c_5$ = 9 | $c_6$ = 10 |
| $c_7$ = 13 | $c_8$ = 15 | $c_{15}$ = 57 | $c_{22}$ = 77 | $c_{31}$ = 99 |
| Rule Consequent. Time Granularity (hours). | | | | |
| $c_{48}$ = 0 | $c_{72}$ = 5 | $c_{96}$ = 9 | $c_{120}$ = 20 | $c_{144}$ = 27 |
| $c_{168}$ = 37 | $c_{192}$ = 54 | $c_{360}$ = 91 | $c_{528}$ = 117 | $c_{744}$ = 128 |

### *4.4.2 Rule Significance Analysis*

Finally, we check the significance of the mined rules to determine their utility for adoption prediction. We accomplish that by comparing the conditional probability of the consequents given the antecedents with the prior probability of the consequents, considering each time-window and time granularity. We present the results in Table 4.7, showing that we obtain probability gains for all possible cases that vary from 145% until 531%.

Table 4.7: Significance Analysis of the Generated Rules.

| Time Granularity (days). | | | | | | | | |
|---|---|---|---|---|---|---|---|---|
| $\Delta t$ = 3 | $\Delta t$ = 4 | $\Delta t$ = 5 | $\Delta t$ = 6 | $\Delta t$ = 7 | $\Delta t$ = 8 | $\Delta t$ = 15 | $\Delta t$ = 22 | $\Delta t$ = 31 |
| %531 | %463 | %361 | %319 | %292 | %273 | %204 | %171 | %145 |
| Time Granularity (hours). | | | | | | | | |
| $\Delta t$ = 72 | $\Delta t$ = 96 | $\Delta t$ = 120 | $\Delta t$ = 144 | $\Delta t$ = 168 | $\Delta t$ = 192 | $\Delta t$ = 360 | $\Delta t$ = 528 | $\Delta t$ = 744 |
| %488 | %410 | %358 | %321 | %293 | %273 | %204 | %172 | %146 |

### 4.4.3 Testing and Performance Analysis

The testing phase consists in generating adoption predictions for each test case that represents a hacker or a sequence of hackers posting in the same topic. We accomplish this task in two steps. First, we identify the rule(s) that match the test case, or the rule(s) whose users in the antecedent are those who form the test case. Then, after selecting those rule(s), we choose from their consequent(s) all distinct user(s) to predict that they will adopt the topic retrieved from the test case.

In order to generate all test cases from our testing set, we use the posts from the last 4 months of our sequential data ($\approx$ 10% of the period analyzed), which totals 33,139 posts. For each time granularity and time-window, we retrieve one topic at a time to locate possible test cases. We start with test cases with size 1 (one user posting) and then move to locate test cases with size 2 (two users posting), size 3 (three users posting), until we reach the limit size identified for the antecedent of rules in our training set (5 users).

We evaluate our model computing two distinct measures. The first one is precision, which is defined as the number of correct predictions divided by the number of predictions made. The second measure is the number of predictions made, which is higher if the training set (our mined sequential rules) matches more test cases. Figure 4.5 presents the results. We observe in panel (a) that, although the two precision curves are similar, our model has slightly higher precision throughout the time-windows when we set "days" as the time granularity. For this setting, the precision successively increases when the time-window is 3 (0.416), 4 (0.510), and 5 (0.572), successively decreases through the time-windows 6 (0.440) and 7 (0.411), and successively increases again reaching the highest value in the last time-window, following 8 (0.442), 15 (0.588), 22 (0.664), 31 (0.786). In addition, panel (b) shows that more predictions are made when we set "hours" as the time granularity, since more test cases are generated. However, the difference in rule magnitude (shown in Table 4.4) between the corresponding time-windows for both time granularities (2-48, 3-72, ..., 31-744) is not reflected in the growing number of predictions, since this number only doubles in size on average (96 until 34,923 and 96 until 71,000 when considering "days" and "hours" as time granularity respectively).

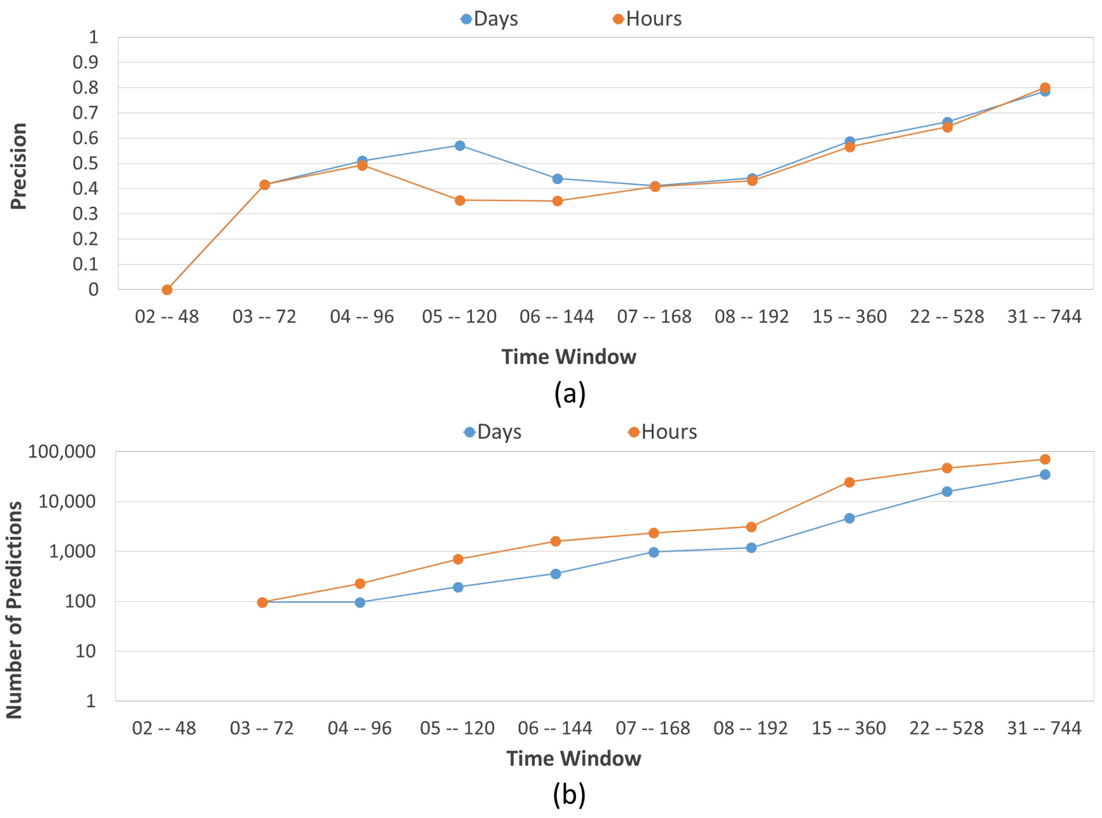

Fig. 4.5: Performance of Our Model When Predicting Hacker Adoption, Considering (a) Precision and (b) Number of Predictions (y-axis is in log-scale).

### *4.4.4 Baseline*

In this section, we informally explain a baseline predictor that we use to compare with our proposed rule-based approach. A very simple baseline approach would be predicting user engagement in any forum topic with a probability equal to the multiplication of two terms: (1) the prior probability that a user would post in any time window of length $\Delta_t$, and (2) the average fraction of forum topics on which he/she posts in any time-window with length of $\Delta_t$. Such quantities should be learned from the training dataset.

However, our baseline is less straightforward, since we assume that users vary in their posting activity. We sought to learn the prior probability of hacker adoption in a time window of length $\Delta_t$, conditioned on the user. Hence, we learn from the training data those prior probabilities and then predict hacker adoption for each test case. Having a prior probability for each user, we can predict adoption in different ways: (1) setting a threshold on prior probability, then predict hacker adoption if their prior probability is greater than the threshold, and (2) predicting hacker adoption randomly with a chance of being predicted equivalent to the prior probability [1] . With (1), few users would be predicted to post on every single topic at each time point we make predictions—such judgment is not desired; hence we use (2). Clearly, this method is non-deterministic. Therefore, we repeat the experiments 10 times and take the average precision of the runs.

Figure 4.6 presents the results. Evidently, the archived precision is way less than the rule-learning approach presented in this work. We observe in panel (a) that both curves are almost identical. They present low precision that successively increases from the first time-window until the last one, with values varying in [0.047, 0.180]. Note how the precision value range is much lower than the one outputted by our model, showing we are able to

[1]We do this by generating a random number in [0,1], sampled from a uniform distribution. If the number falls within the prior probability of a user, we predict his/her adoption, otherwise, we say that user is not going to adopt.

identify patters of sequential hacker postings among forum topics. Our assumption is that these patterns are a natural consequence of the influence process, which encourages hackers to adopt a topic within a time-window because of the influential activities of their peers.

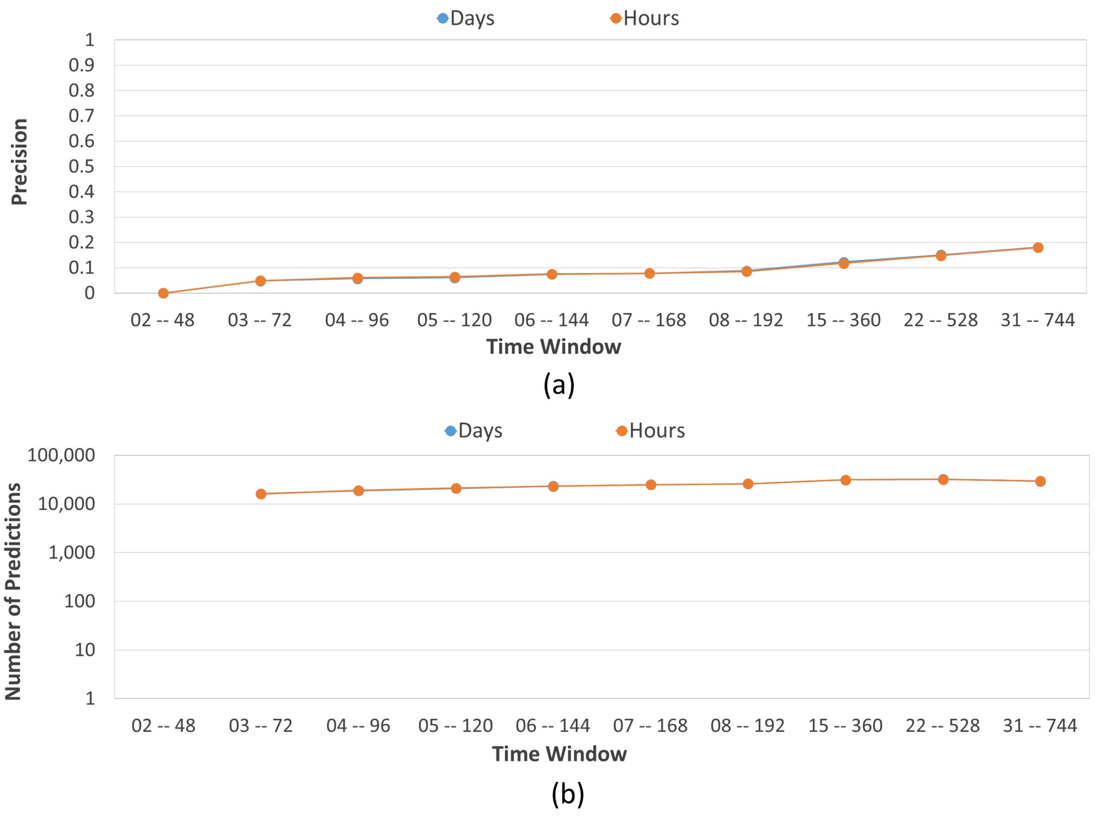

Fig. 4.6: Baseline Evaluation When Predicting Hacker Adoption, Considering (a) Precision and (b) Number of Predictions (y-axis is in log-scale).

In panel (b), we observe practically the same number of predictions for both curves (16,302 until 32,260 when considering "days" as time granularity and 16,171 until 32,015 when considering "hours"). Clearly, the variance is lower than the one produced by our model, since the method only considers the prior probabilities throughout the time-windows, neglecting other social aspects as peer-influence. We verify that, although the number of predictions of our model is relatively small (96 until 702) for short time-windows, when we increase the time-windows, the number of predictions grows until eventually passing the one produced by the baseline. From this particular point on, the precision values of our model are relatively high while the ones produced by the baseline are still very low, which corroborates our influence assumption.

Finally, we also analyze the precision gains of our model when compared to the baseline, showing the results in Figure 4.7. We discover a pattern that ratifies the findings relating to the notion of *Forgettable Span* constraint, —previously introduced in Chapter 3. As it is well known that social influence decreases over time, this constraint was proposed to determine the subset of users who should be predicted to adopt a behavior; it sets a maximum time interval for the adoption of neighbors still be remembered by the influenced users. Running experiments on Twitter and Sina Weibo, we found that when *Forgettable Span* is approximately 1.5 days, the precision of adoption prediction is maximized, decreasing after that [81]. Looking at Figure 4.7, we note the highest precision gains for hacker adoption [785%, 837%] are observed for time-windows in [3,5] days (corresponding to [2,4] days of time interval), successively decreasing for time-windows greater than that (a similar patter can be observed for setting "hours" as time granularity).

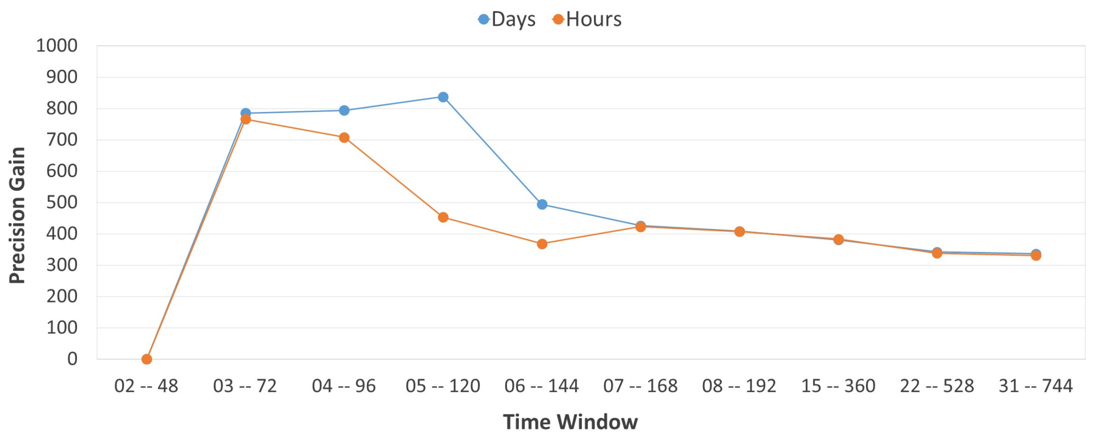

Fig. 4.7: Precision Gain of Our Model Compared to the Baseline.

Assuming that in a darkweb forum, user activity is lower than the one observed on microblogs (where ephemeral hashtags are analyzed to predict user adoption), we understand these both values are very similar. This finding is relevant since predicting within a short time is considerably more difficult than when a large time interval is given, once the latter provides more time to appear hackers posting by chance than the former. Thus, we believe our model captures the social influence process on hacking forums throughout the time.

## 4.5 Related Work

To the best of our knowledge, this is the first applied study where adoption prediction is conducted among malicious hackers on forums of the darkweb. Even so, we introduce here some works carried out on the surfaceweb that could be used to predict opinions, activities, link formation, and also participation of hackers on online forums.

Qiu et al. [101] proposed a model which leveraged user arguments, interactions, and attributes into a collaborative filtering framework for stance prediction on a surfaceweb forum. Although the model is able to infer public opinion, which could be used for understanding the hackers reasoning, it can not estimate where (topic) and when (time) a hacker will post.

Glenski et al. [49] tracked the online activity of 186 users of the popular Reddit forum over a year, in order to predict their future interactions. They formulated the task as a multi-class classification, leveraging ranking and semantic features to estimate browse-content, browse-comments, upvote, downvote, or do-nothing behavior for each post visualized. This technique can be used to predict behaviors with respect to an existing post, but it is not able to anticipate a new one.

Yang et al. [129] analyzed user activity in a popular underground forum of the surfaceweb, combining social network analysis, logistic regression, and clustering to first preselect a list of potential key actors (users who have been linked to criminal activities). Then, they filtered key terms used by those individuals in their posts to predict who is actually a key actor. The idea is relevant to profile skilled hackers, but no predictive method was included to foresee new content.

Sadeque et al. [110] developed a time-series methodology for predicting link formation in real-world datasets from Massive Open Online Course (MOOC) discussion forums. They leveraged neighborhood, path, and post-based quantities between learners as features to a Long-Short Term Memory (LSTM) Recurrent Neural Network (RNN) units, in order to forecast interactions between two users (link) in a thread. Although this model can be used to predict hacker posts, we identify three main drawbacks here: first, training is costly because of the different nature of the features; second, the prediction is done taking into consideration only one neighbor; finally, the links are bidirectional, making the prediction of user $u_2$ given user $u_1$ also valid for cases in the opposite direction.

## 4.6 Summary

In this Chapter, we study the adoption behavior among hackers on the darkweb, aiming to predict their future adoptions of a particular forum topic, given the influence produced by their peers. We accomplish this task by leveraging sequential rule mining to discover user posting rules through sequences of user posts, to later use these rules to make the predictions. We analyze the performance of our model when it uses different time granularities to represent the posts and also multiple time-windows for mining the sequential rules, obtaining results that by far overcome the prior probabilities of hackers posts. Our model provides an alternative strategy for security researchers to anticipate the participation of cyber criminals in hacking-related forum topics. With this insight, organizations can better monitor their networks for threats and exploitable vulnerabilities, extending their reach to cover forums where hackers often share valuable information.

Chapter 5

# DETECTING COMMUNITIES OF MALWARE AND EXPLOIT VENDORS ON DARKWEB MARKETPLACES

## 5.1 Introduction

Recently, darkweb hacking marketplaces have become a central venue for online purchasing of malicious products and services by cyber criminals, who take advantage of the numerous offerings provided especially by trustful and well succeeded key-hackers. An example that illustrates this fact is given by Nunes et. al in [92]. An exploit targeting a Microsoft Windows vulnerability CVE-2015-0057 was for sale on a darkweb marketplace in March 2015. The corresponding vulnerability was disclosed by Microsoft a month earlier, with no publicly available exploit at that time. Four months after the availability of the exploit, FireEye reported that the Dyre banking Trojan - designed to target organizations to steal credit card information - had used the exploit [41]. See [7] for more examples.

In this context, consider the importance of finding communities of vendors with similar hacking expertise for surveillance purposes. Many vendors possibly linked to the Dyre Banking Trojan, could be automatically identified if at least one of them had been already confirmed as offering the exploit online, allowing defenders to anticipate subsequent similar product offerings. In more complex scenarios, those communities might correspond to sets of individuals dealing with similar products or services in some specific subfields of hacking, such as carding, phishing, and keyloggers, which is a feature typically owned by key-hackers. Therefore, detecting all individuals forming specialized hacker communities becomes another form of discovering who are in the the expanding network of key-hackers, helping defenders to anticipate their imminent cybercriminal activities.

In this Chapter, we explore a new method based on (SNA) and (ML) techniques to identify and validate communities of malware and exploit vendors on darkweb hacking marketplaces. As there is no direct communication between vendors in those environments, we start by collecting information about their hacking-related product offerings in 20 different markets, from where we produce a similarity matrix of the vendors. To create this matrix, we leverage unsupervised learning to cluster the vendors' products into the 34 main hacking categories proposed by our prior work published at [80]. Then, we quantify the similarity between vendors by analyzing the number of product categories shared between them and also the number of products they have in each product category. Finally, as a way to address the lack of ground truth (the existing vendor communities in the markets), we split the marketplaces into two disjoint sets to detect the community overlapping between them. Our results demonstrate how the multiplexity of social ties [137, 75, 85, 84], which makes individuals interact in multiple domains, help us to validate a considerable part of the mined communities. This Chapter makes the following main contributions:

- We cluster around 40,000 hacking-related products using 34 product categories;
- We calculate the similarity of hacking vendors applying different metrics over their products and product categories, inferring the implicit connections among them;
- We perform community finding to detect the communities of hacking-related vendors in two disjoint sets of marketplaces, validating our results by checking the overlapping between them. We found the ARI score achieves 0.445 using our method, while randomly assigning individuals to communities yields an ARI of -0.006.

The remaining of this Chapter is structured as follows. Section 5.2 introduces darkweb marketplaces and our dataset. Section 5.3 describes our methodology, detailing its modules, experiments, and corresponding results. We discuss related work in Section 6.6. Finally, Section 6.7 summarizes the Chapter.

## 5.2 Darkweb Hacking Marketplaces

People who want to shield their product offerings from government surveillance may require the cover of the darkweb, and that would not be different for malicious hackers and exploit vendors. These individuals require a marketplace infrastructure to safely commercialize their illegal cyber threats, keeping their activities hidden from law-enforcement agencies. Basically, all darkweb hacking marketplaces require a registration and a valid account to get access. Sometimes, this registration process is not trivial, including effort to answer questions and solve puzzles, mathematical equation or CAPTCHA [80]. Products are often verified before any funds are released to the vendor. As a way to keep the monetary transactions untraceable, Bitcoin is the currency often used in those environments [104].

### *5.2.1 Dataset*

In this work, we select 20 popular English hacking-related marketplaces from the darkweb provided CYR3CON [28]. We anonymously show in Table 5.1 the number of hacking-related products and the number of vendors found in each market.

Table 5.1: Darkweb Marketplace Statistics.

| Marketplace | Products | Vendors | Marketplace | Products | Vendors |
|---|---|---|---|---|---|
| *Market 1* | 22,956 | 525 | *Market 11* | 1,136 | 87 |
| *Market 2* | 13,423 | 1,323 | *Market 12* | 1,122 | 63 |
| *Market 3* | 9,936 | 856 | *Market 13* | 995 | 34 |
| *Market 4* | 7,360 | 243 | *Market 14* | 936 | 40 |
| *Market 5* | 3,443 | 1,439 | *Market 15* | 739 | 61 |
| *Market 6* | 3,437 | 1,625 | *Market 16* | 527 | 6 |
| *Market 7* | 3,328 | 266 | *Market 17* | 328 | 18 |
| *Market 8* | 1,358 | 131 | *Market 18* | 302 | 135 |
| *Market 9* | 1,269 | 589 | *Market 19* | 182 | 26 |
| *Market 10* | 1,264 | 106 | *Market 20* | 159 | 32 |

## 5.3 Methodology

This section explains the steps of our methodology designed to reveal the communities of malicious hacking-related vendors on the darkweb, as illustrated in Figure 5.1.

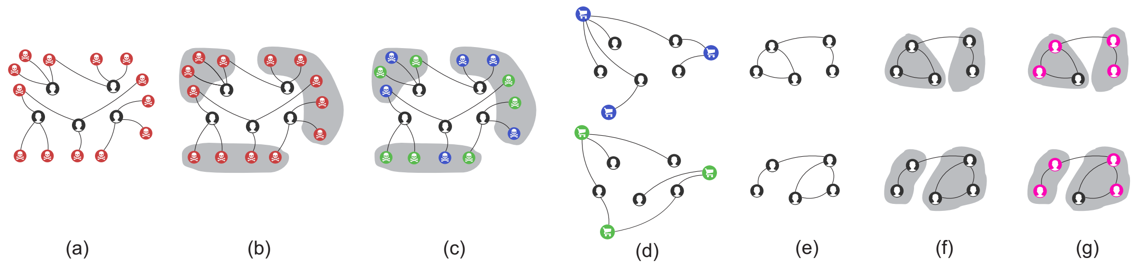

Fig. 5.1: Methodology. (a) Creating a Bipartite Network of Vendors and Products, (b) Clustering the Products in Product Vategories, (c) Splitting the Marketplaces into Two Disjoint Sets (green and blue), (d) Creating Bipartite Networks of Vendors and Product Categories, (e) Projecting Bipartite Networks of Vendors and Products Categories into Monopartite Networks of Vendors, (f) Finding the Communities of Vendors in Each set of Markets, (g) Calculating the Community Overlapping Between the Two Sets of Markets.

### 5.3.1 *Creating a Bipartite Network of Vendors and Products*

The first step of our methodology consists of collecting the malicious hacking products offered by each vendor on the marketplaces to generate a bipartite network of vendors and their corresponding products. Therefore, the nodes of this bipartite graph are formed by vendors and products, while the edges are created only between these two type of nodes. We use the vendors' screen-name and products' names to uniquely identify vendors and products in this Chapter. By analyzing the vendors' screen-names, we note that many products are cross-posted by vendors in multiple sites. This happens since vendors usually adopt the strategy of using the same screen-name in different marketplaces to transfer their reputation [92]. As the great majority of screen-names are personal and exotic, we believe that applying string-match over them is a reasonable approach to uniquely identity individuals [1] . Figure 5.2 (a) shows the distribution of vendors who use the same screen-name across multiple marketplaces. As observed, there is no exclusive vendor for any marketplace, and two of these environments share almost 200 vendors with other markets.

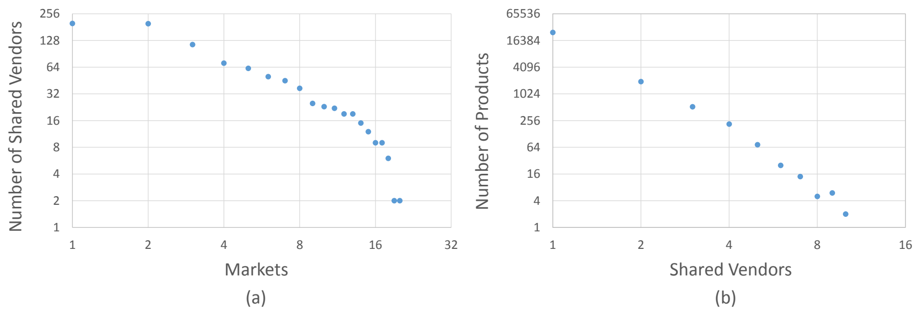

Fig. 5.2: Distribution of (a) Shared Vendors Over Markets, (b) Products Over Shared Vendors (in log-log scale).

As our method uses duplicated vendors in different set of marketplaces to validate the results, we filter our dataset to consider only vendors present in at least two markets, bringing their corresponding products. Table 5.2 shows the size of the original and the filtered datasets. By using this filtered data, we generate a bipartite graph considering the vendors and distinct products as two disjoint sets of nodes, and the total number of products as the connecting edges.

Table 5.2: Scraped Data from Darkweb Marketplaces.

| Original | | Filtered | |
|---|---|---|---|
| Marketplaces | 20 | Marketplaces | 20 |
| Products (Total) | 74,200 | Products (Total) | 40,610 |
| Products (Distinct) | 51,902 | Products (Distinct) | 27,581 |
| Vendors | 7,605 | Vendors | 390 |

[1]We leave other methods of similarity-based comparison to future work.

### *5.3.2 Clustering the Products in Product Categories*

As we collect data from different sites, there is inconsistency as to how products are categorized on each site - if such non-trivial categorization even exists for a given site. Furthermore, there is a clear absence of a standardized method for vendors to register their products. As a consequence, the majority of the products are unique when compared with simple matching or regular expression technique. It is valid even in the case where a pair of vendors with different screen-names post what a human would determine to be the same product. Figure 5.2 (b) shows the distribution of products and the vendors shared between them. We observe that around 70% of the distinct products belong to only a single vendor.

In order to mitigate this inconsistency, we cluster the products into the 34 hacking categories that we defined in [80]. The idea is to make the vendors share more information, assigning similar products to the same product category. This strategy allows us to generate a more precise matrix of vendors similarity, using their shared product categories and the corresponding products. Following the approach in [80], we apply character n-grams (in the range from 3 to 6) over the product names, aiming to engineer features that represent products as vectors. Then, we value all features using term frequency - inverse document frequency (TF-IDF), after eliminating stopping words and executing steaming. Finally, we run K-Means to produce the 34 product categories ranked and detailed in Table 5.3.

To run k-means, we first manually label 400 samples using those 34 product categories (the "K" parameter of K-Means), ensuring at least 10 samples for each cluster. We use those samples to determine the initial centroids for each cluster, instead of doing this task randomly. Finally, we run K-means using cosine similarity as the distance function (spherical K-Means [56]) in the entire dataset (27,581 distinct products). As verified in Table 5.3, "Netflix-related" is the top first product category in terms of number of products assigned, following a trend observed in [80]. Nevertheless, other product categories emerged

Table 5.3: Product Categories.

| Rank | Cluster Name | Nº of Products | Nº of Markets | Nº of Vendors | Rank | Cluster Name | Nº of Products | Nº of Markets | Nº of Vendors |
|---|---|---|---|---|---|---|---|---|---|
| 1 | Netflix-related | 3786 | 16 | 186 | 18 | RDP Servers | 938 | 17 | 130 |
| 2 | Viruses/Counter AntiVirus | 3216 | 14 | 61 | 19 | Physical Layer Hacking | 935 | 18 | 122 |
| 3 | VPN | 3064 | 14 | 66 | 20 | Exploit Kits | 858 | 19 | 123 |
| 4 | Keyloggers | 2662 | 18 | 221 | 21 | Smartphone - General | 791 | 17 | 141 |
| 5 | Linux-related | 1875 | 14 | 69 | 22 | Ebay-related | 780 | 16 | 92 |
| 6 | Carding | 1634 | 17 | 171 | 23 | Windows-related | 708 | 17 | 96 |
| 7 | Hacking Tools - General | 1610 | 15 | 111 | 24 | Password Cracking | 615 | 18 | 113 |
| 8 | PGP | 1609 | 14 | 120 | 25 | Network Security Tools | 615 | 15 | 75 |
| 9 | Facebook-related | 1526 | 15 | 97 | 26 | Botnet | 611 | 18 | 87 |
| 10 | Point of Sale | 1275 | 18 | 131 | 27 | Bitcoin | 595 | 16 | 116 |
| 11 | Dumps - General | 1227 | 16 | 99 | 28 | Phishing | 587 | 16 | 107 |
| 12 | Network Layer Hacking | 1181 | 17 | 134 | 29 | Android-related | 523 | 16 | 69 |
| 13 | PayPal-related | 1148 | 15 | 133 | 30 | Hacking Groups Invitation | 473 | 15 | 92 |
| 14 | Cashing Credit Cards | 1134 | 18 | 124 | 31 | Amazon-related | 464 | 16 | 94 |
| 15 | Browser-related | 1038 | 15 | 104 | 32 | Wireless Hacking | 442 | 15 | 77 |
| 16 | Banking | 959 | 15 | 139 | 33 | Links (Lists) | 409 | 12 | 100 |
| 17 | RATs | 940 | 16 | 104 | 34 | Email Hacking Tools | 382 | 16 | 96 |

such as "Viruses/Counter AntiVirus", "VPN", "Keyloggers", and "Linux-related", followed by the one also pointed by [80] as very active ("Carding"). We also inform the number of markets and vendors assigned to each product category. "Exploit Kits" appears as the product category most spread among the 20 markets (19), while "Keyloggers" appears as the one most spread among vendors (221).

### 5.3.3 Splitting the Marketplaces into Two Disjoint Sets

In this Chapter, we assume that vendors on darkweb hacking marketplaces strive to build social status and trust, and one common way to accomplish that is by using the same screen-name in different environments. This assumption is common across research work on darkweb data [7, 104]. For this reason, we decide to split our dataset into two partitions, using an optimization process to produce a division that maximizes the redundancy of vendors in both partitions. We will leverage this redundancy to check if the communities found in one part of the data are also present in the other one. Formally, we implement an optimization algorithm to produce the best split of all 20 markets (set $M$) into 2 nonempty and disjoint sets. Thus, $M_1 \neq \varnothing$, $M_2 \neq \varnothing$, $M_1 \cap M_2 = \varnothing$, and $M_1 \cup M_2 = M$, and the complexity of the algorithm for $n$ markets is $O(2^{(n-1)} - 1)$. Considering $V_{M_1}$ and $V_{M_2}$as the set of vendors present in $M_1$ and $M_2$ respectively, our objective function seeks to maximize the number of duplicated vendors in these both sets, as shown in equation 5.1:

$$\max f(V_{M_1}, V_{M_2}),\ with\ f(V_{M_1}, V_{M_2}) = |\{V_{M_1} \cap V_{M_2}\}| \tag{5.1}$$

Table 5.4 presents the results of the data split algorithm, showing that we found 329 duplicated vendors in our two disjoint sets of markets. We will use these individuals to verify if they form similar communities in these two different environments.

Table 5.4: Results of the Marketplaces Split.

| | $M_1$ | $M_2$ |
|---|---|---|
| Number of Markets | 10 | 10 |
| Number of Products | 13,486 | 27,124 |
| Number of Vendors | 345 | 374 |
| Number of Duplicated Vendors in Both Sets | 329 | |

### 5.3.4 Creating Bipartite Networks of Vendors and Product Categories

At this point, we are able to connect the vendors to their product categories in a bipartite graph, allowing us to check which categories are shared between them. Figure 5.3 illustrates this process with a subset of the graph within set $M_1$. In panel (a), the vendors are connected to their products, which in turn are connected to their categories. In panel (b), we plot the same graph without the products to better visualize the shared product categories between the vendors. Vendors who were previously disconnected from others (note the 9 disconnected components highlighted in panel (a), since the vendors mostly own exclusive products) are now connected using the shared product categories in panel (b).

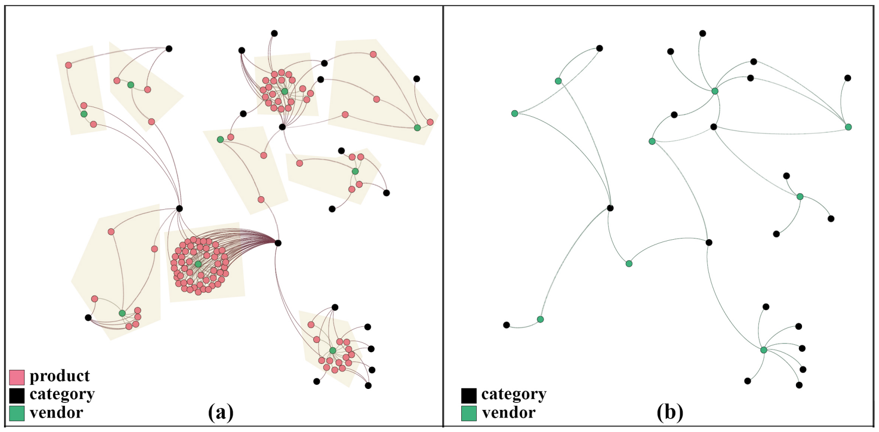

Fig. 5.3: Sample of the Network of Vendors, Products, and Product Categories (a). The Same Network is Shown in Panel (b) but Hiding the Products.

Figure 5.4 shows the distribution vendors over product categories in sets (a) $M_1$ and (b) $M_2$. Both distributions are similar and point out the majority of vendors (≈ 63%) are assigned to more than one product category in both sets of marketplaces. This condition increases the probability of creating new connections in the graph, although vendors assigned to a single product category are in most of the cases sharing it with other individuals.

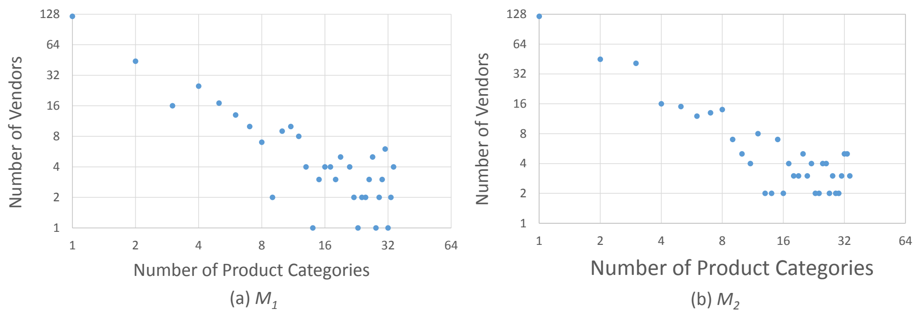

Fig. 5.4: Distribution of Vendors Over Product Categories in Sets (a) $M_1$ and (b) $M_2$.

Overall, the number of connections created between vendors and product categories in both subsets of markets is around 2,500 (7.5 on average for each one of the 329 duplicated vendors).

### 5.3.5 *Projecting Bipartite Networks of Vendors and Product Categories into a Monopartite Network of Vendors*

After discovering the shared product categories between vendors, our next challenge is to project the corresponding bipartite graphs of vendors and product categories into monopartite graphs of vendors. This step is crucial for this work, since the algorithms we are going to use to find the communities of vendors were designed to work with networks with single-type nodes (such as vendors), and not to work with multimodal networks [15].

To accomplish this task, we create a similarity matrix between vendors using two pieces of information: their product categories and their corresponding products. The former information basically creates a binary matrix connecting vendors and product categories, where "1" means the vendor has a least one product in the corresponding product category, and "0" otherwise. The latter information adds magnitude to the product categories owned by vendors, including the number of products vendors have within each product category. We use both information to create a similarity matrix between vendors, considering an edge between two specific individuals if the corresponding similarity (weight) is greater than a given threshold $\delta$. To calculate this weight, we use four different similarity metrics according to Table 5.5.

Table 5.5: Similarity Metrics.

| Metric | Formula |
|---|---|
| Jaccard [130] | $J(V_i, V_j) = \frac{M_{11}}{M_{01}+M_{10}+M_{11}}$, where $V_i$ and $V_j$ are two binary vectors corresponding to the assignment of existing product categories for vendors $i$ and $j$, $M_{11}$ represents the number of product categories where $V_i$ and $V_j$ both have a value of 1, $M_{01}$ represents the number of product categories where the product category of $V_i$ is 0 and the product category of $V_j$ is 1, and $M_{10}$ represents the number of product categories where the product category of $V_i$ is 1 and the product category of $V_j$ is 0. |
| Cosine [130] | $Cos(V_i, V_j) = \frac{V_i \bullet V_j}{\|V_i\|\|V_j\|}$, where $V_i$ and $V_j$ are two non binary vectors corresponding to the assignment of the total number of products within each existing product categories that belong to vendors $i$ and $j$. |
| Correlation [130] | $Corr(V_i, V_j) = \frac{cov(V_i, V_j)}{\sigma_{(V_i)} * \sigma_{(V_j)}}$, where $V_i$ and $V_j$ are two non binary vectors corresponding to the assignment of the total number of products within each existing product categories that belong to vendors $i$ and $j$, $cov(V_i, V_j)$ is the covariance of $V_i$ and $V_j$, and $\sigma_{(V_i)}$ is the standard deviation of $V_i$. |
| Tanimoto [130] | $T(V_i, V_j) = \frac{V_i \bullet V_j}{\|V_i\|^2 + \|V_j\|^2 - V_i \bullet V_j}$, where $V_i$ and $V_j$ are two non binary vectors corresponding to the assignment of the total number of products within each existing product categories that belong to vendors $i$ and $j$. |

The idea of calculating those similarity metrics is to use them to weight the edges of our graphs, since those weights should represent the level of similarity between vendors. We rely on the assumption that vendors with a high similarity based on their product offerings will form a community of interests in the real world. Figure 5.5 illustrates this process of projecting a bipartite network of vendors and product categories - panel (a) - into a monopartite network of vendors - panel (b). The network shown in Figure 5.5 (a) is the one shown in 5.3 (b). Note how we can see the vendors directed connected to each others in a weighed graph in Figure 5.5 (b).

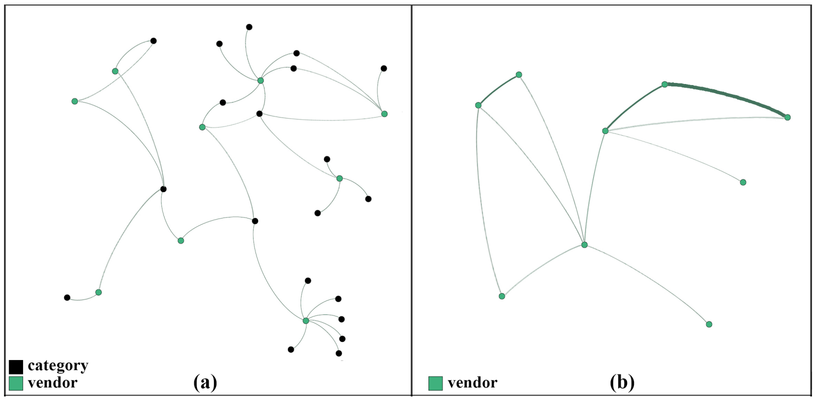

Fig. 5.5: Sample of the Network of Vendors and Product Categories (a) Projected into a Network of Vendors (b).

### *5.3.6 Finding the Communities of Vendors in Each Set of Markets*

After producing the network of vendors, we search for the existing communities in both sets of marketplaces. The methods described in this work assume a non-overlapping community network structure, which means that every vertex (vendor) belongs to only one of the communities. Algorithms in this context can be broadly grouped into three types: (1) *Hierarchical algorithms* construct a tree of communities based on the network topology, being classified as divisive [48] and agglomerative algorithms [24]; (2) *Modularity-*

*based algorithms* optimize the modularity objective function to uncover communities in the networks [90], being our choice for this work; (3) *Other algorithms* include label propagation, spectral methods that use eigenvectors of Laplacian or standard matrix, and methods based on statistical models [43]. In addition, when studying communities, we are interested in detecting either (1) specific members (member-based community detection) or (2) specific forms of communities (group-based community detection) [143]. Here, we work with group-based community detection algorithms, since we are interested in finding communities that own high modularity.

Modularity is a measure designed to compute the strength of a network division into modules (groups), checking how likely the community structure found is created at random [143]. Clearly, community structures should be far from random, therefore, the more distant they are from randomly generated communities, the more structure they exhibit. Modularity defines this distance as a scalar value between -1 and 1, and modularity maximization tries to maximize this distance [90]. Networks with high modularity have dense connections between the nodes within modules but sparse connections between nodes in different modules. Consider an undirected graph $G(V,E), |E| = m$, two nodes $v_i$ and $v_j$, with degrees $d_i$ and $d_j$, respectively, and a partitioning of the graph into $k$ partitions, $P = (P_1, P_2, P_3, ..., P_k)$. For partition $P_x$, the distance from randomly generated communities can be defined as [143]:

$$\sum_{v_i, v_j \in P_x} A_{ij} - \frac{d_i d_j}{2m} \tag{5.2}$$

Then, this distance can be generalized for partitioning $P$ with $k$ partitions as [143]:

$$\sum_{x=1}^{k} \sum_{v_i, v_j \in P_x} A_{ij} - \frac{d_i d_j}{2m} \tag{5.3}$$

The summation is over all edges $m$, and because all edges are counted twice $(A_{ij} = A_{ji})$, the normalized version of this distance is defined as modularity $Q$ as [90]:

$$Q = \frac{1}{2m}(\sum_{1}^{k} \sum_{v_i, v_j \in P_x} A_{ij} - \frac{d_i d_j}{2m}) \tag{5.4}$$

Optimizing the value of $Q$ theoretically results in the best possible grouping of the nodes of a given network. However, going through all possible iterations of the nodes into groups is impractical and heuristic algorithms are used. In this work, we use the Louvain heuristic method of community detection [15] to find our communities of vendors. This method iteratively finds small communities by optimizing modularity locally on all nodes to later group each small community into one node. It is similar to the original method proposed by Newman [90], connecting communities whose combination produces the largest increase in modularity. Figure 5.6 shows the produced communities and inform the modularity $Q$ found in $M_1$ (0.579) and $M_2$ (0.514) using Jaccard similarity metric. These values indicate that both networks present a considerable clustering property. Louvain community detection algorithm found 46 and 37 communities in $M_1$ and $M_2$ respectively.

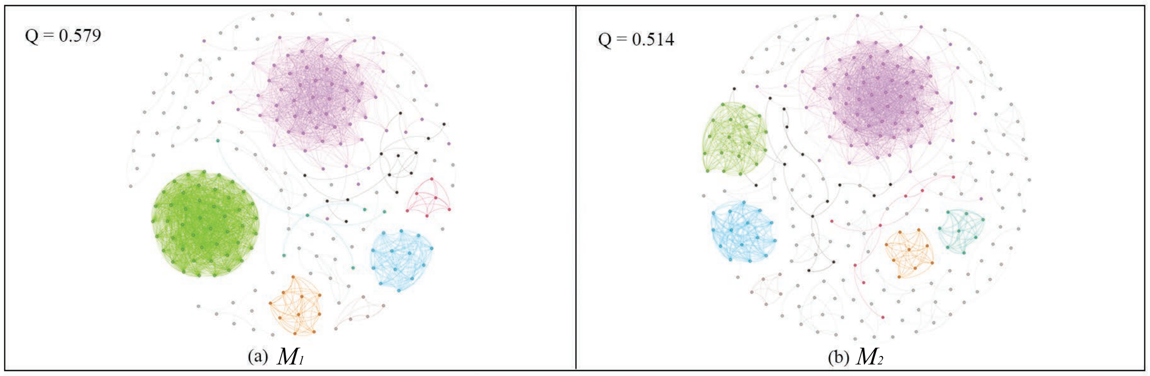

Fig. 5.6: Communities Found for $\delta$ = 0.51 in $M_1$ (a) and $M_2$ (b) Using Jaccard Similarity Metric.

The corresponding distribution of vendors per community is presented in Figure 5.7.

Both sets present a similar power law distribution, with most communities including few vendors while some few communities include many individuals.

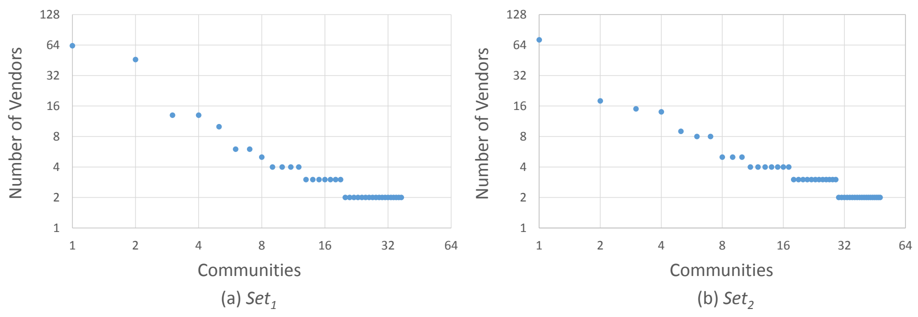

Fig. 5.7: Distribution of Vendors per Community in $M_1$ (a) and $M_2$ (b).

### 5.3.7 *Calculating the Community Overlapping between the Two Sets of Markets*

Finally, we move to the final step of our work: the validation of the communities. As mentioned before, we accomplish this task by checking the community overlapping in both sets. A high agreement here would mean a strong similarity between the vendors and consequently a strong likelihood of them belong to the same community in the real world. In order to calculate this level of agreement between both sets, we use the Adjusted Rand Index (ARI) proposed in [58]. This metric produces a score between [-1,1] according to the number of agreements and disagreements of the groups produced by two sets. Jointly, we prune the generated networks varying the threshold $\delta$ in [0,0.99] (considering the step as 0.01) to verify how the ARI changes accordingly. In addition, we also analyze the trade-off between the threshold $\delta$ and the total number of vendors possible to be identified. Figure 5.8 shows the results for our networks of vendors created using the four similarity metrics.

As verified in Figure 5.8, the highest value identified for ARI (0.445) is produced when we use Jaccard similarity to create the network of vendors, and when we set the value of $\delta$ as 0.51. These results show that only the product categories are relevant to create the similarity matrix of vendors (binary matrix), and their magnitude (number of products in

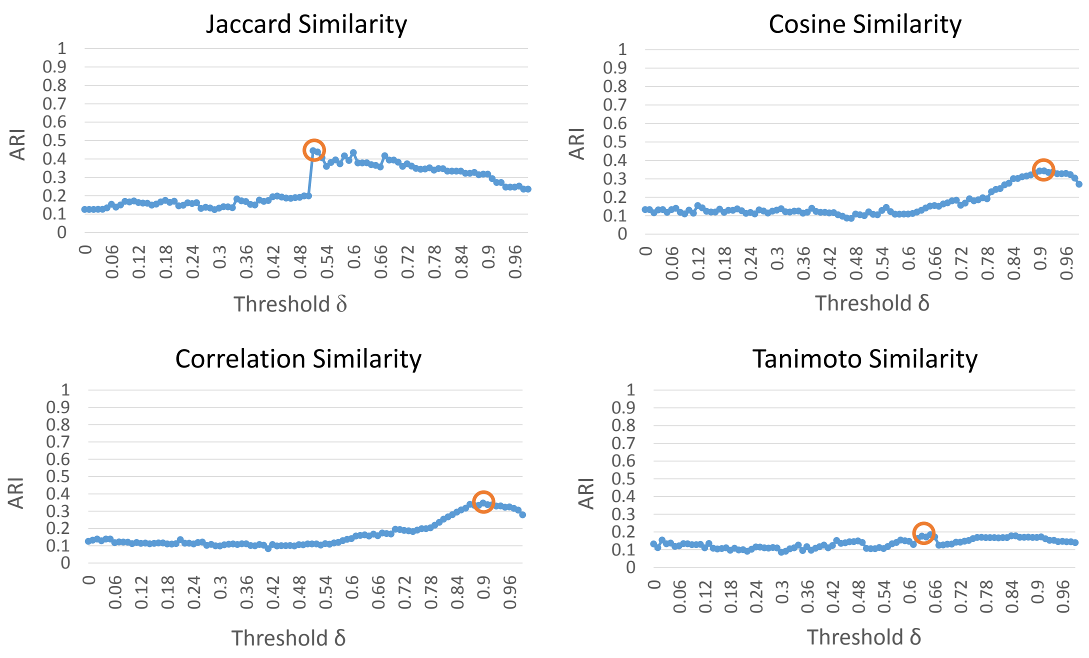

Fig. 5.8: Curve of Adjusted Rand Index (ARI) Produced for Our Four Networks When We Vary the Threshold $\delta$.

each category) should be avoided. We observe that the number of vendors correctly assigned in both sets to the same community is 169, which represents 51.3% of the possible number of vendors that could be matched.

### *5.3.8 Significance analysis*

After identifying the communities of vendors in both sets, we make a final examination of the distribution of vendors per communities shown in Figure 5.7. Our intention here is to check if the creation of those agreements between both sets could not be easily done at random. In order to accomplish that, we get the number of vendors present in each community and apply the same distribution to a randomly community assignment method, carrying out this experiment for both sets. Our results show a value of -0.006 calculated for ARI, which clearly demonstrates a non-randomness property of our method.

## 5.4 Related Work

To the best of our knowledge, this is the first applied study where social network information of malware and exploit vendors is derived from darkweb malicious hacking marketplaces. We note that with the exception of our own work [103, 92, 80, 117] - which laid the groundwork for the current study - no previous work has examined malicious hacking marketplaces in this manner. Previous studies examined characteristics of malicious hacking forums, aspects of non-malicious hacking markets, or the products for sale in a hacking market. In the following, we will introduce some of them.

In [69], two topic-based social networks were created, one from the topic creator perspective and the other from the repliers perspective. The authors tried to identify group of topics as well as group of key-members who created them. These topics could be anything (e.g. potential home land security thread). Both networks were built over the same database that consists of a single forum on the darkweb monitored for about 14 months. Yang et. al [142] used the same dataset with a different approach. They tried to form clusters of users based on their messages' timestamps, and then compared user activeness, instead of depending on messages content or link analysis. The goal was to discover the focused theme of discussion in each cluster. Anwar et. al [10] treated each post as an entity with its own related information (author, timestamp, thread, etc.) and tried to cluster them using agglomerative clustering, based on similarities between each pair of entities. This work used surfaceweb sites including 58 forums.

Additionally, there is a complementary research on malicious hacking forums (i.e. [142, 12, 72, 150, 22, 119, 122, 117]). Unlike our study, the relationships in darkweb forums can be easily observed from the post/reply activities of forum users, while in marketplaces there is no explicit communications amongst vendors. Then, inferring those relationships is a significant novel contribution of this work. Our previous studies on marketplaces [103, 92, 80] focused on: 1) a game theoretic analysis of a small subset of the data in this work; 2) classify products as malicious hacking-related; 3) categorize the malicious hacking-related products for sale; and did not attempt to find any social structure of vendors, such as communities.

## 5.5 Summary

In this Chapter, we mine communities of malware and exploit vendors on 20 darkweb marketplaces, connecting different vendors based on their product offerings. The multiplexity of social ties allows us to find these hidden communities using two different sets of markets (using social network analysis and machine learning techniques) and then successfully validate the results. We start with a bipartite network of vendors and products, transformed it in a bipartite network of vendors and product categories, to finally project this network into a monopartite network of vendors. To accomplish that, we use a combination of product clustering, similarity functions to connect vendors, and community finding algorithms to identify the community of vendors. Finally, we analyze the overlapping of the communities identified in our both sets of markets, observing a reasonable value for this metric. Our method can be considered one further step towards comprehending implicit hacker networks formed on the darkweb, helping law enforcement agencies track suspicious hacking-related organizations and their activities in real time.

Chapter 6

# REASONING ABOUT FUTURE CYBER-ATTACKS THROUGH SOCIO-TECHNICAL HACKING INFORMATION

## 6.1 Introduction

To achieve proactive intelligence-driven security, organizations need to identify whether they will be a target for future cyber-attacks, checking for instance, which software vulnerabilities are about to be exploited by malicious hackers [7]. Unfortunately, this is not a simple predictive task. As cyber-crime absorbs a huge number of vulnerabilities and organizations have limitations on time and resources to keep pace with this underground cyber world, patching all software flaws is usually not an option. As soon as the security teams make a progress, a new batch of vulnerabilities arises, keeping the defenders continuously behind [104]. However, as past research has shown that only a small percentage of those vulnerabilities are actually exploited in cyber-attacks [9, 6], mining the interest of malicious hackers allows for a better assessment of the real risk that each vulnerable target is exposed to. Thus, organizations are constantly trying to identify which are the probable IT targets of cybercriminals, although the available processes for this task are still not effective [7, 17].

In this Chapter, we combine inductive and deductive reasoning into a temporal logical framework to predict cyber-attacks. We use causal reasoning [64] and logic programming (in particular the concepts from Annotated Probabilistic Temporal (APT) logic [121, 123]) to learn predictive rules of the form: "if a relevant malicious hacking activity $x$ is observed, then there will be a cyber-attack of type $y$, targeting organization $o$, after exactly $\Delta t$ time units, with probability in $[l, u]$" [1] . We consider as malicious hacking activity any

[1]We also extend our analysis to make predictions within a period of time $\Delta t$.

vulnerability mentioned by a hacker in a collection of darkweb forums, and its relevance for attack prediction is captured by two factors: 1) socio-personal indicators obtained from the hacker mentioning the vulnerability (e.g., the measured activity, influence or expertise of the individual); 2) technical indicators obtained from the mentioned vulnerability (e.g., a recent patch or an exploitation script being released). Cybersecurity research has been showing that both factors are strongly correlated with cyber-attacks, since skilled and reputable hackers are usually more successful in their endeavors [5], while newly disclosed exploitable vulnerabilities attract more hacker attention worldwide [104].

In addition, we collect 239 real-world cyber incidents from the logs of a commercial enterprise. Thus, malicious hacking activities and cyber incidents are used as pre and post-conditions during the induction phase, where our goal is to inform when (a precise day), where (the target company) [2] and how (the method used) a particular attack is likely to happen. Finally, to improve the accuracy of our model, we perform deduction to combine multiple attack predictions made for a given day. We accomplish that by finding the tightest probability bounds of the corresponding cyber-attacks, adjusting the confidence with which our model makes the predictions. This Chapter makes the following main contributions:

1. We collect more than 7,800 posts with vulnerability mentions from 56 darkweb forums and correlate them with real-world attack incidents, generating an APT-logic program able to predict future cyber-attacks;

2. We consider in our model socio-technical indicators of enterprise attacks, demonstrating how reputable hackers pose credible threats to organizations;

3. During induction, we mine 55,245 APT rules that reach up to 562% in probability gains when compared to the prior probability of attacks. The framework presents

[2]Although we work with real-world data from a single enterprise, the framework is prepared to work with data from multiple enterprises simultaneously.

average F1 score gains of 125%, 104%, 109%, 73%, 70%, 150%, and 58% for $\Delta t$ in [1, 2, 3, 4, 5, 6, 7] days respectively when compared to a baseline predictor. We also obtain F1 scores that reach up to 0.75 and 0.87 when the predictions are made within a period of 2 or 3 days, respectively;

4. During deduction, F1 score increases up to 182% (plus 22.40% compared to the induction phase) when the predictions made for a given day are combined.

The remaining of this Chapter is structured as follows. Section 6.2 presents our datasets. Section 6.3 formalizes APT-logic applied to the cybersecurity domain. Section 6.4 details the inductive and deductive methods that we use to learn rules capable of predicting future cyber-attacks. This section includes all corresponding results. Section 6.6 shows some related work. Finally, Section 6.7 summarizes the Chapter.

## 6.2 Dataset

We combine data from four different datasets to conduct our cyber-attack predictions.

### *6.2.1 Darkweb Hacking Forums*

We collect data from 53 darkweb hacking forums provided by CYR3CON [28], showing details of this original forum data in Table 6.1.

Table 6.1: Darkweb Hacking Forum Data.

| | *Original data* | *Filtered data (including 1,213 distinct CVE's)* |
|---|---|---|
| Time Period | 2016-04-03 : 2017-03-31 | 2016-04-03 : 2017-03-31 |
| Number of Users | 55,224 | 416 |
| Number of Posts | 270,475 | 7,824 |

### 6.2.2 *NVD*

The National Vulnerability Database (NVD) [96], our second dataset, comprises a collection of publicly disclosed vulnerabilities maintained by the National Institute of Standards and Technology [1], where each vulnerability is assigned a unique CVE (Common Vulnerabilities and Exposures) code [95]. To precisely identify vulnerability mentions in the forums analyzed, we filter all posts containing mentions of any disclosed CVE, since they can signal the intention of vulnerability exploitation for future cyber-attacks. Table 6.1 also shows this filtered forum data produced with the 1,213 distinct CVE's identified.

As APT rules are built correlating hacking activity with cyber-attacks, we expect to have multiple posts mentioning the same CVE. However, we note that most of the CVE's identified are not frequently mentioned in the posts, a fact that would necessarily hurt our model. To solve the issue, we map each CVE to pre-identified CPE's (Common Platform Enumeration), which is a list of software programs provided by NVD that are vulnerable to a given CVE [95]. Then, we cluster those CPE's into 88 high-level groups according to their common vendors/products [3] . Figure 6.1 presents the distribution of CVE's per CPE, demonstrating how CPE's group CVE's to generate frequent technical data in the posts.

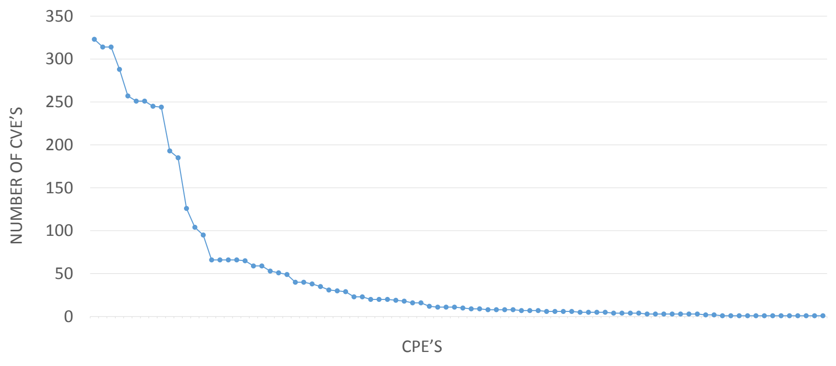

Fig. 6.1: Distribution of CVE's per CPE.

[3]We use soft clustering since each CVE can be mapped to more than one of those 88 CPE groups in the NVD software hierarchy, such as: Microsoft-Office and Microsoft-Word.

### 6.2.3 *EDB*

We also use data from ExploitDB (EDB) [114], which comprises a collection of Proof-of-Concept (PoC) exploits that have corresponding CVEs, being maintained by Offensive Security [133]. Those PoC scripts are provided by the white-hat community and demonstrate approaches to exploit vulnerabilities. We query EDB to check whether a PoC exploit is available for any CVE mined from the forum posts, since this increases the likelihood of future cyber-attacks [7]. We found that 149 CVE's out of 1,213 have verified PoCs in EDB.

### 6.2.4 *Enterprise External Threats*

Finally, the fourth dataset used in this work consists of 239 real-world targeted cyber incidents recorded from the logs of a large enterprise (anonymized here as Enterprise_1). Those records form our ground truth (GT) data, and correspond to malicious attempts to gain unauthorized access, alter/destroy data or interrupt services/resources, all detected in uncontrolled environment by different security defense products. Each (GT) record includes: *ID, Occurrence Time, and Attack Type*, with the reported attack types being classified as:

- **Malicious Email (**$m\_e$**).** A received email containing either a malicious attachment or a link (embedded URL or IP address) to a known malicious destination;
- **Malicious Destination (**$m\_d$**).** A visit to URL or IP address that host malicious content;
- **Endpoint Malware (**$e\_m$**).** A malware discovered on an endpoint device, such as ransomware or spyware.

Figure 6.2 shows the distribution of cyber-attacks reported by the targeted enterprise during the period analyzed.

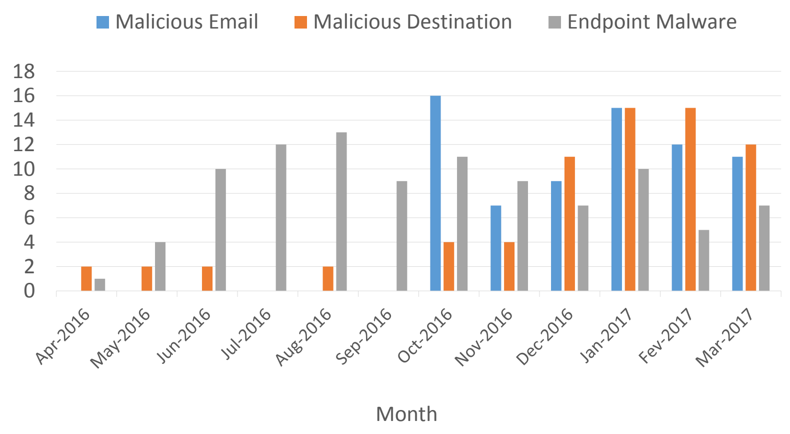

Fig. 6.2: Month-Wise Distribution of Cyber-Attacks Reported by Enterprise_1.

## 6.3 Annotated Probabilistic Temporal Logic (APT-logic)

In formal logic, the syntax of the representation language specifies the sentences that are well formed in the knowledge base, while the semantics define the truth of the sentences with respect to each possible world [107]. In this section, we define the syntax and semantics of APT-logic programs applied to our cybersecurity domain, which is mainly built upon the work proposed by Shakarian et al. in [121, 123].

### *6.3.1 Syntax*

We assume the existence of a first-order logical language $\mathcal{L}$, with a finite set $\mathcal{L}_{cons}$ of constant symbols, a finite set $\mathcal{L}_{pred}$ of predicate symbols, and an infinite set $\mathcal{L}_{var}$ of variables. In the following, we formalize the allowable sentences of $\mathcal{L}$.

**Conventions:** We define that constant and predicate symbols will begin with lowercase letters. For example, we might use the constant symbols $adobe\_reader$, $enterprise\_1$, and $m\_e$ to represent the CPE "adobe:reader", the organization "Enterprise_1", and the attack type "malicious email" respectively. Differently, variables are all uppercase letters. Both, constants and variables are used as arguments of predicates, such as $hackerDiscussion(CVE, ACTOR)$ or $mapping(CVE, adobe\_reader)$.

**Terms and Atoms:** A term is any member of $\mathcal{L}_{cons} \cup \mathcal{L}_{var}$, while ground terms must be present only in $\mathcal{L}_{cons}$. Atomic sentences (atoms) are formed from a predicate symbol followed by a parenthesized list of terms. Each predicate symbol $p \in \mathcal{L}_{pred}$ has an arity that informs the number of arguments. If $tr_1, \ldots, tr_n$ are (ground) terms and $p \in \mathcal{L}_{pred}$, then $p(tr_1, \ldots, tr_n)$ is also a (ground) atom.

**Herbrand base (Conditions and Actions):** We use $B_{\mathcal{L}}$ to denote the Herbrand base of $\mathcal{L}$, or its finite set of ground atoms. Then, we divide $B_{\mathcal{L}}$ into two disjoint sets: $B_{\mathcal{L}\{conditions\}}$ and $B_{\mathcal{L}\{actions\}}$, so that $B_{\mathcal{L}} \equiv B_{\mathcal{L}\{conditions\}} \cup B_{\mathcal{L}\{actions\}}$. $B_{\mathcal{L}\{conditions\}}$ comprehends the atoms allowed only in the pre-conditions of our APT rules. They represent *conditions* or the malicious activities performed by hackers on darkweb forums, as well as the socio-personal and technical indicators of attacks, e.g., $hackerDiscussion(CVE, ACTOR)$ or $recentPatch(CVE)$. On the other hand, $B_{\mathcal{L}\{actions\}}$ comprehends the atoms allowed only in the post-conditions of our APT rules, representing *actions* or the cyber incidents reported by the target organizations in their facilities, e.g., $cyberAttack(enterprise\_1, m\_e)$.

**Regular Formulas:** In general, complex sentences (formulas) are constructed recursively from simpler ones, using parentheses and three logical connectives: ($\neg$ negation, $\vee$ disjunction, $\wedge$ conjunction). A (ground) atom is a (ground) formula, and if $F$ and $F'$ are (ground) formulas, then $F \vee F'$, $F \wedge F'$, and $\neg F$ are also (ground) formulas. In this work, a formula could either be a single atom or a conjunction of atoms. As specified for atoms, formulas representing conditions must be located only in the pre-conditions of APT rules, while formulas representing actions must be located only in the post-conditions of those rules. As we want to predict one attack at a time, formulas are always formed by a single atom in the post-conditions of our APT rules.

**Time Formulas:** If $F$ is a (ground) formula and $t$ is a time point, then $F_t$ is a (ground) time formula that states that $F$ is true at time $t$. If $\phi$, $\rho$ are (ground) time formulas, then $\phi \vee \rho$,

$\phi \wedge \rho$, and $\neg\phi$ are also (ground) time formulas. We will represent time and regular formulas by using Greek ($\phi$, $\rho$) and capital ($F$, $G$) letters respectively.

**Probabilistic Time Formulas:** If $\phi$ and $[l,u]$ represent a (ground) time formula and a probability interval $\subseteq$ [0,1], then $\phi : [l,u]$ is a (ground) probabilistic time formula ($ptf$). Intuitively, $\phi : [l,u]$ states that $\phi$ is true with a probability in $[l,u]$ (or by using the full notation, $F_t : [l,u]$ states that $F$ is true at time $t$ with a probability in $[l,u]$). To illustrate the ptf's generation process, Figure 6.3 shows a timeline with past data (when $t$ is in $[1,6]$) and future data (when $t$ is in $[7,8]$).

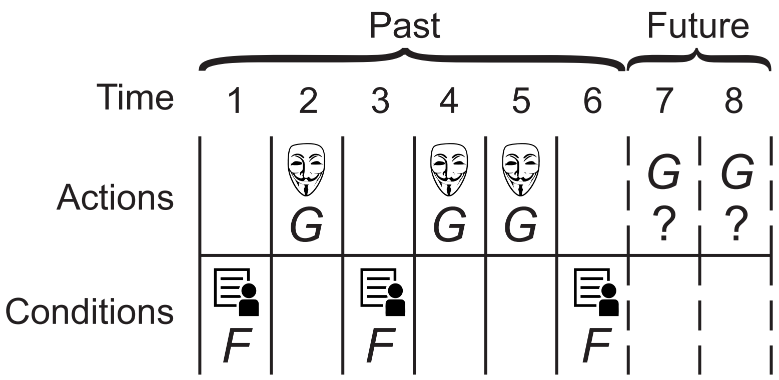

Fig. 6.3: Sample Timeline of Conditions and Actions.

Past data (conditions and actions) can only be annotated with [1,1], since they refer to facts that have been already observed. On the other hand, future data can only be annotated with [0,1] [4] without additional information. Equation 6.1 illustrates the ptf's derived by using the data of Figure 6.3.

$$KB = \begin{pmatrix} F_1 : [1,1] & G_2 : [1,1] & F_3 : [1,1] & G_4 : [1,1] \\ G_5 : [1,1] & F_6 : [1,1] & G_7 : [0,1] & G_8 : [0,1] \end{pmatrix} \tag{6.1}$$

[4]Alternative models can also use the prior probabilities of events as an estimation for annotating future events, and then, make even farther predictions.

We want to learn the temporal relationship between past conditions and actions to predict the probability of actions in the future (induction phase). Then, we want to combine and tighten the probability boundaries $[l, u]$ of the predictions made for a given day to adjust the confidence of our model, consequently improving its performance (deduction phase).

**APT Rules and Programs:** Suppose condition $F$ and action $G$ are (ground) formulas, $\Delta t$ is a time interval, $[l, u]$ is a probability interval, and $pfr$ is a frequency function (these functions will be defined later with the semantics of APT rules). Then $F \overset{pfr}{\leadsto} G : [\Delta t, l, u]$ is an (ground) APT (Annotated Probabilistic Temporal) rule. We will explain the formal semantics of APT rules in the next section, but informally saying, this rule computes the probability of $G$ becomes true exactly $\Delta t$ time units after $F$ becomes true. Consider for instance, the APT rule illustrated in equation 6.2:

$$\begin{aligned} &hackerDiscussion(CVE, ACTOR) && \wedge \\ &mapping(CVE, adobe\_reader) && \wedge \\ &hasMinPageRank(ACTOR, 0.1) && \wedge \\ &recentPatch(CVE) \overset{pfr}{\leadsto} cyberAttack(enterprise\_1, m\_e) \ : \ [2, 0.8, 0.9] \end{aligned} \tag{6.2}$$

This APT rule is informing that the probability of Enterprise_1 being attacked by a malicious email, exactly 2 time units after a hacker with minimal PageRank of 0.1 mentions a CVE that has a recently released patch and that is mapped to the CPE adobe:reader, is in [0.8,0.9]. APT Rules with high and tight boundaries like this one produce precise information that can be leveraged by organizations to allocate their limited resources and patch vulnerabilities before the attacks. Finally, we say an APT-logic program is a finite set of APT rules and ptf's (probabilistic time formulas).

### *6.3.2 Semantics*

In this section, we provide and detail a formal declarative semantics for APT-logic programs.

**World:** A world is any set of ground atoms that belong to $B_{\mathcal{L}}$. The power set of $B_{\mathcal{L}}$ (denoted $2^{B_{\mathcal{L}}}$) is the set of all possible worlds (Herbrand interpretations) that describe possible states of the domain being modeled by an APT-logic program. A few possible worlds in our cybersecurity domain are:

- $\{cyberAttack(enterprise\_1, m\_e), cyberAttack(enterprise\_1, e\_m)\}$
- $\{cyberAttack(enterprise\_1, e\_m)\}$
- $\{cyberAttack(enterprise\_1, m\_e)\}$
- $\{\}$

We say a world $w$ satisfies a ground formula $F$ (denoted $w \models F$), if the following four conditions hold [70]:

- If $F = a$ for some ground atom $a$, then $a \in w$;
- If $F = \neg F'$ for some ground formula $F'$, then $w$ does not satisfy $F'$;
- If $F = F_1 \wedge F_2$ for some ground formulas $F_1$ and $F_2$, then $w$ satisfies $F_1$ and $w$ satisfies $F_2$;
- If $F = F_1 \vee F_2$ for some ground formulas $F_1$ and $F_2$, then $w$ satisfies $F_1$ or $w$ satisfies $F_2$.

**Thread:** A sequence of worlds modeling the domain over time form a thread. $Th(t)$ informs that according to the thread $Th$, the world at time $t$ will be $Th(t)$. Given a thread $Th$ and a time formula $\phi$, we say $Th$ satisfies $\phi$ (denoted $Th \models \phi$) iff:

- If $\phi \equiv F_t$ for some ground time formula $F_t$, then $Th(t)$ satisfies $F$;
- If $\phi \equiv \neg\rho$ for some ground time formula $\rho$, then $Th$ does not satisfy $\rho$;
- If $\phi \equiv \rho_1 \wedge \rho_2$ for some ground time formulas $\rho_1$ and $\rho_2$, then $Th$ satisfies $\rho_1$ and $Th$ satisfies $\rho_2$;
- If $\phi \equiv \rho_1 \vee \rho_2$ for some ground time formulas $\rho_1$ and $\rho_2$, then $Th$ satisfies $\rho_1$ or $Th$ satisfies $\rho_2$.

We also specify how a ptf can be satisfied. If we consider $A$ as the set of all ptf's satisfied by a given thread $Th$, we say $Th$ satisfies $F_t : [l, u]$ (denoted $Th \vDash F_t : [l, u]$) iff:

- If $F = a$ for some ground atom $a$, then $\exists\, a_t : [l', u'] \in A\ s.t.\ [l, u] \subseteq [l', u']$;
- If $F_t : [l, u] = \neg F'_t : [l, u]$ for some ground formula $F'$, then $Th \vDash F'_t : [1 - u, 1 - l]$;
- If $F_t : [l, u] = F'_t : [l, u] \wedge F''_t : [l, u]$ for some ground formulas $F'$ and $F''$, then $Th \vDash F'_t : [l, u]$ and $Th \vDash F''_t : [l, u]$;
- If $F_t : [l, u] = F'_t : [l, u] \vee F''_t : [l, u]$ for some ground formulas $F'$ and $F''$, then $Th \vDash F'_t : [l, u]$ or $Th \vDash F''_t : [l, u]$.

If we have a thread $Th'$ satisfying each ptf of a knowledge base, then we can state that $Th'$ satisfies a given APT-logic program $\mathcal{K}$ formed only by those ptf's (denoted $Th' \vDash \mathcal{K}$), which makes $\mathcal{K}$ consistent. In this work, we assume the existence of a single thread $Th$ that corresponds to our historical corpus of data. This thread shows how malicious hackers are posting on darkweb forums and how cyber-attacks are occurring at Enterprise_1.

**Frequency Functions:** A frequency function $fr$ captures temporal relationships between worlds within a thread. From the functions proposed by Shakarian et al. in [121], we choose here the *Point Frequency Function (pfr)* to construct our APT rules [121], as it captures precise temporal relationships between events. Formally, $pfr$ maps quadruples of the form $(Th, F, G, \Delta t)$ to [0,1], specifying how frequently the condition $F$ is followed by the action $G$ after *exactly* $\Delta t$ time points within the thread $Th$, as shown in equation 6.3:

$$pfr(Th, F, G, \Delta t) = \frac{|\{t | Th \vDash F_t : [l, u] \land Th \vDash G_{t+\Delta t} : [l', u']\}|}{|\{t | Th \vDash F_t : [l, u]\}|} \tag{6.3}$$

As past data is only annotated with $[1, 1]$, $[l, u]$ and $[l', u']$ of equation 6.3 are equal to $[1, 1]$ while we learn the APT rules (induction).

**Satisfaction APT Rules and Programs:** We say the thread $Th$ satisfies an APT rule $F \overset{pfr}{\rightsquigarrow} G : [\Delta t, l, u]$ (denoted $Th \vDash F \overset{pfr}{\rightsquigarrow} G : [\Delta t, l, u]$) iff:

$$pfr(Th, F, G, \Delta t) \subseteq [l, u] \tag{6.4}$$

Finally, we say a thread $Th$ satisfies an APT-logic program $\mathcal{K}$ if $Th$ satisfies all ptf's and APT rules of $\mathcal{K}$.

## 6.4 Inductive and Deductive Learning

In this section, we detail how we leverage induction to learn APT rules and predict imminent cyber-attacks and how we apply deduction to improve the accuracy of our model.

### *6.4.1 Induction*

For the induction phase, we use a modified version of the algorithm proposed in [121]. We show the PFR-APTRule-Extract in Algorithm 1. This algorithm expects as inputs: a thread $Th$ containing historical data, a time interval $\Delta t$ in days, and a lower bound $minSup$ for the rule support [5] . Equation 6.2 shows a sample of APT rules that can be extracted by

[5]The support of a rule is the fraction of times where its pre-condition appears before its post-condition exactly $\Delta t$ time units [76].

this algorithm.

**Algorithm 1** The PFR-APTRule-Extract.

```
1: procedure PFR-APTRULE-EXTRACT($Th$, $\Delta t$, $minSup$)
2:     $Rules \leftarrow \varnothing$, $WeakRules \leftarrow \varnothing$
3:     for each desired combination of conditions and actions do
4:         $F \leftarrow$ current condition, $G \leftarrow$ current action
5:         $F_{atoms} \leftarrow$ set of atoms of $F$, $G_{atom} \leftarrow$ atom of $G$
6:         if $\{F_{atoms} \cup G_{atom}\} \not\supseteq$ of any item of $WeakRules$ then
7:             $supCountF \leftarrow 0$, $supCountFG \leftarrow 0$, $supFG \leftarrow 0$, $trials \leftarrow 0$
8:             for $t = minTime(Th)$ to $maxTime(Th) - \Delta t$ do
9:                 if $Th \models F_t : [1, 1]$ then
10:                    $supCountF \leftarrow supCountF + 1$
11:                    if $Th \models G_{t+\Delta t} : [1, 1]$ then
12:                        $supCountFG \leftarrow supCountFG + 1$
13:                $trials \leftarrow trials + 1$
14:            $supFG \leftarrow supCountFG/trials$
15:            if $supFG \geq minSup$ then
16:                $conFG \leftarrow supCountFG/supCountF$
17:                if $conFG > PRIOR(G)$ then
18:                    $\sigma_{prob} \leftarrow \frac{\sqrt{nTrials*conFG*(1-conFG)}}{nTrials}$
19:                    $rule \leftarrow F \overset{pfr}{\rightsquigarrow} G : [\Delta t, conFG - \sigma_{prob}, conFG + \sigma_{prob}]$
20:                    $Rules \leftarrow Rules \cup \{rule\}$
21:            else
22:                $WeakRules \leftarrow WeakRules \cup \{F_{atoms} \cup G_{atom}\}$
23:    Return $Rules$
```

Overall, the PFR-APTRule-Extract generates all combinations of conditions and actions using their predefined atoms, returning rules that satisfy two constraints: 1) the rule support $supFG$ is not lower than the user-defined threshold $minSup$ (line 15); 2) the rule condition $F$ is a *prima facie* cause [64] for the rule action $G$ (line 17). This second constraint is satisfied when the probability of $G$ occurring after $F$ is greater than the prior probability of $G$. To compute the probability intervals of the APT rules, we use one standard deviation of the corresponding point probability (the rule confidence $conFG$) in a binomial distribution [136] (line 18 of the algorithm), where $nTrials$ is the number of events that produced the probability $conFG$. This standard deviation $\sigma_{prob}$ is used to define some error margin for each APT rule in $[conFG - \sigma_{prob}, conFG + \sigma_{prob}]$ for all pairs $[l, u]$. We keep together in a set named $WeakRules$, the atom(s) forming the current condition $F_{atoms}$ and the atom forming the current action $G_{atom}$, for cases when $supFG$ is lower than $minSup$. Then, supersets of irrelevant solutions can be eliminated without testing. Finally, we analyze the border cases of our data (line 8 of PFR-APTRule-Extract), to guarantee that we always have $\Delta t$ days (not less) to find the post-condition of a rule.

**Rule Predicates:** Table 6.2 presents the predicates we use to create the atoms of APT rules. Those predicates are categorized into four groups: 1) captures the discussion content; 2) captures socio-personal indicators of attacks by analyzing the hackers involved; 3) captures technical indicators of attacks by analyzing the targeted vulnerabilities; 4) captures the cyber incident.

Table 6.2: Predicate Symbols Used to Learn APT Rules.

| **Predicate** | **Cat.** | **Description** |
|---|---|---|
| $hackerDiscussion(X, Y)$ | 1 | A set of CVE's $X$ mentioned by hackers $Y$. |
| $mapping(X, Y)$ | 1 | A set of CVE's $X$ mapped to the CPE $Y$. |
| $hasMinTopicDensity(X, Y)$ | 2 | A set of hackers $X$ with a minimal number $Y$ of users posting in their topics. |
| $hasMinKnowledgeProvision(X, Y)$ | 2 | A set of hackers $X$ with a minimal number $Y$ of messages including knowledge provision. |
| $hasMinPageRank(X, Y)$ | 2 | A set of hackers $X$ with a minimal PageRank value of $Y$. |
| $presentLargestCommunities(X, Y)$ | 2 | A set of hackers $X$ who are present in the $Y$ largest communities. |
| $recentPatch(X, Y)$ | 3 | There is a patch disclosed at maximal $Y$ days before each CVE of set $X$ is mentioned. |
| $proofOfConcept(X)$ | 3 | There is a PoC disclosed for each CVE of set $X$. |
| $cyberAttack(X, Y)$ | 4 | There is a cyber-attack of type $X$ at the enterprise $Y$. |

The PFR-APTRule-Extract algorithm only considers desired combinations of conditions and actions to learn APT rules (line 3 of the algorithm), which are formed when at least the three following components are present in those rules: one unique atom including each predicate of category 1 and one unique atom including the predicate of category 4. We want to investigate the possible combinations of atoms to check which ones produce more accurate predictions. We detail the predicates now.

- $hackerDiscussion(X, Y)$: This mandatory predicate generates atoms that inform mentioned CVE's and their authors. The example here is $hackerDiscussion(CVE, ACTOR)$, where the first argument is a variable receiving CVE's (e.g., *cve-2016-0167*), while the second is a variable receiving hackers' ID, such as $darkwolf$.

- $mapping(X, Y)$: This mandatory predicate generates atoms that inform in which CPE a set of CVE's are mapped to. One example is $mapping(CVE, apache\_tomcat)$, where the first argument is a variable receiving CVE's, while the second is a constant receiving a CPE, such as $apache\_tomcat$.

- $hasMinTopicDensity(X, Y)$: This optional predicate generates atoms that inform hackers with a minimal number of users posting in their topics. One example is $hasMinTopicDensity(ACTOR, 0.05)$, where the first argument is a variable receiving hackers, while the second is a constant receiving a topic density [6] .

- $hasMinKnowledgeProvision(X, Y)$: This optional predicate generates atoms that inform hackers who have a minimal number of messages including knowledge provision key-words, such as "yourself", "recommend" or "suggest". One example is $hasMinKnowledgeProvision(ACTOR, 0.011)$, where the first argument is a variable receiving hackers, while the second is a constant receiving a knowledge provision activity[6].

[6]After normalizing feature values to avoid problems with the different scales of the forums, we check the data distribution to define two thresholds. For topic density, we consider the values 0.008 and 0.05. For knowledge provision, we consider 0.0003 and 0.011. For PageRank, we consider 0.0002 and 0.0005. For the largest communities, we consider 2 and 3. For recent patch, we consider 30 and 60 (days).

- $hasMinPageRank(X, Y)$: This optional predicate generates atoms that inform the hackers who have a minimal PageRank network value [143]. One example is $hasMinPageRank(ACTOR, 0.0005)$, where the first argument is a variable receiving hackers, while the second is a constant receiving the PageRank[6]. To generate multiple network of hackers (one for each forum) and compute metrics like PageRank, we use the same strategy proposed in Chapter 2.

- $presentLargestCommunities(X, Y)$: This optional predicate generates atoms that inform which hackers are present in the largest communities. The example is $presentLargestCommunities(ACTOR, 3)$, where the first argument is a variable receiving hackers, while the second is a constant informing the number of communities[6]. We use the Louvain heuristic method to find the existing communities of hackers [15]).

- $recentPatch(X, Y)$: This optional predicate generates atoms that inform CVE's with a recent patch disclosed at NVD (compared to the CVE's mention). One example is $recentPatch(CVE, 30)$, where the first argument is a variable receiving CVE's, while the second is a constant receiving a maximal number of days[6].

- $proofOfConcept(X)$: This optional predicate generates atoms that inform CVE's with a disclosed PoC. One example is $proofOfConcept(CVE)$, where the argument is a variable receiving CVE's.

- $cyberAttack(X, Y)$: This mandatory predicate generates atoms that inform cyber-attacks happening in organizations. One example is $cyberAttack(enterprise\_1, m\_e)$, where the first argument is a constant receiving an organization, such as $enterprise\_1$, while the second is a constant receiving an attack type, such as $m\_e$.

**Training:** We run the PFR-APTRule-Extract algorithm over the first 70% of the forum posts that include vulnerability mentions (≈ 5,470 messages constitute our training set). Then, we analyze the significance of the rules obtained for attack prediction by comparing the conditional probability of the actions given their conditions with the prior probability of the actions, computing the corresponding probability gains. For this computation, we analyze multiple useful time intervals for $\Delta t$ in [1, 2, 3, 4, 5, 6, 7] days, different number of predicates from 2 (mandatory) to 8 (6 optional) forming the conditions, and multiple values for $minSup$. Figure 6.4 presents the results, showing probability gains that vary from 0.22% to 562% (those values are obtained when $minSup$ = 0.02, which means at least 3 occurrences of the rule within the thread).

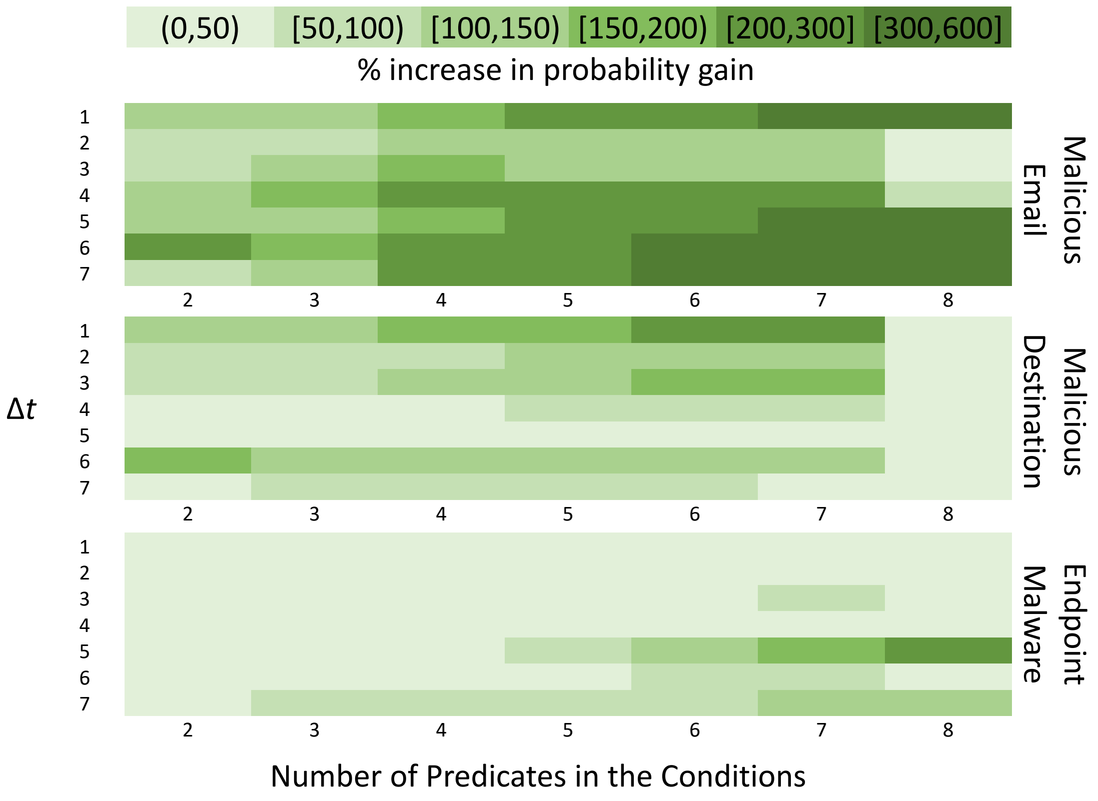

Fig. 6.4: Significance Analysis of the Generated APT Rules.

Overall, we verify that probability gains increase as we include a greater number of predicates in the conditions, pointing out the relevance of capturing socio-personal and technical indicators of cyber-attacks by analyzing the hackers and their strategies. The highest probability gains are located in the zone where the number of predicates is between 6 and 8, indicating which type of APT rules would potentially produce the best cyber-attack predictions during testing. The total number of rules generated for $\Delta t$ in [1, 2, 3, 4, 5, 6, 7] are 8,581, 6,290, 5,627, 6,713, 7,252, 10,456, and 10,326 respectively, adding up 55,245 APT rules. We also observe higher probability gains for the extreme tested values of $\Delta t$, such as 1, 6, and 7, signaling which time intervals could potentially generate more accurate predictions.

**Testing:** After learning the APT rules, we generate cyber-attack predictions for the last 30% of the forum posts that include vulnerability mentions (≈ 2,350 messages constitute our testing set). To accomplish that, we first search for APT rules that match a test case, or those whose atoms forming their conditions are all applied to the two components of the test case (vulnerability and hacker). Then, after selecting a rule from this pool, we use its post-condition to predict the corresponding attack type exactly $\Delta t$ days after the vulnerability mention (this approach will be properly formalized later in Theorem 1). Table 6.3 presents our prediction results. We sort those results according to the highest % gain in F1 score obtained by our model when compared to a baseline predictor that solely uses the prior probability of each attack type (the absolute F1 score values are also sorted in descending order). The highest performance (in F1 gain) is observed for malicious destination, followed by malicious email and endpoint malware.

As verified in Table 6.3, the conditions of the best performing APT rules for all attack types include 6 or 7 predicates, following the pattern identified in Figure 6.4. This confirms the relevance of the indicators integrated into our *pfr-based* temporal logical framework to predict cyber-attacks. Overall, those conditions are formed by all predicates but

Table 6.3: Prediction Results Compared to the Baseline.

| Malicious Email | | | | | |
|---|---|---|---|---|---|
| $\Delta_t$ | Number of Predicates | Precision | Recall | F1 | % gain in F1 |
| 1 | 7 | 0.601 | 0.404 | 0.483 | 125.86 |
| 2 | 6 | 0.578 | 0.285 | 0.382 | 78.51 |
| 5 | 6 | 0.445 | 0.309 | 0.365 | 70.41 |
| 3 | 6 | 0.431 | 0.261 | 0.325 | 52.07 |
| 7 | 7 | 0.302 | 0.261 | 0.280 | 30.97 |
| 6 | 7 | 0.318 | 0.214 | 0.256 | 19.57 |
| 4 | 7 | 0.317 | 0.190 | 0.238 | 11.15 |
| Malicious Destination | | | | | |
| $\Delta_t$ | Number of Predicates | Precision | Recall | F1 | % gain in F1 |
| 6 | 6 | 0.642 | 0.333 | 0.439 | 150.24 |
| 3 | 6 | 0.447 | 0.311 | 0.367 | 109.19 |
| 2 | 6 | 0.545 | 0.266 | 0.358 | 104.17 |
| 4 | 6 | 0.484 | 0.222 | 0.304 | 73.71 |
| 1 | 6 | 0.382 | 0.244 | 0.298 | 69.68 |
| 7 | 7 | 0.454 | 0.2 | 0.277 | 58.33 |
| Endpoint Malware | | | | | |
| $\Delta_t$ | Number of Predicates | Precision | Recall | F1 | % gain in F1 |
| 7 | 6 | 0.372 | 0.360 | 0.366 | 41.82 |
| 1 | 7 | 0.376 | 0.280 | 0.321 | 24.49 |
| 6 | 7 | 0.297 | 0.310 | 0.308 | 19.38 |

$proofOfConcept(X)$, which means that only (PoC) exploits were not meaningful for the predictions. Finally, as expected because of the rule significance analysis conducted before, the extreme tested values of $\Delta t$ indeed improve the performance of our model, which obtains F1 score gains of 150.24% for malicious destination (when $\Delta t$ = 6), 125.86% for malicious email (when $\Delta t$ = 1), and 41.82% for endpoint malware (when $\Delta t$ = 7). We interpret this phenomenon as: once a malicious hacking activity is detected, the start and end of the week beginning the day after the detection is crucial for organizations to allocate their resources and patch the corresponding vulnerability.

### 6.4.2 Deduction

During the testing task of the induction phase, we make 1,560, 2,879, and 1,702 general predictions for malicious-destination, malicious-email, and endpoint-malware attacks respectively. However, we observe that only 100, 108, and 105 distinct days were actually predicted for those types of attacks. Those results inform that several APT rules (with different combinations of atoms and time windows) triggered by the test cases are leading to the same attack type on the same day. As general predictions are made with different confidence $[l, u]$ (each learned APT rule analyzes specific data correlations over time), we want to define a method that combines as most as possible the predictive power of multiple APT rules to deduct a final attack probability. Then, we can compare this deducted probability with a proper threshold to decide whether there will be or not a cyber-attack on a given day. Therefore, we address in this section the "tight entailment problem" [123], where the goal is to find the tightest interval $[l, u]$ such that $F_t : [l, u]$ is entailed by an APT-logic program for a given time $t$ and formula $F$. By finding this tightest probability bound, we could adjust the confidence of our model, helping to improve the accuracy of our attack predictions. Before detailing our solution to the problem, we first formally define *entailment* between an APT-logic program and APT rules/ptf and *tight entailment* between an APT-logic program and a ptf:

**Definition 1.** *Entailment: Let $\mathcal{K}$ be an APT-logic program. We say that $\mathcal{K}$ entails $F \overset{pfr}{\rightsquigarrow} G : [\Delta t, l, u]$ (denoted, $\mathcal{K} \models F \overset{pfr}{\rightsquigarrow} G : [\Delta t, l, u]$) iff for all threads $Th$ s.t. $Th \models \mathcal{K}$ then $Th \models F \overset{pfr}{\rightsquigarrow} G : [\Delta t, l, u]$, and that $\mathcal{K}$ entails $F_t : [l, u]$ (denoted, $\mathcal{K} \models F_t : [l, u]$) iff for all threads $Th$ s.t. $Th \models \mathcal{K}$ then $Th \models F_t : [l, u]$.*

**Definition 2.** *Tight entailment: An APT-logic program $\mathcal{K}$ tightly entails a ptf $F_t : [l, u]$ (denoted $k \Vdash F_t : [l, u]$) iff $\mathcal{K} \models F_t : [l, u]$ and $\nexists\ F_t : [l', u']$ s.t. $\mathcal{K} \models F_t : [l', u']$ and $[l', u'] \subset [l, u]$.*

Now, suppose an APT-logic program $\mathcal{K}_{cyber1}$ is composed of the APT rule $r$ (inducted using the PFR-APTRule-Extract algorithm) and the ptf $\phi$ shown in Table 6.4:

Table 6.4: APT-Logic Program $\mathcal{K}_{cyber1}$.

| **ID** | **Type** | **Definition** |
|---|---|---|
| $r$ | APT rule | $F \overset{pfr}{\rightsquigarrow} G : [\Delta t, l, u]$ |
| $\phi$ | ptf | $F_t : [1,1]$ |

As $\mathcal{K}_{cyber1}$ entails $r$ and $\phi$, we can place $\phi$ into the condition of $r$ to infer that $\mathcal{K}_{cyber1}$ will also entail $G_{t+\Delta t} : [l, u]$. We formally present this inference in Theorem 1 (this is the logic used to make the predictions shown in Table 6.3):

**Theorem 1.** *Let $\mathcal{K}$ be an APT-logic program, $F \overset{pfr}{\rightsquigarrow} G : [\Delta t, l, u]$ be an APT rule and $F_t : [1,1]$ be a ptf. If $\mathcal{K} \vDash F \overset{pfr}{\rightsquigarrow} G : [\Delta t, l, u]$ and $\mathcal{K} \vDash F_t : [1,1]$ then $\mathcal{K} \vDash G_{t+\Delta t} : [l, u]$.*

*Proof.* The proof here is straightforward by applying Modus Ponens, which states that $(F \Rightarrow G,\ F)/G$ [107]. As we have the APT rule $F \overset{pfr}{\rightsquigarrow} G : [\Delta t, l, u]$ informing that if $F$ happens at time $t$, then $G$ will happen with a probability within $[l, u]$ in exactly $t + \Delta t$, and we also have the ptf $F_t : [1,1]$ informing that $F$ happened at time $t$, then we can infer that $G$ will happen at $t + \Delta t$ with probability within $[l, u]$ (keeping all constraints specified in the APT rule). Formally, the ptf $G_{t+\Delta t} : [l, u]$ can be logically inferred. $\square$

Now, consider an APT-logic program $\mathcal{K}_{cyber2}$ composed of the four components (APT rules and ptf's) shown in Table 6.5. By using Theorem 1 over the APT rules and ptf's ($r$ and $\phi$), ($s$ and $\rho$), and ($u$ and $\gamma$), we can respectively infer the ptf's: $G_{t+\Delta t} : [l, u]$, $G_{t'+\Delta t'} : [l', u']$, $G_{t''+\Delta t''} : [l'', u'']$. If $t + \Delta t$, $t' + \Delta t'$, and $t'' + \Delta t''$ lead to the same time point $t_i$, then we can deduct a combined probability for $G$ happening at $t_i$, which is formally presented in Theorem 2:

Table 6.5: APT-Logic Program $\mathcal{K}_{cyber2}$.

| **ID** | **Type** | **Definition** |
|---|---|---|
| $r$ | APT rule | $F \overset{pfr}{\rightsquigarrow} G : [\Delta t, l, u]$ |
| $s$ | APT rule | $F' \overset{pfr}{\rightsquigarrow} G : [\Delta t', l', u']$ |
| $u$ | APT rule | $F'' \overset{pfr}{\rightsquigarrow} G : [\Delta t'', l'', u'']$ |
| $\phi$ | ptf | $F_t : [1, 1]$ |
| $\rho$ | ptf | $F'_{t'} : [1, 1]$ |
| $\gamma$ | ptf | $F''_{t''} : [1, 1]$ |

**Theorem 2.** *Let $\mathcal{K}$ be an APT-logic program, and $G_t : [l, u]$, $G_t : [l', u']$ be two ptf's. If $\mathcal{K} \models G_t : [l, u]$ and $\mathcal{K} \models G_t : [l', u']$ then $\mathcal{K} \models G_t : [max(l, l'), min(u, u')]$ s.t. $[l, u] \cap [l', u'] \neq \varnothing$.*

*Proof.* This proof uses the notion of entailment between two ptf's and the combination of probabilities. Reasoning from [123, 36], we say a ptf $\lambda : [l, u]$ entails another ptf $\lambda' : [l', u']$ (denoted $\lambda : [l, u] \models \lambda' : [l', u']$) iff for all threads $Th$ s.t. $Th \models \lambda : [l, u]$ then $Th \models \lambda' : [l', u']$, which is an implication that becomes true only when $[l, u] \subset [l', u']$. Also, if there are two models predicting the same event on a given day with different lower bound probabilities, the higher one will be valid for both models. On the other hand, if these models predict with different upper bound probabilities, then the lower one will be valid for both models. This way, if there exists an intersection between the probability boundaries of $G_t : [l, u]$ and $G_t : [l', u']$ so that both predictions can be considered in our model, this intersection is formed by the interval $[max(l, l'), min(u, u')]$, which is a subset of $[l, u]$ and also a subset of $[l', u']$. Therefore, we can say that $G_t : [max(l, l'), min(u, u')] \models G_t : [l, u]$ and that $G_t : [max(l, l'), min(u, u')] \models G_t : [l', u']$, which leads to $\mathcal{K} \models G_t : [max(l, l'), min(u, u')]\ s.t.\ [l, u] \cap [l', u'] \neq \varnothing$. □

Note that Theorem 2 can be applied recursively if there is an extra ptf possible to be combined with a previously deducted ptf. For instance, if we consider that:

$\mathcal{K} \models G_t : [max(l,l'), min(u,u')]$ and $\mathcal{K} \models G_t : [l'', u'']$, then we can state that:

$\mathcal{K} \models G_t : [max(max(l,l'),l''), min(min(u,u'),u'')]$ *s.t.* $[max(l,l'), min(u,u')] \cap [l'', u''] \neq \varnothing$.

This way, by using Theorem 1 and Theorem 2, we can guarantee tight entailment conditions for the APT-logic programs $K_{cyber1}$ and $K_{cyber2}$ as shown below:

$\mathcal{K}_{cyber1} \Vdash G_{t+\Delta t} : [l, u]$.

$\mathcal{K}_{cyber2} \Vdash G_t : [max(max(l,l'),l''), min(min(u,u'),u'')]$ *s.t.* $[max(l,l'), min(u,u')] \cap [l'', u''] \neq \varnothing$.

If there is a case where there is no intersection between the probability boundaries of two ptf's leading to the same action at the same time, then our deductive model cannot consider both ptf's for predictions. Thus, we eliminate the ptf with the lower probability boundaries from our APT-logical program. Finally, to decide whether we should make a prediction or not after combining the probability boundaries of two or more ptf's, we test different thresholds $\delta$ in [0,1] with step 0.05. Then, if the upper bound of the deducted ptf is greater or equal to $\delta$, we make the prediction. Figure 6.5 presents the results for this deduction task, where we compute more than 3,300 combinations of probability intervals.

We compare the highest performances obtained by our model after the deduction phase with those obtained after the induction (training/testing) phase and also with the ones provided by the baseline predictor. As observed, the F1 scores increase considerably for all situations analyzed, with gains varying from 73.83% until 182.38% when compared with the baseline predictor, and with gains varying from 11.80% until 22.40% when compared with performance obtained after induction. Those results demonstrate how the combination

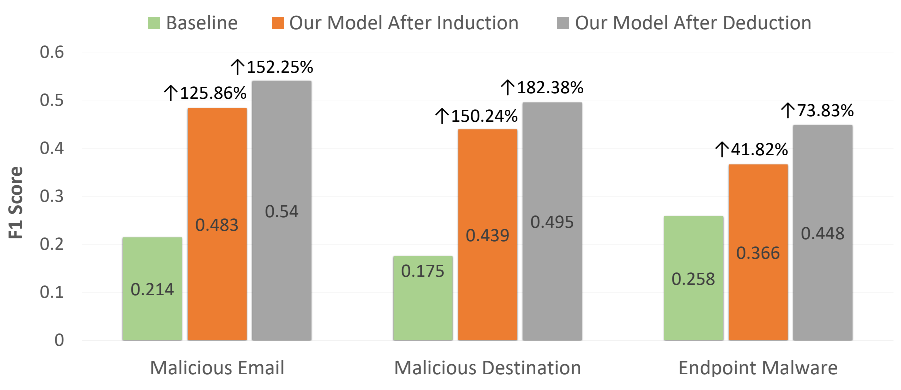

Fig. 6.5: Performance (F1 Score) Comparison Between the Baseline and Our Model After the Induction and Deduction Phases.

of ptf's is a relevant strategy to improve the accuracy of our cyber-attack predictions. We note that our model achieves the highest prediction performance after deduction when we set $\delta$ in [0.2, 0.4], as shown in Figure 6.6. On average, those threshold values imply the prior probability plus $\approx 35\%$.

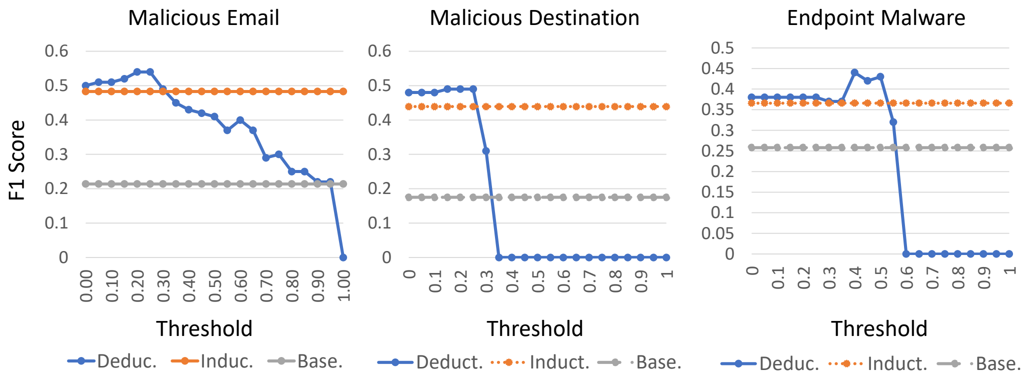

Fig. 6.6: Threshold Analysis for Final Predictions After Deduction.

## 6.5 Extending the Framework to Predict Within a Period of Time $\Delta t$

As the *Point Frequency Function (pfr)* captures precise temporal relationships between events, we can use mined hacking activity to make cyber-attack predictions for a specific day. However, we also analyze the utility of making predictions withing a period of time $\Delta t$, using the *Existential Frequency Function (efr)* to construct our APT rules [121]. Formally, $efr$ maps quadruples of the form $(Th, F, G, \Delta t)$ to [0,1], specifying how frequently the condition $F$ is followed by the action $G$ *within* $\Delta t$ time points in the thread $Th$, as shown in equation 6.5. Thus, $efr$ allows for the action to fall (becomes true) within some period of time $\Delta t$ rather than exactly $\Delta t$ time points after the condition becomes true.

$$efr(Th, F, G, \Delta t) = \frac{|\{t | Th \vDash F_t : p \wedge Th \vDash \bigcup_{t'=1}^{\Delta t} G_{t+t'} : p'\}|}{|\{t | Th \vDash F_t : p\}|} \tag{6.5}$$

Note how for $efr$ we do not compute probability intervals $[l, u]$ but point probabilities $p$. This happens since we will not know the exact day for which a prediction is made when $\Delta t > 1$, considering that a prediction is true if there is an attack in any of the days covered by $\Delta t$. Thus, we also do not conduct the deduction phase in this analysis, keeping our experiments focused only on the induction phase. Based on that, we say the thread $Th$ satisfies an APT rule $F \overset{efr}{\rightsquigarrow} G : [\Delta t, p]$ (denoted $Th \vDash F \overset{efr}{\rightsquigarrow} G : [\Delta t, p]$) iff:

$$efr(Th, F, G, \Delta t) \geq p \tag{6.6}$$

We extend the PFR-APTRule-Extract to propose the EFR-APTRule-Extract algorithm shown in Algorithm 2. Note how this new algorithm addresses the requirements of existential frequency functions, considering a period of time $\Delta t$ for the action to be true after the condition is triggered (line 11 of the algorithm) and outputting point probabilities instead of probability intervals for the mined APT rules (line 18 of the algorithm). We use the same predicates shown in Table 6.2 and the same constraints regarding valid combinations of conditions and actions to learn APT rules. The parameters $Th$, $minSup$, and the training and test set ratio of 70/30 are also kept the same. However, we make the values of $\Delta t$ to include now only 2 or 3 days. The reason is because we want to make predictions for short periods of time, since a value for $\Delta t$ greater or equal to 5 (around a week) will basically create a tautology and will not be useful given the high frequency of attacks in our data.

**Algorithm 2** The EFR-APTRule-Extract.

```
1: procedure EFR-APTRULE-EXTRACT($Th$, $\Delta t$, $minSup$)
2:     $Rules \leftarrow \varnothing, WeakRules \leftarrow \varnothing$
3:     for each desired combination of conditions and actions do
4:         $F \leftarrow$ current condition, $G \leftarrow$ current action
5:         $F_{atoms} \leftarrow$ set of atoms of $F$, $G_{atom} \leftarrow$ atom of $G$
6:         if $\{F_{atoms} \cup G_{atom}\} \not\supseteq$ of any item of $WeakRules$ then
7:             $supCountF \leftarrow 0, supCountFG \leftarrow 0, supFG \leftarrow 0, trials \leftarrow 0$
8:             for $t = minTime(Th)$ to $maxTime(Th) - \Delta t$ do
9:                 if $Th \models F_t : 1$ then
10:                    $supCountF \leftarrow supCountF + 1$
11:                    if $Th \models \bigcup_{t'=1}^{\Delta t} G_{t+t'} : 1$ then
12:                        $supCountFG \leftarrow supCountFG + 1$
13:                $trials \leftarrow trials + 1$
14:            $supFG \leftarrow supCountFG / trials$
15:            if $supFG \geq minSup$ then
16:                $conFG \leftarrow supCountFG / supCountF$
17:                if $conFG > PRIOR(G)$ then
18:                    $rule \leftarrow F \overset{pfr}{\rightsquigarrow} G : [\Delta t, conFG]$
19:                    $Rules \leftarrow Rules \cup \{rule\}$
20:            else
21:                $WeakRules \leftarrow WeakRules \cup \{F_{atoms} \cup G_{atom}\}$
22:     Return $Rules$
```

Figure 6.7 shows the significance of the rules obtained for attack prediction with EFR-APTRule-Extract algorithm. Repeating the pattern observed for PFR-APTRule-Extract, we verify that probability gains increase as we include a greater number of predicates in the conditions. However, we verify that probability gains tend to decrease as we make $\Delta t$ greater, showing how the prior probability of attacks grows fast when we consider higher $\Delta t$ values. We also note the highest probability gains are located in a zone where the number of predicates is between 4 and 7, repeating what we observed for PFR-APTRule-Extract.

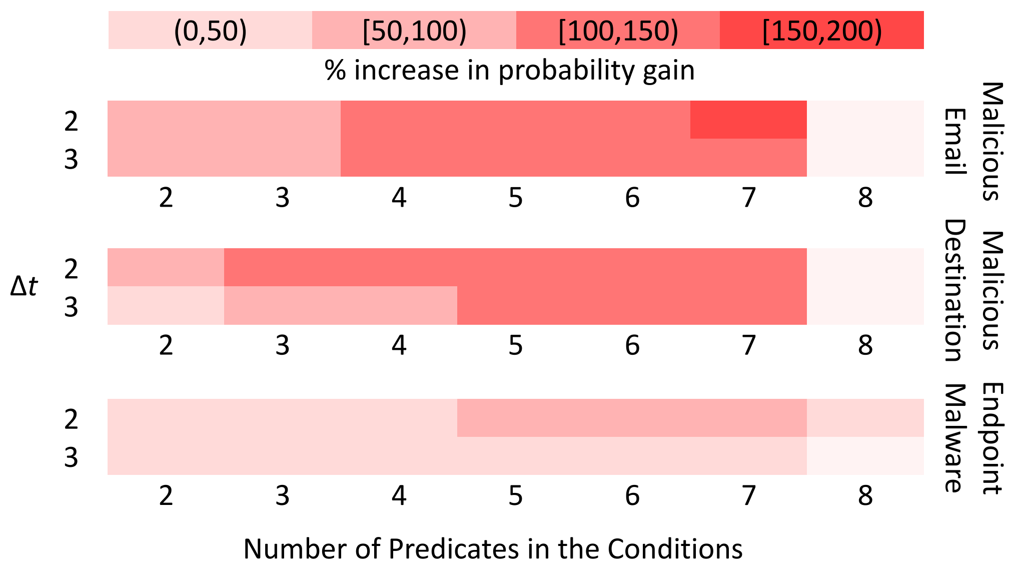

Fig. 6.7: Significance Analysis of the Generated APT Rules Considering $efr$.

Table 6.6 presents our prediction results, where we inform which conditions (combination of atoms generated according to the predicates) obtain the highest percentage in F1 gain when compared to a baseline predictor that uses the prior probability of each attack type. The table shows gains from 1% to 123%, with the highest gains observed for the attack type malicious email, followed by malicious destination and endpoint malware. As the baseline has its accuracy increased with a greater $\Delta t$, and the performance of our model does not improve with the same rate, the F1 gains are generally smaller if compared to the ones obtained when the point frequency function is used. However, the absolute values of the F1 score are higher, since now we have a period of 2 or 3 days to observe the cyber-attack.

Note how in 50% of the cases (3 out of 6 cases analyzed), the conditions are formed by 5 predicates, which follows the pattern shown of Figure 6.7. Since we observe a lower number of predicates forming the conditions compared to the $pfr$ analysis (5 against 6 or 7), we investigate which are the recurrent indicators that effectively contribute for more accurate predictions. For instance, $hasMinPageRank$ is present in 83.3% of the cases (5 out of 6), indicating how social network metrics that estimate the hackers' centrality can be important

Table 6.6: Prediction Results.

| Enterprise | Attack Type | $\Delta t$ | APT Rule Conditions | Baseline (Prior Prob.) F1 | Prop. Framework F1 | % gain in F1 |
|---|---|---|---|---|---|---|
| $enterprise\_1$ | $m\_e$ | 2 | $hackerDiscussion(X,Y) \wedge mapping(X,Y) \wedge hasMinTopicDensity(X,Y) \wedge presentLargestCommunities(X,Y)$ | 0.336 | 0.751 | 123% |
| | | 3 | $hackerDiscussion(X,Y) \wedge mapping(X,Y) \wedge hasMinKnowledgeProvision(X,Y) \wedge hasMinPageRank(X,Y) \wedge recentPatch(X,Y)$ | 0.603 | 0.872 | 45% |
| | $m\_d$ | 2 | $hackerDiscussion(X,Y) \wedge mapping(X,Y) \wedge hasMinTopicDensity(X,Y) \wedge hasMinPageRank(X,Y) \wedge presentLargestCommunities(X,Y)$ $recentPatch(X,Y)$ | 0.371 | 0.566 | 52% |
| | | 3 | $hackerDiscussion(X,Y) \wedge mapping(X,Y) \wedge hasMinKnowledgeProvision(X,Y) \wedge hasMinPageRank(X,Y)$ | 0.705 | 0.748 | 6% |
| | $e\_m$ | 2 | $hackerDiscussion(X,Y) \wedge mapping(X,Y) \wedge hasMinTopicDensity(X,Y) \wedge hasMinKnowledgeProvision(X,Y) \wedge hasMinPageRank(X,Y)$ | 0.469 | 0.508 | 8% |
| | | 3 | $hackerDiscussion(X,Y) \wedge mapping(X,Y) \wedge hasMinTopicDensity(X,Y) \wedge hasMinPageRank(X,Y) \wedge recentPatch(X,Y)$ | 0.643 | 0.650 | 1% |

to identify credible threats. Following, $hasMinTopicDensity$ is present in 4 out of 6 cases, again strengthening the relevance of finding hackers that produce the most interesting and useful cyber threats. Also, $hasMinKnowledgeProvision$ occurs in 3 out of 6 cases, indicating how relevant it is to find hackers with expertise to share. Similarly, $recentPatch$ is present in 3 out of 6 cases, showing the importance of the vulnerability disclosure information in NVD during the first 30 or 60 days. Finally, $presentLargestCommunities$ occurs in 2 out of 6 cases, pointing out the relevance of analyzing the biggest communities of hackers, where reputable individuals are usually coordinating activities.

Overall, those results evidence how the analysis of malicious hackers can be relevant to identify credible threats in the future, signaling that: once a vulnerability is mentioned, the next step should be a deep analysis of the hackers involved.

## 6.6 Related Work

Different research works have been proactively investigating cybersecurity either by searching cyber-threats to mitigate risks [103, 7, 5] or by predicting the exploitation of software vulnerabilities [109, 9, 17]. However, only a few of those studies focus on predicting cyber-attacks against specific corporations by analyzing online hacking discussions.

For instance, Khandpur et al. [63] proposed an unsupervised approach to detect ongoing cyber-attacks discussed on Twitter. They achieved a reasonable performance by using a limited set of seed event triggers and adding a query expansion strategy based on convolutional kernels and dependency parses. Goyal et al. [52] described deep neural networks and autoregressive time series models that leveraged external signals to predict attacks. They showed how information from security blogs and vulnerability databases are useful to make the predictions. Deb et al. [30] applied sentiment analysis to darkweb forum posts to assess sentiment trends over time, demonstrating a higher prediction performance compared to a time series model. More similar to our work, Almukaynizi et al. [8] proposed a logical framework to predict cyber-attacks against specific corporations by mining cyber threat intelligence from the darkweb. The authors tried to predict the magnitude of a particular type of attack, achieving reasonable performance when compared to the designed baselines.

Although all those works proposed interesting strategies that help organizations to monitor the cyberspace while searching for credible threats, their implementations partially or totally fail to be timely, actionable, accurate, and transparent. These four key desired properties of a cyber-attack prediction tool are successfully addressed by our temporal logic framework. Besides, those works basically neglected the individuals behind the events. In addition to the technical information involved, such as the release of a recent patch for a software vulnerability, we also rely on social-personal indicators of attacks by checking the hackers and their communities. Then, we are able to differentiate the cybercriminals and their strategies in terms of capability, significantly increasing the accuracy of our predictions.

## 6.7 Summary

In this Chapter, we present a temporal logic framework capable of predicting cyber-attacks in the near future. Particularly, our framework learns Annotated Probabilistic Temporal (APT) rules that correlate malicious hacking activity with real-world cyber incidents, leveraging these rules for predicting when, where, and how a particular attack is likely to happen. Then, we leverage a deductive approach to adjust the confidence with which our model makes attack predictions. Considering socio-personal and technical indicators of enterprise attacks, our method analyzes the malicious hackers and their strategies, helping security teams to effectively identify which will be the probable IT targets of cybercriminals.

# Chapter 7

# CONCLUSION

Today's widespread of cyber-attack incidences makes them one of the primary threat faced by organizations worldwide. The current methods that attempt to neutralize hacking attempts have been failing to demonstrate effectiveness, probably for concentrating only on the technical aspects involved and neglect the actors behind the incidents. We believe that an intimate understanding of the malicious hacker communities will greatly aid power to proactive cyber threat intelligence, allowing defenders to be more effective while anticipating cyber threats. However, as the hacking market is in clear expansion in terms of players and traded exploits, there are important limitations still largely unexplored, such as: who are the skilled and influential individuals forming those hacker groups, how hacker communities organize along the lines of technical expertise, how ideas propagate within those communities, and which internal patterns can signal imminent cyber offensives.

## 7.1 Summary of the Contributions

This dissertation proposes a hacker centric perspective to empower cyber defense, demonstrating how the hackers' digital traces existing in malicious hacking communities yield valuable insights into evolving cyber threats.

In Chapter 2, we mine "key-hackers" on popular darkweb forums, identifying individuals who are likely to succeed in their cybercriminal goals. We develop a profile for each forum member using features derived from content, social network, and seniority analysis, aiming to differentiate standard from key cyber-actors. Then, after defining a metric for collecting ground truth data based on user reputation, we train our model on a given forum using optimization (EC) and (ML) algorithms fed with those features to later test its performance on a different forum. Our results show that we are able to identify up to 52% of the existing key-hackers, demonstrating how our model generalizes relatively well.

In Chapter 3 and Chapter 4, we investigate how social influence contributes to user/hacker engagement online, developing two lines of research for analyzing user adoption behavior. In Chapter 3, we investigate whether microblog users on social media will adopt a hashtag considering the influence exerted by their active neighbors. We introduce two time constraints to extend standard (SNA) measures used to quantify social influence, noting that: 1) their correlation with adoption probability improves up to 488.24% for all influence measures analyzed; 2) their ability to predict adoption in a (ML) classification task improves up to 13.69% in F1 score when comparing to recent machine learning techniques that aim to predict adoption. In Chapter 4, we investigate where and when darkweb forum hackers will post a message in the future considering their recurrent interactions with other hackers. We formulate this problem as a (ML) sequential rule mining task, designing experiments using multiple posting time granularities and time-windows. We observe precision results of up to 0.78 and precision gains up of to 837% when compared to the prior probabilities of hackers' posts. The analysis of user adoption behavior in both research works can be used by security specialists to reveal the potential expansion degree of the key-hackers' networks.

In Chapter 5, we search for communities of darkweb marketplaces' vendors with similar expertise in specific subfields of hacking, a feature typically owned by key-hackers that can be used for surveillance purposes. We develop a method based on (SNA) techniques that identifies communities of hacking-related vendors using the similarity of their products, validating our method by cross-checking the community assignments of these individuals on two mutually exclusive sets of marketplaces. Our model achieves 0.445 of consistency between more than 30 communities of vendors revealed in each subset of markets.

In Chapter 6, we integrate the social models proposed in the previous chapters into a temporal logic framework capable of predicting cyber-attacks. Particularly, the framework induct rules that correlate malicious hacking activity with real-world cyber incidents and deduct more accurate security warnings by combining multiple attack predictions. By considering technical and socio-personal indicators of cyber-attacks, we demonstrate considerable prediction gains in F1 score (up to 150.24%) compared to the baseline. Those results are particular evidenced when the pre-conditions of the rules include relevant information about the hackers behind the attacks, highlighting the relevance of the socio-personal indicators for the identification of imminent threats. Besides, we also obtain gains in F1 score of up to 182.38% when the predictions made for a given day are combined using deduction.

By proposing the models detailed in this dissertation, we provide methods for the identification of credible cyber threats, allowing organizations to protect assets likely to be targeted before the attackers even have a chance to start their offensives.

## 7.2 Future Directions

The work conducted in this dissertation can be extended in many ways in order to enhance proactive cyber threat intelligence, either by addressing current limitations or by proposing new models, methods, frameworks, and algorithms. In the following, some potential research areas that will go towards this goal are discussed.

- Vulnerability Exploitation Prediction. This task comprises the prediction which known software vulnerabilities are likely to be exploited by malicious hackers. Standard vulnerability score systems like CVSS [6, 9] are known not to be useful for patch prioritization due to their high false positive rates. Machine learning techniques can be applied over features computed from malicious hacking environments to mine vulnerabilities directly or indirectly discussed by credible hackers, so that security specialists can have a better map of the assets at risk.

- Identification of Zero-Day Exploits. Another important security challenge is the potential identification of zero-day attacks, as defenders cannot be protected against "invisible" threats. Although zero-day exploits target unknown vulnerabilities, they usually exist "in the wild" for over 300 days before identification [14]. Thus, researchers can gather cyber threat intelligence to discover what kind of zero-day exploit is being developed and offered on hacking communities.

- Social Network Extraction of Malicious Hackers. Many research works conducted on darkweb forums [78, 79, 83, 7] explore social network features to accomplish their goals. However, due to the fragmented and interactionally disjointed natures of those environments, extracting social network structure by using only hacker interaction data is difficult and inaccurate. Thus, Natural language Processing (NLP) methods can be used to derive more accurate reply-to information on darkweb forums, leading to a better approximation of the real hacker network topology.

- Forum Spidering. In order to automate data collection from darkweb websites, designed spiders need to automatically find and download relevant HTML pages. Malicious hacking sites, especially those existing in encrypted networks like Tor, are able to easily detect and block those robots [92]. Thus, one main contribution to the cyber threat intelligence area should be the design of intelligent human-like-spiders. Those robots should be able to bypass detection methods by mimicking human browsing behavior, and also learn which hacking information is important to be collected.

- Adversarial Reasoning. Malicious hackers are continually evolving and adjusting their strategies to defeat defense postures. To address this threat, defenders should also employ adaptive strategies to assess hackers' capabilities, perceptions, intents, actions, and behaviors [103]. Thus, the development of models combining game theory, AI, control theory, cognitive modeling, and machine learning to reason about how, why, where, and when cyber-attacks will occur is crucial to successfully defeat attackers.

- Cascade Prediction: Predicting when a hacking message will go “viral” is important for cybersecurity, since information cascades can signal hacktivism campaigns or mass adoption of cyber threats [119]. Then, defenders will benefit from modeling information diffusion on hacking communities to investigate which influential and topological patterns can be leveraged for the early extraction of popular threads.

## REFERENCES

[1] National Institute of Standards and Technology (NIST). https://https://www.nist.gov//, Last Accessed: June 2019.

[2] A. Abbasi, W. Li, V. Benjamin, S. Hu, and H. Chen. Descriptive analytics: Examining expert hackers in web forums. In *Proceeding of ISI 2014*, pages 56–63. IEEE, Sept 2014.

[3] O. Abbosh and K. Bissell. Securing the digital economy: Reinventing the internet for trust. , Accenture, 2019.

[4] I. Ajzen and M. Fishbein. *Understanding attitudes and predicting social behavior*. Prentice-Hall, 1980.

[5] L. Allodi. Economic factors of vulnerability trade and exploitation. In *Proceedings of the 2017 ACM SIGSAC Conference on Computer and Communications Security*, CCS '17, pages 1483–1499, New York, NY, USA, 2017. ACM.

[6] L. Allodi and F. Massacci. Comparing vulnerability severity and exploits using case-control studies. *ACM Trans. Inf. Syst. Secur.*, 17(1):1:1–1:20, Aug. 2014.

[7] M. Almukaynizi, A. Grimm, E. Nunes, J. Shakarian, and P. Shakarian. Predicting cyber threats through hacker social networks in darkweb and deepweb forums. In *Proceedings of the 2017 International Conference of The Computational Social Science Society of the Americas*. ACM, 2017.

[8] M. Almukaynizi, E. Marin, E. Nunes, P. Shakarian, G. I. Simari, D. Kapoor, and T. Siedlecki. Darkmention: A deployed system to predict enterprise-targeted external cyberattacks. In *Proceeding of 2018 IEEE International Conference on Intelligence and Security Informatics (ISI)*. IEEE, 2018.

[9] M. Almukaynizi, E. Nunes, K. Dharaiya, M. Senguttuvan, J. Shakarian, and P. Shakarian. Proactive identification of exploits in the wild through vulnerability mentions online. In *2017 International Conference on Cyber Conflict (CyCon U.S.)*, pages 82–88, Nov 2017.

[10] T. Anwar and M. Abulaish. Identifying cliques in dark web forums - an agglomerative clustering approach. In *2012 IEEE International Conference on Intelligence and Security Informatics*, pages 171–173, June 2012.

[11] A.-L. Barabasi and R. Albert. Emergence of scaling in random networks. *Science*, 286(5439):509–512, 1999.

[12] V. Benjamin, W. Li, T. Holt, and H. Chen. Exploring threats and vulnerabilities in hacker web: Forums, irc and carding shops. In *2015 IEEE International Conference on Intelligence and Security Informatics (ISI)*, pages 85–90, May 2015.

[13] V. Benjamin, B. Zhang, J. Jr., and H. Chen. Examining hacker participation length in cybercriminal internet-relay-chat communities. *Journal of Management Information Systems*, 33(2):482–510, 2016.

[14] L. Bilge and T. Dumitras. Before we knew it: An empirical study of zero-day attacks in the real world. In *CCS '12 Proceedings of the 2012 ACM conference on Computer and Communications Security*, CCS '12, pages 833 – 844. ACM, ACM, 2012 2012.

[15] V. D. Blondel, J.-L. Guillaume, R. Lambiotte, and E. Lefebvre. Fast unfolding of communities in large networks. *Journal of Statistical Mechanics: Theory and Experiment*, 2008(10):P10008, 2008.

[16] S. P. Borgatti, K. M. Carley, and D. Krackhardt. On the robustness of centrality measures under conditions of imperfect data. *Social Networks*, 28(2):124–136, 2006.

[17] B. L. Bullough, A. K. Yanchenko, C. L. Smith, and J. R. Zipkin. Predicting exploitation of disclosed software vulnerabilities using open-source data. In *Proceedings of the 3rd ACM on International Workshop on Security And Privacy Analytics*, IWSPA '17, pages 45–53, New York, NY, USA, 2017. ACM.

[18] R. S. Burt. Social contagion and innovation: Cohesion versus structural equivalence. *American Journal of Sociology*, 92(6):1287–1335, 1987.

[19] B. Buunk and W. Schaufeli. Reciprocity in interpersonal relationships: An evolutionary perspective on its importance for health and well-being. *European Review of Social Psychology*, 10(1):259–291, 1999.

[20] D. Carr. How Obama Tapped into Social Networks' Power, 2008. `https://www.nytimes.com/2008/11/10/business/media/10carr.html` (accessed on 07-03-2018).

[21] M. Cha, H. Haddadi, F. Benevenuto, and K. P. Gummadi. Measuring user influence in twitter: The million follower fallacy. In *Proceedings of the Fourth ICWSM*. AAAI Press, 2010.

[22] Y.-D. Chen, S. A. Brown, P. J.-H. Hu, C.-C. King, and H. Chen. Managing emerging infectious diseases with information systems: Reconceptualizing outbreak management through the lens of loose coupling. *Information Systems Research*, 22(3):447–468, 2011.

[23] J. Cheng, L. Adamic, P. A. Dow, J. M. Kleinberg, and J. Leskovec. Can cascades be predicted? In *Proceedings of the 23rd International Conference on World Wide Web*, WWW '14, pages 925–936, New York, NY, USA, 2014. ACM.

[24] A. Clauset, M. E. J. Newman, and C. Moore. Finding community structure in very large networks. *Phys. Rev. E*, 70:066111, Dec 2004.

[25] G. Coleman. *Hacker, Hoaxer, Whistleblower, Spy: The Many Faces of Anonymous*. Verso Books, 2014.

[26] J. S. Coleman, E. Katz, and H. Menzel. Medical innovation: A diffusion study. *Social Forces*, 46(2):291, 1967.

[27] P. Cui, S. Jin, L. Yu, F. Wang, W. Zhu, and S. Yang. Cascading outbreak prediction in networks: A data-driven approach. In *Proceedings of the 19th ACM SIGKDD International Conference on Knowledge Discovery and Data Mining*, KDD '13, pages 901–909, New York, NY, USA, 2013. ACM.

[28] I. Cyber Reconnaissance. CYR3CON, 2020. `https://www.cyr3con.ai//` (accessed on 02-01-2020).

[29] G. Das, K.-I. Lin, H. Mannila, G. Renganathan, and P. Smyth. Rule discovery from time series. In *Proceedings of the Fourth International Conference on Knowledge Discovery and Data Mining*, KDD'98, pages 16–22. AAAI Press, 1998.

[30] A. Deb, K. Lerman, and E. Ferrara. Predicting cyber-events by leveraging hacker sentiment. *Information*, 9(11):280, 2018.

[31] D. Décary-Hétu and B. Dupont. Reputation in a dark network of online criminals. *Global Crime*, 14(2-3):175–196, 2013.

[32] J. Deogun and L. Jiang. Prediction mining – an approach to mining association rules for prediction. In D. Ślezak, J. Yao, J. F. Peters, W. Ziarko, and X. Hu, editors, *Rough Sets, Fuzzy Sets, Data Mining, and Granular Computing*, pages 98–108. Springer Berlin Heidelberg, 2005.

[33] P. Domingos and M. Richardson. Mining the network value of customers. In *Proceedings of the Seventh ACM SIGKDD International Conference on Knowledge Discovery and Data Mining*, KDD '01, pages 57–66, New York, NY, USA, 2001. ACM.

[34] S. Dowdy, S. Wearden, and D. Chilko. *Statistics for Research*. Wiley, 2004.

[35] M. Edkrantz and A. Said. Predicting cyber vulnerability exploits with machine learning. In *Proceedings of the 13th Scandinavian Conference on Artificial Intelligence*, volume 278, pages 48–57, 2015.

[36] M. V. Emden. Quantitative deduction and its fixpoint theory. *The Journal of Logic Programming*, 3(1):37 – 53, 1986.

[37] S. Enderby. Remediation vs. prevention: How to place your bets, 2017. `https://blog.malwarebytes.com/101/2017/09/remediation-vs-prevention-how-to-place-your-bets/` (accessed on 10-26-2018).

[38] Z. Fang, X. Zhao, Q. Wei, G. Chen, Y. Zhang, C. Xing, W. Li, and H. Chen. Exploring key hackers and cybersecurity threats in chinese hacker communities. In *Proceeding of ISI 2016*. IEEE, 2016.

[39] C. Fink, A. Schmidt, V. Barash, C. J. Cameron, and M. Macy. Complex contagions and the diffusion of popular twitter hashtags in nigeria. *Social Netw. Analys. Mining*, 6(1):1:1–1:19, 2016.

[40] C. Fink, A. Schmidt, V. Barash, J. Kelly, C. Cameron, and M. Macy. Investigating the observability of complex contagion in empirical social networks. *Tenth International AAAI Conference on Web and Social Media*, 2016.

[41] FIREEYE. Threat Research. Dyre Banking Trojan Exploits CVE-2015-0057, 2018. `https://www.fireeye.com/blog/threat-research/2015/07/dyre_banking_trojan.html/` (accessed on 08-15-2018).

[42] N. Fisk. *Social learning theory as a model for illegitimate peer-to-peer use and the effects of implementing a legal music downloading service on peer-to-peer music piracy*. PhD thesis, Rochester Institute of Technology, 2006.

[43] S. Fortunato. Community detection in graphs. *Physics Reports*, 486(3):75 – 174, 2010.

[44] P. Fournier-Viger, U. Faghihi, R. Nkambou, and E. M. Nguifo. Cmrules: Mining sequential rules common to several sequences. *Knowledge-Based Systems*, 25(1):63 – 76, 2012. Special Issue on New Trends in Data Mining.

[45] P. Fournier-Viger, T. Gueniche, and V. S. Tseng. Using partially-ordered sequential rules to generate more accurate sequence prediction. In *Advanced Data Mining and Applications*, pages 431–442, Berlin, Heidelberg, 2012. Springer Berlin Heidelberg.

[46] P. Fournier-Viger, C. Wu, V. S. Tseng, L. Cao, and R. Nkambou. Mining partially-ordered sequential rules common to multiple sequences. *IEEE Transactions on Knowledge and Data Engineering*, 27(8):2203–2216, Aug 2015.

[47] P. Fournier-Viger, C.-W. Wu, V. S. Tseng, and R. Nkambou. Mining sequential rules common to several sequences with the window size constraint. In *Advances in Artificial Intelligence*, pages 299–304, Berlin, Heidelberg, 2012. Springer Berlin Heidelberg.

[48] M. Girvan and M. E. J. Newman. Community structure in social and biological networks. *Proceedings of the National Academy of Sciences*, 99(12):7821–7826, 2002.

[49] M. Glenski and T. Weninger. Predicting user-interactions on reddit. In *Proceedings of the 2017 IEEE/ACM International Conference on Advances in Social Networks Analysis and Mining 2017*, ASONAM '17, pages 609–612, New York, NY, USA, 2017. ACM.

[50] S. Goel, A. Anderson, J. M. Hofman, and D. J. Watts. The structural virality of online diffusion. *Management Science*, 62:180–196, 2016.

[51] A. Goyal, F. Bonchi, and L. V. Lakshmanan. Learning influence probabilities in social networks. In *Proceedings of the 3rd ACM WSDM*, WSDM '10, pages 241–250, New York, NY, USA, 2010. ACM.

[52] P. Goyal, K. Hossain, A. Deb, N. Tavabi, N. Bartley, A. Abeliuk, E. Ferrara, and K. Lerman. Discovering signals from web sources to predict cyber attacks. *DeepAI*, Jun 2018.

[53] R. Guo and P. Shakarian. A comparison of methods for cascade prediction. In *Proceedings of the 2016 IEEE/ACM International Conference on Advances in Social Networks Analysis and Mining*, ASONAM '16, pages 591–598, Piscataway, NJ, USA, 2016. IEEE Press.

[54] H. J. Hamilton and K. Karimi. The timers ii algorithm for the discovery of causality. In T. B. Ho, D. Cheung, and H. Liu, editors, *Advances in Knowledge Discovery and Data Mining*, pages 744–750, Berlin, Heidelberg, 2005. Springer Berlin Heidelberg.

[55] T. Holt, D. Strumsky, O. Smirnova, and M. Kilger. Examining the social networks of malware writers and hackers. *International Journal of Cyber Criminology*, 6(1):891–903, 1 2012.

[56] K. Hornik, M. Kober, I. Feinerer, and C. Buchta. Spherical k-means clustering. *Journal of Statistical Software*, 50, Sep 2012.

[57] J. Huang and J. Xue. The predictive power of content and temporal features of posts in information dissemination in microblogging. *Journal of China Tourism Research*, 11(2):150–165, 2015.

[58] L. Hubert and P. Arabie. Comparing partitions. *Journal of Classification*, 2(1):193–218, Dec. 1985.

[59] B. Hunter. The importance of reciprocity in relationships between community-based midwives and mothers. *Midwifery*, 22(4):308–322, 2006.

[60] IdentityForce. 2019 Data Breaches - The Worst So Far. https://www.identityforce.com/blog/2019-data-breaches, Access: 2019.

[61] M. Jenders, G. Kasneci, and F. Naumann. Analyzing and predicting viral tweets. In *Proceedings of the 22Nd International Conference on World Wide Web*, WWW '13 Companion, pages 657–664, New York, NY, USA, 2013. ACM.

[62] D. Kempe, J. Kleinberg, and E. Tardos. Maximizing the spread of influence through a social network. In *Proceedings of the Ninth ACM SIGKDD International Conference on Knowledge Discovery and Data Mining*, KDD '03, pages 137–146, New York, NY, USA, 2003. ACM.

[63] R. P. Khandpur, T. Ji, S. Jan, G. Wang, C.-T. Lu, and N. Ramakrishnan. Crowdsourcing cybersecurity: Cyber attack detection using social media. In *Proceedings of the 2017 ACM on Conference on Information and Knowledge Management*, CIKM '17, pages 1049–1057, New York, NY, USA, 2017. ACM.

[64] S. Kleinberg and B. Mishra. The temporal logic of causal structures. In *Proceedings of the Twenty-Fifth Conference on Uncertainty in Artificial Intelligence*, UAI '09, pages 303–312, Arlington, Virginia, United States, 2009. AUAI Press.

[65] A. Knowles. How Black Hats and White Hats Collaborate to Be Successful, 2016. https://securityintelligence.com/how-black-hats-and-white-hats-collaborate-to-be-successful/ (accessed on 08-20-2018).

[66] K. Lab. Kaspersky Security Bulletin 2019. Statistics, 2019. https://securelist.com/kaspersky-security-bulletin-2019-statistics/95475/ (accessed on 01-27-2020).

[67] S. Laxman and P. S. Sastry. A survey of temporal data mining. *Sadhana*, 31(2):173–198, Apr 2006.

[68] J. Lewis. Economic Impact of Cybercrime - No Slowing Down. , McAfee, 02 2018.

[69] G. L'Huillier, H. Alvarez, S. A. Ríos, and F. Aguilera. Topic-based social network analysis for virtual communities of interests in the dark web. *SIGKDD Explor. Newsl.*, 12(2):66–73, Mar. 2011.

[70] J. W. Lloyd. *Foundations of Logic Programming*. Springer-Verlag New York, Inc., New York, NY, USA, 1984.

[71] Z. Ma, A. Sun, and G. Cong. On predicting the popularity of newly emerging hashtags in twitter. *Journal of the American Society for Information Science and Technology*, 64, 07 2013.

[72] M. Macdonald, R. Frank, J. Mei, and B. Monk. Identifying digital threats in a hacker web forum. In *Proceedings of the 2015 IEEE/ACM International Conference on Advances in Social Networks Analysis and Mining 2015*, ASONAM '15, pages 926–933, New York, NY, USA, 2015. ACM.

[73] MANDIANT. APT1: Exposing one of China's cyber espionage units, 2013. https://www.fireeye.com/content/dam/fireeye-www/services/pdfs/mandiant-apt1-report.pdf/ (accessed on 11-07-2018).

[74] C. Manski. *Identification for Prediction and Decision*. Harvard University Press, 2009.

[75] E. Marin. Fluzz Redes Sociais: Geração, Visualização e Buscas que Maximizam a Probabilidade de Influência entre Indivíduos (in Portuguese). Master's thesis, Universidade Federal de Goiás - Instituto de Informática, Goiânia, Goiás, Brazil, 2012.

[76] E. Marin, M. Almukaynizi, E. Nunes, J. Shakarian, and P. Shakarian. Predicting hacker adoption on darkweb forums using sequential rule mining. In *2018 11th International Conference on Social Computing and Networking (SocilCom)*. IEEE, December 2018.

[77] E. Marin, M. Almukaynizi, E. Nunes, and P. Shakarian. Community finding of malware and exploit vendors on darkweb marketplaces. In *2018 1st International Conference on Data Intelligence and Security (ICDIS)*, pages 81–84, April 2018.

[78] E. Marin, M. Almukaynizi, and P. Shakarian. Reasoning about future cyber-attacks through socio-technical hacking information. In *2019 IEEE 31th International Conference on Tools with Artificial Intelligence (ICTAI)*, Nov 2019.

[79] E. Marin, M. Almukaynizi, and P. Shakarian. Inductive and deductive reasoning to assist in cyber-attack prediction. In *2020 IEEE Annual Computing and Communication Workshop and Conference*, Jan 2020.

[80] E. Marin, A. Diab, and P. Shakarian. Product offerings in malicious hacker markets. In *2016 IEEE Conference on Intelligence and Security Informatics (ISI)*, pages 187–189, Sept 2016.

[81] E. Marin, R. Guo, and P. Shakarian. Temporal analysis of influence to predict users' adoption in online social networks. In *Proceedings of the International Conference on Social Computing, Behavioral-Cultural Modeling & Prediction and Behavior Representation in Modeling and Simulation (SBP-BRiMS '17)*, pages 254–261, 05 2017.

[82] E. Marin, R. Guo, and P. Shakarian. Measuring time-constrained influence to predict adoption in online social networks. *Trans. Soc. Comput.*, 2(1), Feb. 2020.

[83] E. Marin, J. Shakarian, and P. Shakarian. Mining key-hackers on darkweb forums. In *2018 1st International Conference on Data Intelligence and Security (ICDIS)*, pages 73–80, April 2018.

[84] E. S. Marin and C. L. d. Carvalho. Search in social networks: Designing models and algorithms that maximize human influence. In *2014 47th Hawaii International Conference on System Sciences*, pages 1586–1595, Jan 2014.

[85] E. S. Marin and C. L. de Carvalho. Small-scale: A new model of social networks. In *2013 Winter Simulations Conference (WSC)*, pages 2972–2983, Dec 2013.

[86] N. Memon and R. Alhajj. *From Sociology to Computing in Social Networks: Theory, Foundations and Applications*. Lecture Notes in Social Networks. Springer Science & Business Media, 2010.

[87] M. Mitchell. *An Introduction to Genetic Algorithms*. MIT Press, Cambridge, MA, USA, 1996.

[88] R. G. Morris and A. G. Blackburn. Cracking the code: an empirical exploration of social learning theory and computer crime. *Journal of Crime and Justice*, 32(1):1–34, 2009.

[89] M. Motoyama, D. McCoy, K. Levchenko, S. Savage, and G. M. Voelker. An analysis of underground forums. In *Proceedings of the 2011 ACM SIGCOMM Conference on Internet Measurement Conference*, IMC '11, pages 71–80, New York, NY, USA, 2011. ACM.

[90] M. E. J. Newman. Finding community structure in networks using the eigenvectors of matrices. *Phys. Rev. E*, 74:036104, Sep 2006.

[91] M. Nouh and J. Nurse. Identifying key-players in online activist groups on the facebook social network. In *2015 IEEE International Conference on Data Mining Workshop (ICDMW)*, pages 969–978, Nov 2015.

[92] E. Nunes, A. Diab, A. Gunn, E. Marin, V. Mishra, V. Paliath, J. Robertson, J. Shakarian, A. Thart, and P. Shakarian. Darknet and deepnet mining for proactive cybersecurity threat intelligence. In *Proceeding of ISI 2016*, pages 7–12. IEEE, 2016.

[93] E. Nunes, P. Shakarian, and G. I. Simari. At-risk system identification via analysis of discussions on the darkweb. In *2018 APWG Symposium on Electronic Crime Research (eCrime)*, pages 1–12, May 2018.

[94] OCCUPYTHEWEB. The Essential Skills to Becoming a Master Hacker, 2016. `https://null-byte.wonderhowto.com/how-to/essential-skills-becoming-master-hacker-0154509/` (accessed on 02-21-2019).

[95] N. I. of Standards and T. (NIST). Common vulnerabilities and exposures. https://cve.mitre.org/, Last Accessed: June 2019.

[96] N. I. of Standards and T. (NIST). National vulnerability database. https://nvd.nist.gov/, Last Accessed: June 2019.

[97] A. Oprea, Z. Li, T. Yen, S. H. Chin, and S. Alrwais. Detection of early-stage enterprise infection by mining large-scale log data. In *2015 45th Annual IEEE/IFIP International Conference on Dependable Systems and Networks*, pages 45–56, June 2015.

[98] J. Pei, J. Han, B. Mortazavi-Asl, J. Wang, H. Pinto, Q. Chen, U. Dayal, and M.-C. Hsu. Mining sequential patterns by pattern-growth: the prefixspan approach. *IEEE Transactions on Knowledge and Data Engineering*, 16(11):1424–1440, Nov 2004.

[99] A. Pitman and M. Zanker. An empirical study of extracting multidimensional sequential rules for personalization and recommendation in online commerce. In *Wirtschaftsinformatik*, 2011.

[100] A. Pons and E. Pons. Social learning theory and ethical hacking: Student perspectives on a hacking curriculum. In *Proceedings of the Information Systems Education Conference*, ISECON 2015, pages 289–299, New York, NY, USA, 2015. Foundation for IT Education.

[101] M. Qiu, Y. Sim, N. A. Smith, and J. Jiang. Modeling user arguments, interactions, and attributes for stance prediction in online debate forums. In *Proceedings of the 2015 SIAM International Conference on Data Mining*, SIAM'2015, pages 855–863. SIAM Press, 2015.

[102] J. Radianti. A study of a social behavior inside the online black markets. In *2010 Fourth International Conference on Emerging Security Information, Systems and Technologies*, pages 189–194, July 2010.

[103] J. Robertson, A. Diab, E. Marin, E. Nunes, V. Paliath, J. Shakarian, and P. Shakarian. Darknet mining and game theory for enhanced cyber threat intelligence. *The Cyber Defense Review*, 1(2):95 – 121, 2016.

[104] J. Robertson, A. Diab, E. Marin, E. Nunes, V. Paliath, J. Shakarian, and P. Shakarian. *Darkweb Cyber Threat Intelligence Mining*. Cambridge University Press, 2017.

[105] J. L. Rodgers and W. A. Nicewander. Thirteen ways to look at the correlation coefficient. volume 41, pages 59–66. Taylor & Francis, 1988.

[106] R. Rogers. Debanalizing twitter: The transformation of an object of study. In *Proceedings of the 5th Annual ACM Web Science Conference*, WebSci '13, pages 356–365, New York, NY, USA, 2013. ACM.

[107] S. Russell and P. Norvig. *Artificial Intelligence: A Modern Approach*. Prentice Hall Series in Artifi. Prentice Hall, 2010.

[108] G. M. S. The strength of weak ties. *American Journal of Sociology*, 78(6):1360–1380, 1973.

[109] C. Sabottke, O. Suciu, and T. Dumitraş. Vulnerability disclosure in the age of social media: Exploiting twitter for predicting real-world exploits. In *Proceedings of the 24th USENIX Conference on Security Symposium*, SEC'15, pages 1041–1056, Berkeley, CA, USA, 2015. USENIX Association.

[110] F. Sadeque, T. Solorio, T. Pedersen, P. Shrestha, and S. Bethard. Predicting continued participation in online health forums. In *In Proceedings of the International Workshop on Health Text Mining and Information Analysis*, INFOCOM '18, pages 12–20. ACL, 2015.

[111] K. Saito, R. Nakano, and M. Kimura. Prediction of information diffusion probabilities for independent cascade model. In *Proceedings of the 12th International Conference on Knowledge-Based Intelligent Information and Engineering Systems, Part III*, KES '08, pages 67–75, Berlin, Heidelberg, 2008. Springer-Verlag.

[112] S. Samtani and H. Chen. Using social network analysis to identify key hackers for keylogging tools in hacker forums. In *Proceeding of ISI 2016*, pages 319–321, Sept 2016.

[113] A. Sapienza, A. Bessi, S. Damodaran, P. Shakarian, K. Lerman, and E. Ferrara. Early warnings of cyber threats in online discussions. In *2017 IEEE International Conference on Data Mining Workshops (ICDMW)*, pages 667–674, Nov 2017.

[114] O. Security. Exploitdb (edb). https://www.exploit-db.com/, Last Accessed: June 2019.

[115] R. Seebruck. A typology of hackers: Classifying cyber malfeasance using a weighted arc circumplex model. *Digital Investigation*, 14:36–45, 2015.

[116] R. Senthilkumar, R. Deepika, R. Saranya, and M. D. Govind. Generating adaptive partially ordered sequential rules. In *Proceedings of the International Conference on Informatics and Analytics*, ICIA-16, pages 110:1–110:8, New York, NY, USA, 2016. ACM.

[117] J. Shakarian, A. Gunn, and P. Shakarian. Exploring malicious hacker forums. In S. Jajodia, V. Subrahmanian, V. Swarup, and C. Wang, editors, *Cyber Deception: Building the Scientific Foundation*. Springer, 2016.

[118] J. Shakarian, A. T. Gunn, and P. Shakarian. *Exploring Malicious Hacker Forums*, pages 259–282. Springer International Publishing, Cham, 2016.

[119] J. Shakarian, P. Shakarian, and A. Ruef. Cyber Attacks and Public Embarrassment: A Survey of Some Notable Hacks. *CoRR*, abs/1501.05990, 2015.

[120] P. Shakarian, A. Bhatnagar, A. A., E. Shaabani, and R. Guo. *Diffusion in Social Networks*. Springer, 2014.

[121] P. Shakarian, A. Parker, G. Simari, and V. V. S. Subrahmanian. Annotated probabilistic temporal logic. *ACM Trans. Comput. Logic*, 12(2):14:1–14:44, Jan. 2011.

[122] P. Shakarian and J. Shakarian. Socio-cultural modeling for cyber threat actors. In *AAAI Workshop on Artificial Intelligence and Cyber Security (AICS)*, 2016.

[123] P. Shakarian, G. I. Simari, and V. S. Subrahmanian. Annotated probabilistic temporal logic: Approximate fixpoint implementation. *ACM Trans. Comput. Logic*, 13(2):13:1–13:33, Apr. 2012.

[124] W. F. Skinner and A. M. Fream. A social learning theory analysis of computer crime among college students. *Journal of Research in Crime and Delinquency*, 34(4):495–518, 1997.

[125] B. State and L. Adamic. The diffusion of support in an online social movement: Evidence from the adoption of equal-sign profile pictures. In *Proceedings of the 18th ACM Conference on Computer Supported Cooperative Work*, CSCW '15, pages 1741–1750, New York, NY, USA, 2015. ACM.

[126] X. Sun, J. Dai, P. Liu, A. Singhal, and J. Yen. Using bayesian networks for probabilistic identification of zero-day attack paths. *IEEE Transactions on Information Forensics and Security*, 13(10):2506–2521, Oct 2018.

[127] J. Swarner. Before WannaCry was Unleashed, Hackers Plotted About it on the Dark Web., 2017. `http://slate.me/2xQvscu` (accessed on 07-03-2017).

[128] J. Swearingen. The Creator of the Mirai Botnet Is Probably a Rutgers Student With the Bad Habit of Bragging., 2017. `http://slct.al/2wpr54I` (accessed on 08-12-2017).

[129] C. J.-W. T. Yang, C. Brinton. Predicting learner interactions in social learning networks. In *IEEE Conference on Computer Communications (INFOCOM)*, INFOCOM '18, 2018.

[130] P. Tan, M. Steinbach, and V. Kumar. *Introduction to Data Mining*. Always learning. Pearson Addison Wesley, 2006.

[131] P. Tan, M. Steinbach, and V. Kumar. *Introduction to Data Mining*. Addison-Wesley, 2013.

[132] N. Tavabi, P. Goyal, M. Almukaynizi, P. Shakarian, and K. Lerman. Darkembed: Exploit prediction with neural language models. In *Proceedings of AAAI Conference on Innovative Applications of AI (IAAI2018)*. AAAI, 2018.

[133] The Offensive Security Team. Offensive Security. https://www.offensive-security.com/, Last Accessed: June 2019.

[134] J. Ugander, L. Backstrom, C. Marlow, and J. Kleinberg. Structural diversity in social contagion. *Proceedings of the National Academy of Sciences*, 109(16):5962–5966, 2012.

[135] T. Valente. *Network Models of the Diffusion of Innovations*, volume 2. Hampton Press, 1995.

[136] G. Wadsworth and J. Bryan. *Introduction to Probability and Random Variables*. Probability & Statistics. McGraw-Hill, 1960.

[137] D. Watts. *Six Degrees: The Science of a Connected Age*. W. W. Norton, 2004.

[138] D. J. Watts. A simple model of global cascades on random networks. *Proceedings of the National Academy of Sciences*, 99(9):5766–5771, 2002.

[139] D. J. Watts and P. S. Dodds. Influentials, networks, and public opinion formation. *Journal of Consumer Research*, 34:441–458, 2007.

[140] L. Weng, F. Menczer, and Y.-Y. Ahn. Virality prediction and community structure in social networks. *Scientific Reports*, 3(2522), 8 2013.

[141] Z. Xu, Y. Zhang, Y. Wu, and Q. Yang. Modeling user posting behavior on social media. In *Proceedings of the 35th International ACM SIGIR Conference on Research and Development in Information Retrieval*, SIGIR '12, pages 545–554, New York, NY, USA, 2012. ACM.

[142] C. C. Yang, X. Tang, and X. Gong. Identifying dark web clusters with temporal coherence analysis. In *Proceedings of 2011 IEEE International Conference on Intelligence and Security Informatics*, pages 167–172, July 2011.

[143] R. Zafarani, M. Abbasi, and H. Liu. *Social Media Mining: An Introduction*. Cambridge University Press, 2014.

[144] H. Zhang, Q. Zhao, H. Liu, K. xiao, J. He, X. Du, and H. Chen. Predicting retweet behavior in weibo social network. In *WISE 2012*, pages 737–743, Berlin, Heidelberg, 2012. Springer Berlin Heidelberg.

[145] J. Zhang, B. Liu, J. Tang, T. Chen, and J. Li. Social influence locality for modeling retweeting behaviors. In *Proceedings of the 13th International Joint Conference on Artificial Intelligence*, IJCAI '13, pages 2761–2767. AAAI Press, 2013.

[146] J. Zhang, J. Tang, J. Li, Y. Liu, and C. Xing. Who influenced you? predicting retweet via social influence locality. *ACM Trans. Knowl. Discov. Data*, 9(3):25:1–25:26, Apr. 2015.

[147] X. Zhang and L. C. Survival analysis on hacker forums. *2013 SIGBPS Workshop on Business Processes and Service*, pages 106–2013, 2013.

[148] X. Zhang, A. Tsang, W. Yue, and M. Chau. The classification of hackers by knowledge exchange behaviors. *Inform. Systems Frontiers*, 17(6):1239–1251, 2015.

[149] Z. Zhang, B. Li, W. Zhao, and J. Yang. A study on the retweeting behaviour of marketing microblogs with high retweets in sina weibo. In *2015 Third International Conference on Advanced Cloud and Big Data*, pages 20–27, Oct 2015.

[150] Z. Zhao, G.-J. Ahn, H. Hu, and D. Mahi. SocialImpact: Systematic Analysis of Underground Social Dynamics. In S. Foresti, M. Yung, and F. Martinelli, editors, *ESORICS*, volume 7459 of *Lecture Notes in Computer Science*, pages 877–894. Springer, 2012.